

OCDO-94010907

OHIO COAL RESEARCH CONSORTIUM

SUBCONTRACT AGREEMENT NO. OCRC/92-1.6

OCDO Grant No. CDO/R-87-2C/B

SORBENT PREPARATION/MODIFICATION/ADDITIVES

Final Report for the Period
September 1, 1992 to November 30, 1993

by

RECEIVED

Michael E. Prudich

MAY 06 1994

Rajesh Venkataramakrishnan

DEPARTMENT OF DEVELOPMENT
OHIO COAL DEV OFFICE

Ohio University, Athens, OH

February 1994

Project Manager: Michael E. Prudich, Professor, Chemical Engineering,
Ohio University, Athens, OH 45701
(614) 593-1501

This project was funded in part by the Ohio Coal Development Office, Department of
Development, State of Ohio.

MASTER

DISTRIBUTION OF THIS DOCUMENT IS UNLIMITED

SUBCONTRACT AGREEMENT NO. OCRC/92-1.6

SORBENT PREPARATION/MODIFICATION/ADDITIVES

TABLE OF CONTENTS

EXECUTIVE SUMMARY	i
1.0 GENERAL DESCRIPTION AND BACKGROUND	1-1
1.1 Background	1-1
1.2 Sorbent Preparation	1-1
1.2.1 <u>Chemical Form</u>	1-1
1.2.2 <u>Calcium/Magnesium Ratio</u>	1-2
1.2.3 <u>Morphology</u>	1-2
1.2.4 <u>Preparation by Aqueous Hydration</u>	1-4
1.3 The Use of Additives to Enhance Reactivity	1-7
1.3.1 <u>Deliquescents, Buffers, and Sodium Additives</u>	1-7
1.3.2 <u>Alcohol and Sucrose Hydration</u>	1-9
1.3.3 <u>Silicate Additives</u>	1-11
1.3.4 <u>Miscellaneous Additives - High Temperature Additives</u>	1-12
1.4 Long-Term Goals	1-15
2.0 PROJECT YEAR #1 ACCOMPLISHMENTS	2-1
2.1 Acquisition of Limestone/Lime Samples	2-1
2.2 Characterization of Limestone/Lime Samples	2-2
2.3 Calcination Reactor	2-2
2.4 Slaking Reactor	2-2
2.5 Calcination Reactions	2-5
2.6 Slaking Reactions	2-5

SUBCONTRACT AGREEMENT NO. OCRC/92-1.6

SORBENT PREPARATION/MODIFICATION/ADDITIVES

TABLE OF CONTENTS (continued)

3.0	PROJECT YEAR #2 ACCOMPLISHMENTS	3-1
3.1	Sorbent Preparation	3-1
3.2	Chemical Additives	3-3
4.0	PROJECT YEAR #3 PLANS	4-1
5.0	PROJECT YEAR #3 ACCOMPLISHMENTS	5-1
5.1	Effect of Chemical Additives on Duct Injection/ Spray Drying Performance	5-1
5.1.1	<u>Introduction/ General Description</u>	5-1
5.1.2	<u>Chemical Effects of Additives</u>	5-6
5.1.3	<u>Model Comparisons</u>	5-19
5.1.4	<u>Conclusions and Recommendations</u>	5-20
5.2	Solid State Chemistry at High Temperatures	5-21
5.2.1	<u>Introduction/ General Description</u>	5-21
5.2.2	<u>Literature Review</u>	5-21
5.3	Effect of Sorbent "Inert" Contents at Low Temperature	5-26
5.3.1	<u>Introduction/ General Description</u>	5-26
5.3.2	<u>Experimental</u>	5-26
5.3.3	<u>Results and Discussion</u>	5-30
REFERENCES		R-1
APPENDIX		A-1

EXECUTIVE SUMMARY

Sorbent preparation techniques used today have generally been adapted from techniques traditionally used by the lime industry. Traditional "dry" hydration and slaking processes have been optimized to produce materials intended for use in the building industry. These preparation techniques should be examined with an eye to optimization of properties important to the SO₂ capture process.

The study of calcium-based sorbents for sulfur dioxide capture is complicated by two factors: (1) little is known about the chemical mechanisms by which the "standard" sorbent preparation and enhancement techniques work, and (2) a sorbent preparation technique that produces a calcium-based sorbent that enjoys enhanced calcium utilization in one regime of operation [flame zone (>2400°F), in-furnace (1600-2400°F), economizer (800-1100°F), after air preheater (<350°F)] may not produce a sorbent that enjoys enhanced calcium utilization in the other reaction zones. Again, an in-depth understanding of the mechanism of sorbent enhancement is necessary if a systematic approach to sorbent development is to be used.

As a long-term goal, an experimental program is being carried out for the purpose of (1) defining the effects of slaking conditions on the properties of calcium-based sorbents, (2) determining how the parent limestone properties and preparation techniques interact to define the SO₂ capture properties of calcium-based sorbents, and (3) elucidating the mechanism(s) relating to the activity of various dry sorbent additives.

Project Year #1 research work focussed in the areas of experimental set-up (all experimental apparatus has been built from the ground up) and the learning/selection of analytical techniques for sorbent characterization. Accomplishments during the first year include: (1) the collection of a series of limestone/ hydrated lime/ quicklime samples representing a range of Ohio limestone products, (2) initial analyses of the suite of Ohio limestones, (3) the set-up/shakedown of a mercury porosimeter, (4) the design and construction of a bench-scale slaking reactor, and (5) the design and construction of a bench-scale calcination reactor.

Project Year #2 research work included: (1) a continuation of the collection and characterization of a set of Ohio limestones, (2) the production of a complete set of calcined and hydrated products from the set of Ohio limestones, and (3) an investigation of the importance of lime solubility enhancement in the evolution of surface area during the slaking process.

Project Year #3 research work has included a model/paper study of the effects of chemical additives on the performance in spray drying and in-duct injection processes. A one-dimensional model formulated by the Energy and Environmental Research Corporation (EER, 1989) was selected as the basic vehicle for this study. The basic EER model was modified to allow for a range of additive effects. A brief experimental study was made in an effort to quantify the effects of both magnesium and "inert" contents on the low temperature dry capture effectiveness of hydrated lime. The results of this experimental study were inconclusive.

1.0 GENERAL DESCRIPTION AND BACKGROUND

1.1 Background

Sorbent preparation techniques used today have generally been adapted from techniques traditionally used by the lime industry. Traditional "dry" hydration and slaking processes have been optimized to produce materials intended for use in the building industry. These preparation techniques should be examined with an eye to optimization of properties important to the SO₂ capture process.

The study of calcium-based sorbents for sulfur dioxide capture is complicated by two factors: (1) little is known about the chemical mechanisms by which the "standard" sorbent preparation and enhancement techniques work, and (2) a sorbent preparation technique that produces a calcium-based sorbent that enjoys enhanced calcium utilization in one regime of operation [flame zone (>2400°F), in-furnace (1600-2400°F), economizer (800-1100°F), after air preheater (<350°F)] may not produce a sorbent that enjoys enhanced calcium utilization in the other reaction zones. Again, an in-depth understanding of the mechanism of sorbent enhancement is necessary if a systematic approach to sorbent development is to be used.

The sorbent modification studies reviewed below relate to both SO₂ capture in the 1600-2400°F range and the <350°F range in a roughly 80:20 ratio. For the purposes of the review section, studies performed in the temperature range 1600-2400°F will be called high temperature studies and studies performed in the temperature range <350°F will be called low temperature studies. No additive studies are offered to describe the application of promoted sorbents to the problem of SO₂ capture in the 800-1100°F reaction range.

1.2 Sorbent Preparation

1.2.1 Chemical Form

High Temperature Studies. Cole et al. [1986], using an isothermal reactor at 2000°F, Ca/S = 2, and 2000 ppm SO₂ showed that calcitic hydrates were more reactive than calcitic carbonates. They attributed this observation to a combination of three reasons: (1) Dehydration occurs much more rapidly than CO₂ evolution, therefore the time available for sulfation after the calcination process is significantly greater for hydrates than for carbonates, (2) hydrates begin with a much higher initial surface area, and (3) the dehydration process generally produces a reduction in the mean particle size of the sorbent thereby reducing the internal diffusion resistance to SO₂ diffusion.

Between the two types of calcium-based sorbents generally used in in-furnace injection, it is well documented that CaO derived from Ca(OH)₂ (h-CaO) is more

reactive than CaO derived from CaCO_3 (c-CaO) [Silcox et al., 1987]. This is attributed in part to the smaller particle size of h-CaO, and more importantly, to the pore structure of the CaO produced. The h-CaO has a slit or plate-like structure while the structure of c-CaO is in the form of cylindrical pores (or spherical grains). The plate-like structure retains its porosity to a greater extent by allowing for particle expansion [Gullett and Bruce, 1987], and results in higher rates of diffusion of the reactant through the product layer [Bruce et al., 1989].

1.2.2 Calcium/Magnesium Ratio

High Temperature Studies. Snow et al. [1986], injecting sorbents into a flue gas stream produced by the combustion of Pittsburgh No. 8 coal (injection temperature = 2210°F; quench rate = 468 °F/s; average residence time at reaction temperature = 1.3 s; Ca/S mole ratio = 2; 1900 ppm SO_2) found that sorbent SO_2 capture reactivity varied in the order dolomitic hydrates > calcitic hydrates > carbonates (based on equal molar Ca/S ratios). However, for a given sorbent type there was no clear correlation between physical properties (BET surface area, mass mean particle size, elemental stoichiometry) and SO_2 capture performance. A summary of their data is given in Table 1-1.

Teixeira et al. [1986], testing sorbents for SO_2 removal from flue gases generated by burning low-sulfur Western coals (injection temperature = 2000°F; average residence time = 0.33 s; 500 ppm SO_2) also found that SO_2 capture reactivity varied in the order dolomitic hydrates > calcitic hydrates > carbonates. This observation was further confirmed by Beittel et al. [1985], Overmoe et al. [1985], and Bortz and Flament [1985].

Gooch et al. [1986] have observed that the increased utilization of pressure-hydrated dolomitic lime is often only sufficient to compensate for the decreased calcium content. This balance results in no net reduction of the mass of sorbent required to accomplish a given SO_2 reduction.

1.2.3 Morphology

High Temperature Studies. Gooch et al. [1986] tested 11 commercial calcitic hydrates under furnace injection conditions. No obvious correlation of properties of the raw sorbent with SO_2 removal was identified. However, when testing four specially-prepared sorbents with widely varying BET surface areas, particle sizes, and pore structures, it was found that a two-fold increase in raw sorbent surface area resulted in a 20% relative increase in calcium utilization. The increased surface area also served to decrease the dependence of sulfur dioxide capture efficiency on injection temperature.

TABLE 1-1

EFFECT OF SORBENT PROPERTIES ON
HIGH TEMPERATURE SO₂ CAPTURE PERFORMANCE
[After Snow et al., 1986]

Sorbent	Mass Mean	BET	<u>Percent by Weight</u>		SO ₂
	Particle Dia. (μm)	Surface Area (m ² /g)	Ca (%)	Mg (%)	Removal (%)
Vicron Limestone	11.0	1.01	39.01	0.49	38
Mercer CAH	7.10	17.8	50.5	0.4	59
Kemikal CAH	3.88	18.0	49.0	1.0	62
Marblehead CAH	7.79	14.3	50.3	0.49	69
Detroit Lime CAH	8.33	14.9	50.2	0.51	60
Black River CAH	5.53	13.3	49.7	1.6	61
Kemidol DAH	19.71	20.6	29.9	18.5	73
Ivory Finish DPH	13.72	18.4	28.6	18.1	75

CAH --- Calcitic Atmospheric Hydrate

DAH --- Dolomitic Atmospheric Hydrate

DPH --- Dolomitic Pressure Hydrate

Percent SO₂ removal at Ca/S=2; 2210°F injection temperature.

McCarthy et al. [1986] also agree that reactivity in furnace injection does not correlate with hydrate surface area. They did show, however, that SO_2 capture reactivity did correlate with the surface area of the calcined hydrate, with an increase in reactivity being associated with a higher calcined surface area (Figure 1-1).

Low Temperature Studies. Yoon et al. [1986] have prepared high BET surface area calcitic hydrates using atmospheric hydration under N_2 followed by filtration and vacuum drying. Using these hydrates Yoon was able to show a strong relationship between sorbent utilization in dry/dry capture (150°F, 60% relative humidity, 20°F approach to saturation, 1000 ppm SO_2) and raw sorbent BET surface area (Figure 1-2a). Using hydrates whose BET surface areas varied between 10 and 50 m^2/g he was able to effect calcium utilizations from between 12% and 45%.

Borgwardt and Bruce [1986] confirmed the work of Yoon et al. [1986] by preparing a series of high surface area hydrates and showing the strong effect of hydrate BET surface area on dry/dry humidified SO_2 capture (Figure 1-2b).

1.2.4 Preparation by Aqueous Hydration

High Temperature Studies. Kirchgessner et al. [1986], using calcines and hydrates prepared from Eldorado limestone, found a slight decrease in the SO_2 capture reactivity of the product hydrate with increasing particle size of the parent calcine. As the mean calcine particle size increased from 0.5mm to 9.5mm the percent Ca utilization of the product hydrate dropped from 14.5% to 13.0%. The observed effect was attributed to the larger particle surface area present for the smaller-sized calcine.

McCarthy et al. [1986] report that pressure hydrates generated under well-controlled conditions are more reactive than commercially produced atmospheric hydrates. They reported that important hydration process variables include size and composition of the parent quicklime, the hydration temperature and pressure, the rate of water addition to the hydration reactor, and the pressure progression during the discharge of the hydrate from the hydration reactor. However, Gooch et al. [1986] found that pressure-hydrated calcitic lime produced and evaluated in laboratory-scale apparatus could not be distinguished from its companion atmospheric hydrate on the basis of either particle morphology, chemical composition, or SO_2 capture ability.

Low Temperature Studies. Borgwardt and Bruce [1986] prepared calcitic hydrates using steam hydration. The hydrate sorbents prepared in this manner show inferior BET surface areas (9-11 m^2/g) when compared to hydrates produced through the use of a liquid water phase. The SO_2 capture performance of the steam hydrated samples was substantially less than that of liquid water hydrated samples. Borgwardt suggested that this observation might explain the sometimes contradictory results

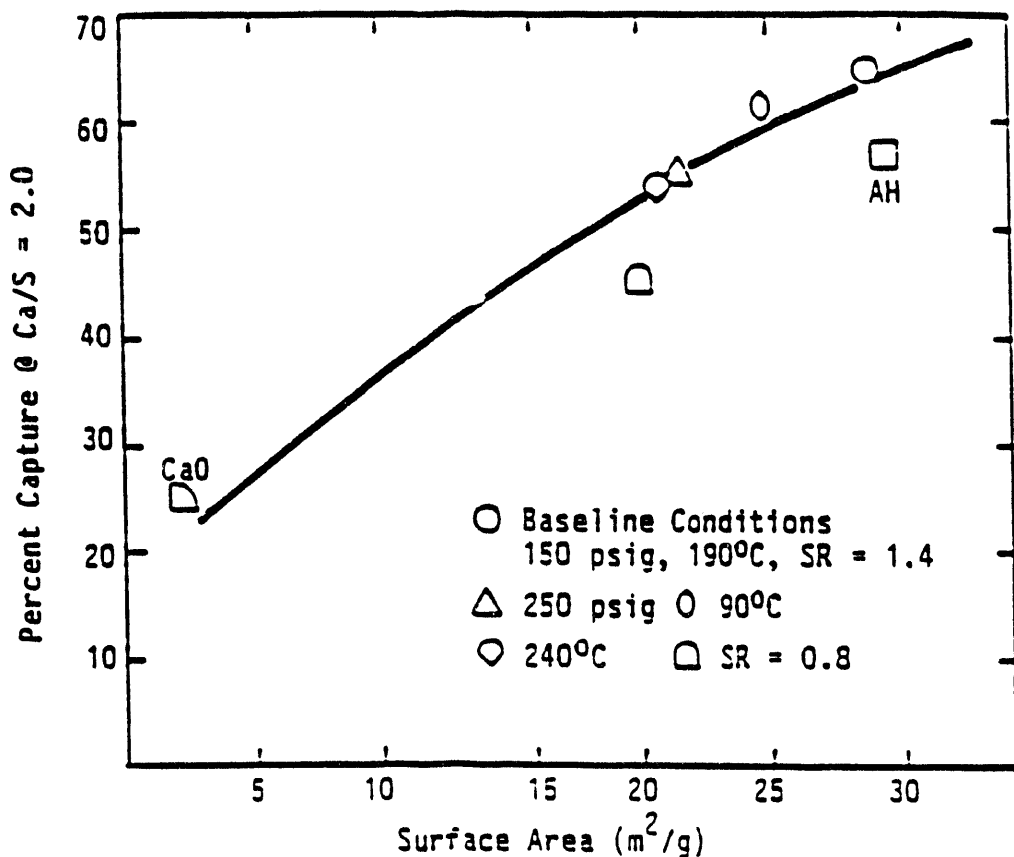
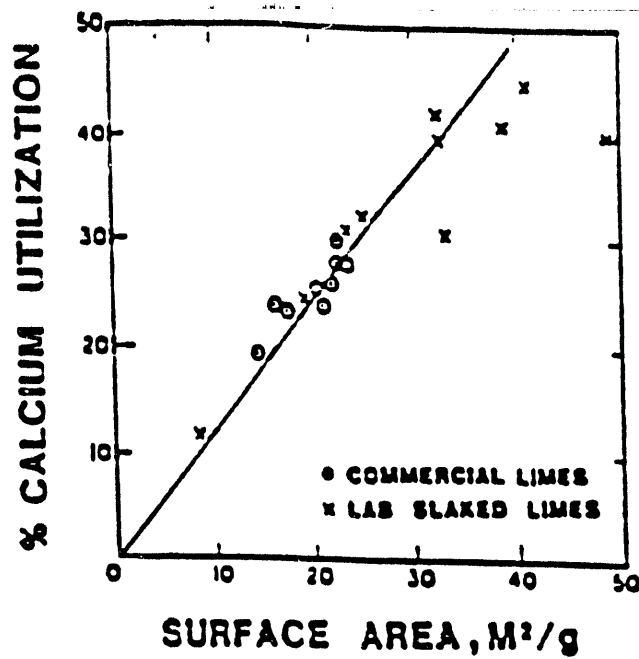
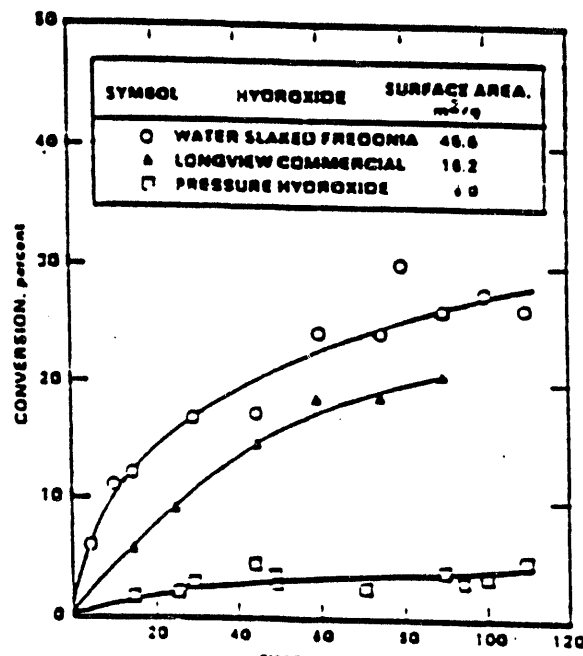


Figure 1-1. SO_2 capture reactivity versus surface area of the calcined hydrate [McCarthy et al., 1986].



(a)



(b)

Figure 1-2. Effect of sorbent surface area on low temperature SO₂ capture performance: (a) 150°F, 60% relative humidity, 1000 ppm SO₂, 60 minutes [Yoon et al., 1986]; (b) 150°F, 20 vol% H₂O, 1500 ppm SO₂ [Borgwardt and Bruce, 1986].

obtained during pressure hydration. The performance of the pressure hydration process might in part be controlled by a delicate balance between the positive effects of decompressive drying and the negative effects of steam exposure.

1.3 The Use of Additives to Enhance Reactivity

The use of additives to enhance the $\text{Ca}(\text{OH})_2$ reactivity with SO_2 have been explored by a number of investigations. The type of additives investigated to date may be classified as [Gooch et al., 1989]:

- deliquescent inorganic salts and related inorganic salts
- sodium-containing basic compounds
- organic compounds
- oxidation catalysts

The majority of the compounds tested fall into the first category above, although there is some cross-classification among the compounds evaluated to date. For example, NaOH is capable of reacting directly with SO_2 as a basic solution but it is also a deliquescent compound.

1.3.1 Deliquescents, Buffers, and Sodium Additives

High Temperature Studies. Sodium compounds have also been tried, with varying success, in the in furnace (1600-2400°F) regime. Generally these additives are added to the water phase during the hydration process. Teixeira et al. [1986] found that sodium carbonate, sodium bicarbonate, and sodium hydroxide all enhance the sulfur removing capability of dolomitic hydrates when removing sulfur from SO_2 -doped natural gas flue gases. However, the benefit of the sodium compounds disappeared when western coal-derived fly ash was present in the flue gas stream. No ash analyses were offered in their paper.

Weber et al. [1986] also remarked on the capability of NaOH to enhance the behavior of a pressure-hydrated calcitic hydrate for in furnace SO_2 capture when using doped natural gas flue gas. However, they also saw this advantage disappear when they used a flue gas generated by burning a Beulah lignite. The high calcium and sodium content of the ash from lignite (15.5wt% CaO , 4.0 wt% Na_2O) probably contributed significantly to this effect.

Snow et al. [1986] investigated NaHCO_3 as an additive for capture of SO_2 at 2210°F from a flue gas generated by burning Pittsburgh No. 8 coal. At a Ca/s ratio of 2, the addition of the NaHCO_3 additive increased the capture efficiency of a calcitic atmospheric hydrate from 63-69% to 83% and for atmospheric and pressure dolomitic hydrates from 73-75% to 88%. Ashes from eastern bituminous coals are not expected to contain significant amounts of calcium or sodium.

Muzio et al. [1986] have investigated the effects of nine additives added to the hydration water on SO_2 capture. The nine additives studied include: NaOH , NaCl , Na_2CO_3 , Li_2SO_4 , LiNO_3 , K_2CO_3 , Cs_2SO_4 , $\text{Fe}(\text{NO}_3)_3$, and FeCl_3 . For experiments at 2100 °F, $\text{Ca/S} = 2$, and a metal promoter/ CaO weight ratio of 0.03 the use of the promoters resulted in the following increases in SO_2 capture when compared to a nonpromoted, base hydrate: $\text{Cs}(33\%) > \text{K}(29\%) > \text{Na}(20\%) > \text{Li}(0\%), \text{Fe}(0\%)$. In all cases where improvement was observed, the improvement was greater than that which would have been predicted if all of the promoting material was transformed to its sulfate form. Muzio also showed that the form of sodium added had essentially no effect on the sulfur capture performance of the promoted sorbent. This was particularly interesting in light of the wide variation in BET surface areas of the raw hydrated sorbents (Na_2CO_3 , 16 m^2/g ; NaOH , 7.8 m^2/g ; NaCl , 4.5 m^2/g). Muzio et al. speculated that for the promoted hydrates, alkali crystals may block the pores at room temperature but, as a result of melting and vaporization in the combustion zone, the pore structure may reopen at reaction conditions. Physical mixtures of CaO and Na_2CO_3 were found to be less effective than addition of the same amount of Na_2CO_3 to the hydration water for the same CaO sorbent (38% SO_2 capture versus 45% SO_2 capture). The presence of fly ash in the flue gas served to totally eliminate any promotion effect of the sodium metal additives.

Low Temperature Studies. Ruiz-Alsop and Rochelle [1985] tested the effectiveness of 18 additives (two buffers, three organic deliquescents, and thirteen inorganic deliquescents) towards improving calcium utilization in dry/dry SO_2 capture. Their experiments were performed in a sand bed reactor at 54-74% relative humidity. Reaction conditions were set to simulate the conditions found in bag filters during flue gas spray drying. It has been postulated that deliquescent salts should increase the efficiency of sulfur capture in dry/dry systems by enhancing the moisture content in the sorbent solids. This study found that the two buffers and the three organic deliquescents caused a degradation in SO_2 capture efficiency while the inorganic deliquescents caused a increase in the SO_2 capture efficiency, in some cases almost doubling the efficiency (Table 1-2). The most effective inorganic deliquescents were LiCl , KCl , NaBr , and Na_2NO_3 . Ruiz-Alsop and Rochelle [1985] found a poor correlation between the relative deliquescence of the inorganic salts and their ability to enhance SO_2 capture. They speculated that some of the salts also acted to favorably modify the sulfite reaction product layer formed on the surface of the sorbent particles.

Huang et al. [1987] have reported that the addition of NaOH in the lime slurry used for an industrial-sized spray dryer caused the partial oxidation of NO to NO_2 . This is a significant development in that NO_2 is more reactive with a variety of gaseous compounds and could conceivably be removed as a particle [Keener, 1977].

Yoon et al. [1986] used additives to promote the activity of samples of hydrated lime in conjunction with tests on the Coolside process (a process operating in the <350°F regime). The action of both "co-sorptive" and "non-cosorptive"

additives were evaluated. Examples of co-sorptive additives include NaOH, Na₂CO₃, and possibly NaCl, Na₂SO₃, and Na₂NO₃. Examples of non-cosorptive additives include CaCl₂, KCl, FeCl₃, and MgCl₂. The additives were either added to the hydrated lime in an aqueous solution or were added to the lime during the hydration process. Both sets of compounds were found to be highly effective in enhancing the capture behavior of the hydrated lime, even when the co-sorptive properties of the sodium salts were subtracted out. Treating -325 mesh hydrated lime particles with NaCl using a promotion mole ratios of 0.05 to 0.2 Na⁺/Ca⁺⁺ in a laboratory reactor (operated in the dry/dry sorption mode) resulted in relative calcium utilization increases of 80% to 114% over those achieved using unpromoted hydrated lime samples. It was speculated that the additives might act to enhance SO₂ capture in any one of three ways: (1) changing the sorbent particle's physical properties, particularly the surface area of the hydrate, (2) enhancing the basicity of the sorbent, and (3) increasing or retaining moisture at the sorbent surface. No evidence was offered to support any of these three proposed mechanisms.

Organic acids and buffers have been studied as wet FGD additives and have been found to be effective in increasing the overall rate of SO₂ capture in CaO or CaCO₃ slurries. This wet FGD slurry work should shed some light on behavior that might be expected for wet/dry SO₂ capture systems.

Jarvis et al. [1986] evaluated the performance of several organic acid additives (adipic acid, maleic acid, formic acid, glutamic acid, succinic acid) in a bench-scale wet FGD system. The use of these additives increased the removal of SO₂ by 15%. Other investigators have confirmed the effectiveness of organic acid and buffer additives for wet FGD systems [Chang and Brna, 1986 - adipic acid, citric acid, sodium formate; Wang and Burbank, 1982 - adipic acid; Rochelle et al., 1982 - sulfopropionic acid, sulfosuccinic acid, acetic acid, adipic acid, hydroxypropionic acid, aluminum sulfate]. Works by Chan and Rochelle [1982] and Rochelle and King [1977] have provided models for the mass-transfer enhancement actions of organic acids, alkali additives, and buffers in wet FGD systems.

1.3.2 Alcohol and Sucrose Hydration

High Temperature Applications. Gooch et al. [1986] evaluated alcohol (methanol, ethanol, isopropanol), acetone, and sucrose hydration techniques. It was observed that while the alcohols are all removed from the final product by evaporation (and therefore can be recovered and reused) the sucrose remains in the final product. For hydration tests conducted at 60-70°C, an atmospheric hydrate with a BET surface area of 22 m²/g was produced starting with a parent CaO with a surface area of 2.2 m²/g. Hydration with aqueous acetone and methanol solutions under "optimum" conditions produced hydrates with surface areas of 50 m²/g and 80 m²/g, respectively. Hydrates produced using an aqueous mixture of sucrose and methanol had a BET surface area of 85 m²/g.

TABLE 1-2

EFFECT OF ADDITIVES ON LIME REACTIVITY
[Ruiz-Alsop and Rochelle, 1985]

Additive	Lime Conversion at 60 minutes		
	74% RH	54% RH	
	64.4°C	66 °C	
No Additive	22.4	11.8	
Buffers			
5 wt% Glycolic Acid	11.3	----	
1 wt% Adipic Acid	20.3	----	
Organic Deliquescents			
5 wt% Monoethanolamine	19.6	----	
5 wt% Ethylene Glycol	20.3	----	
5 wt% TEG	20.5	----	
Inorganic Deliquescents			
5 mole% Na_2SO_4	28.3	----	
5 mole% Na_2SO_3	29.8	16.1	
5 mole% CaCl_2 (*)	34.6	16.4	
10 mole% NaCl	38.5	27.0	
10 mole% NaOH	38.8	17.3	
5 mole% $\text{Ca}(\text{NO}_3)_2$ (*)	39.4	12.3	
10 mole% NaNO_2	40.0	----	
10 mole% NaNO_3	41.5	27.2	
$\text{BaCl}_2 \cdot 2\text{H}_2\text{O}$	----	19.4	
$\text{Na}_2\text{S}_2\text{O}_3$	----	21.6	
KCl	----	37.3	
$\text{NaBr} \cdot 2\text{H}_2\text{O}$	----	42.0	
LiCl	----	43.9	
100% SO_2 Removal	48.2	48.2	

(*) ---- Solid phase are $\text{CaCl}_2 \cdot \text{Ca}(\text{OH})_2 \cdot \text{H}_2\text{O}$ and $\text{CaN}_2\text{O}_7 \cdot 2\text{H}_2\text{O}$ respectively.
RH ---- Relative Humidity.

Gooch et al. [1986] presented the speculation that alcohols act to improve sorbent surface area by abstracting the heat of hydration from the sorbent surfaces by evaporation and that sucrose acts by increasing the solubility of CaO in water (0.1 wt% in water and 9.8 wt% in 35% sucrose/65% water at 25°C). No experimental evidence was reported to support either of these proposed mechanisms.

1.3.3 Silicate Additives

Low Temperature Studies. The use of product recycle (with included fly ash) has been shown to improve spray dryer performance in pilot plant tests [Blythe et al., 1983].

Also, bench scale studies with a packed bed reactor have shown substantial improvements in SO₂ uptake for Ca(OH)₂ slurried with several different fly ashes. [Jozewicz and Rochelle, 1986]. They speculate that the fly ash reacts with Ca(OH)₂ to produce calcium silicates with more reactive surface area than the original Ca(OH)₂. Reagent-grade Al₂O₃, Fe₂O₃, and H₂SiO₃ were also found to enhance calcium utilization for dry/dry SO₂ scrubbing systems.

A potential problem in the use of fly ash as a silica source is the apparent increased solids loading to the atomizer which must be used in order to achieve increased SO₂ removal. The quality of sorbent material entrained in the gas stream is directly proportional to the amount of recycle, and thus, represents an increased load to the particle collection device. A direct injection technology utilizing silica enhanced Ca(OH)₂ is being developed and is known as the ADVACATE process [Gooch et al., 1989].

The impact of coal chloride concentration on SO₂ removal in a spray dryer has been reported by Brown et al. [1988]. In tests conducted at the TVA 10-MW spray dryer/ESP test facility a SO₂ removal level of 85% was achieved over an extended test period for a 4.0% sulfur, 0.05% chloride coal with a reagent ratio of 1.6 for operation at an 18°F approach to adiabatic saturation and an inlet gas temperature of 320°F. For similar operating conditions, a SO₂ removal level of 93% was achieved when the coal was changed to one containing 4.0% sulfur and 0.25% chloride. On high chloride coal (i.e. % chloride > 0.2%), 90% removal appears to be achievable at a reagent ratio between 1.4 and 1.5. The role of chloride in promoting greater SO₂ reactivity is postulated to be caused by the formation of higher concentrations of HCl in the flue gas which subsequently react with the slurry in the spray dryer. Calcium chloride, a classical deliquescent salt, has been reported by others [Karlsson et al., 1983] to greatly improve SO₂ uptake in calcium-based sorbents.

1.3.4 Miscellaneous Additives - High Temperature Applications

Effects of Sintering and Pore Structure. Borgwardt et al. [1987] pointed out that diffusion through the product layer in a solid, when it occurs through solid-state mechanisms, increases with the concentration of lattice defects. These can exist as point defects, which involve individual atoms, or as extended defects, which involve lines or planes of disorder in the crystal structure [West, 1984]. At a given temperature, the concentration of point defects in the product layer may depend on the concentration of foreign ions. Thus, higher diffusivities can be expected in impure materials, when a solid-state mechanism prevails. From their results, they concluded that the higher reactivity of impure CaO is due to defects inherent with the crystal structure of the limestone derivatives. Impurities in the form of aliovalent ions are known to generate defects in the crystal structure [Berniere and Catlow, 1983; Bardakci, 1984].

Accordingly, Borgwardt et al. [1987] studied the effects of alkali metal ions doped on the surface of well-annealed CaO. They added sulfates of lithium, sodium or potassium to pre-calcined and pre-sintered CaO by grinding in a mortar, and observed significant increase in sorbent utilization during sulfation. However, doping CaCO_3 or $\text{Ca}(\text{OH})_2$ with Na^+ prior to calcination and sintering was not successful. This, they explain, is because these ions enhance the diffusion and hence the overall rate during sintering as well, which in turn causes a decrease in the surface area of the sorbent available for sulfation.

According to Haji-Sulaiman et al. [1987], higher impurity content in the sorbent increases the extent of calcination. Thus, sorbents with a more open pore structure are obtained resulting in improved sulfation efficiency by preventing early pore blockage. Shadman and Dombek [1988] view the role of additives solely as structure modifiers. They prepared flakes of modified sorbents by mixing the additives with a slurry of hydrated lime and spreading the mixture in a thin layer followed by drying. The additives used were bauxite, silica and kaolin. For all three additives, both the reaction rate and the maximum achievable conversion increased significantly. Between these additives, when their concentration and particle size were the same, they observed little difference in their performance. Hence they concluded that the effect of the additives is purely physical in nature, specifically an increase in macroporosity.

Following SEM micrograph analysis, they assumed that the sorbent flakes consist of spherical grains of lime mixed with inert additives. This leads to a bimodal pore size distribution where micropores account for pores in the particles and macropores represent the void space between particles. They developed a diffusion-controlled model with micropore and macropore diffusivities as the adjustable parameters. Model simulation supported their experimental finding that initial macroporosity is a critical factor in determining the sulfation performance of the modified sorbent.

Organic Surfactants. Kirchgessner and Lorrain [1987] modified the sorbent Ca(OH)_2 with calcium lignosulfonate, an additive added with the water of hydration. They observed that the utilization of the modified sorbent increases with increasing additive content, reaches a maximum, and then decreases, as shown in Figure 1-3. The maximum occurred at an additive content of 1.5 dry weight percent, where the sorbent utilization was 20% higher than the unmodified hydroxide. Through size analysis of the modified particles, they showed that the superior performance is due to particle size reduction achieved primarily through de-agglomeration and secondarily through crystal size reduction. They suggested that above the optimal level of 1.5%, the large lignosulfonate molecule may block access of the SO_2 molecule to the reactive CaO sites, causing the relative utilization to decrease.

Subsequently, Kirchgessner and Jozewicz [1989] performed extensive studies of the changes in pore structure during sintering of CaO produced from Ca(OH)_2 modified with the 1% calcium lignosulfate. They first noted that modified Ca(OH)_2 calcined more quickly, and retained more of its original surface area and porosity than the conventional Ca(OH)_2 . With increasing time and temperature the difference between the surface area and pore structure between modified and original sorbents due to sintering became more pronounced. Their pore size measurements confirm that sintering involves pore filling, with the smallest pores filled first. This is reflected in the dramatic difference in pore volume with time and temperature for pore sizes less than 50 Å. They noted that the drastic changes in surface area and pore size are complete within 1.5 seconds at 700°C and 0.8 second at 1000°C.

Since sintering of CaO is known to be catalyzed by H_2O , differences in the rates of water loss for modified and unmodified Ca(OH)_2 may explain the differences in the rates of surface area loss and in pore structure. Their measurements show that water loss from modified hydroxide is indeed greater than the loss from unmodified hydroxide. However, the difference in water loss between the two types took place before 0.6 second, whereas the difference in surface areas do not become pronounced until after 0.6 second. Therefore, water loss does not fully explain the difference the structure of the two sorbents.

One of the mechanisms of sintering is the mobility of grain boundary. Because of the large size of the hydrated lignosulfate molecule, it is believed to be located at the grain boundaries and the surfaces of Ca(OH)_2 rather than within the crystal structure. In this structure, it reduces grain mobility, thus reducing the sintering effects. Thus, smaller particle size, increased extent of calcination, and lower sintering all contribute to the better performance of the hydrate sorbent modified with lignosulfate.

Metal Oxides. Slaughter et al. [1986] investigated the addition of chromium (Cr_2O_3), sodium (NaHCO_3), and iron (Fe_2O_3) compounds to the sorbent for injection at 2150°F and 2600°F. Unlike the previously cited studies, the promoters were

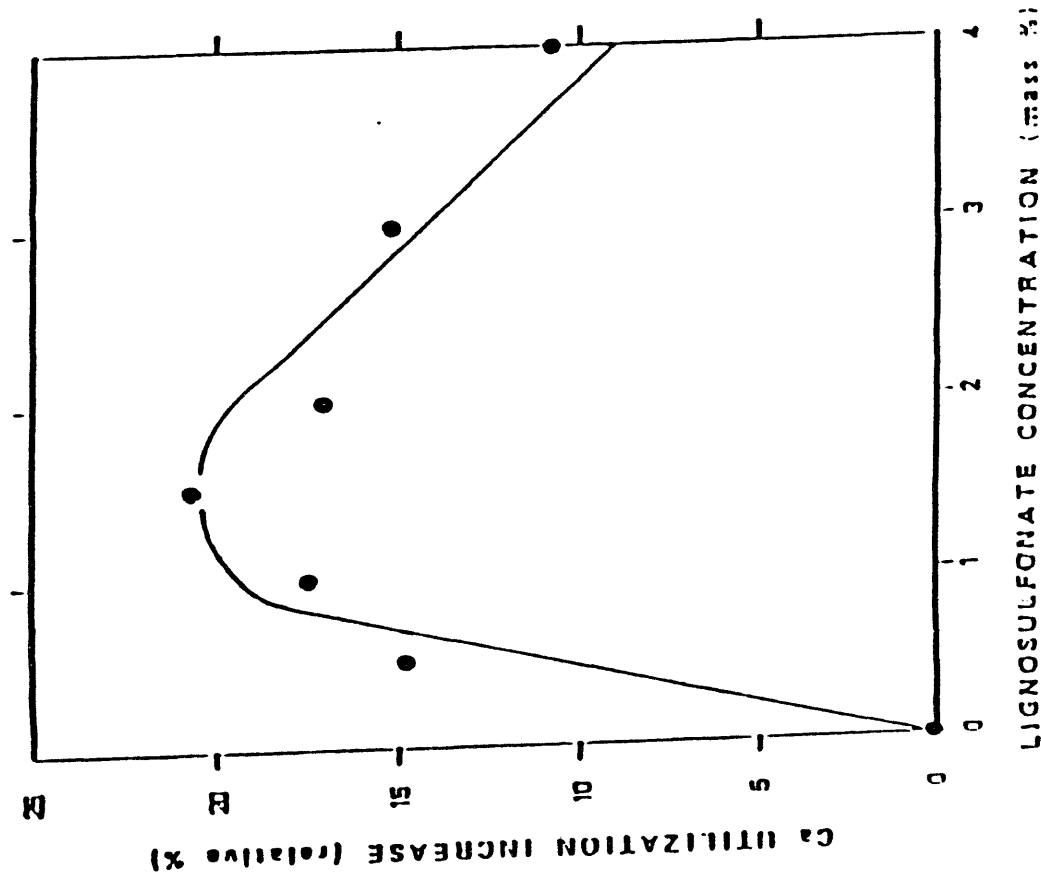


Figure 1-3. Effect of additive concentration on sorbent utilization [Kirchgessner and Lorrain, 1987].

injected in powder form along with the calcine instead of being added to the hydration water during the preparation of the hydrate. Both the chromium compound (18% SO₂ capture without, 39% SO₂ capture with at 2600°F) and the sodium compound (12% SO₂ capture without, 42% SO₂ capture with at 2600°F) were effective in promoting SO₂ capture by the calcine when added at a 15:1 calcium:promoter metal atomic ratio. The iron compound was not effective in promoting sulfur capture. Slaughter indicated that both chromium and sodium react with the calcium sorbent creating large cracks or pores, particle fragmentation and the formation of a liquid phase, all of which serve to increase SO₂ accessibility to the CaO sites. The presence of mineral matter ash in the flue gas stream acted to reduce the effectiveness of both promoters. The effectiveness of the sodium promoter showed a strong dependence on mineral ash concentration while the effectiveness of the chromium promoter showed only a weak dependence on mineral ash concentration.

This is an important area of research. Alternate additives should be considered, chosen on the basis of solid state chemistry. Systematic characterization of reactivity of similar sorbents through crystal structure analysis may explain the difference between them and lead to a better choice of sorbents.

1.4 Long-Term Goals

An experimental program will be carried out in order to (1) define the effects of "dry" hydration and slaking conditions on the properties of calcium-based sorbents, (2) determine how parent limestone properties and sorbent preparation techniques (calcination/hydration) interact to define SO₂ capture properties of calcium-based sorbents, (3) elucidate the mechanism(s) relating to the activity of various dry sorbent additives, and (4) identify promising new dry sorbent additives. Sorbent preparation techniques to be studied include, but are not limited to, atmospheric hydration, pressure hydration and hydration in the presence of additives. The prepared sorbents will be characterized in terms of BET surface area, porosity, pore size distribution, and surface morphology.

2.0 PROJECT YEAR #1 ACCOMPLISHMENTS

2.1 Acquisition of Limestone/Lime Samples

Several limestone and limestone products have been selected for characterization and evaluation as a part of this project. The limestones and limes selected include:

Ohio limestones:

Maxville limestone: Approximately 80:20 weight basis $\text{CaCO}_3/\text{MgCO}_3$ ratio. This limestone was used in the fixed-bed LEC work. This limestone is currently being used in the moving-bed LEC work.

Vanport limestone: Approximately 97:03 weight basis $\text{CaCO}_3/\text{MgCO}_3$ ratio. This limestone was used in the fixed-bed LEC work.

"Mid-Ohio" limestone, hydrate, quicklime: This quicklime is being used at the in-duct injection work taking place at the Ohio Power Company Muskingum River Station.

Bucyrus limestone, hydrate: Approximately 80:20 weight basis $\text{CaCO}_3/\text{MgCO}_3$ ratio. This limestone has been used in several FBC and CFBC projects. Bucyrus limestone has been used in TRW's slagging coal combustor. Samples of this limestone were not received during Project Year #1.

Carey limestone, hydrate, quicklime: Approximately 55:45 weight basis $\text{CaCO}_3/\text{MgCO}_3$ ratio. This limestone was used in the fixed-bed LEC work. Samples of this limestone were not received during Project Year #1.

Other limestones:

Mississippi limestone, hydrate, quicklime: This limestone and its lime products has been used in many national FGD tests (including LIMB and Coolside). This is not an Ohio limestone.

Samples of all but the Carey and Bucyrus limestones and limestone products were acquired during Project Year #1.

2.2 Characterization of Limestone/Lime Samples

All collected limestone and lime samples were characterized using the following tests:

- (a) BET surface area. Raw BET surface areas will be determined for all samples using a Quantisorb Jr. BET sorption apparatus. A BET surface area versus average particle size curve will be determined for each limestone sample in order to identify the individual contributions of its internal and external surface areas.
- (b) Total pore volume and pore size distribution. These analyses will be performed using a mercury porosimeter (Micromeritics AutoPore II 9220). Intrusion pressures of up to 60,000 psia will be used in determining the pore size distribution.
- (c) Chemical composition. Limestone samples will be subjected to elemental analysis in order to confirm their chemical composition. [This analysis was not completed during Project Year #2.]
- (d) Particle size analysis. Particle sizing will be performed on the hydrate products using a Horiba CAPA-300 centrifugal particle size analyzer. [This analysis was not completed during Project Year #2.]

2.3 Calcination Reactor

A bench-scale calcination reactor (Figure 2-1) was designed and constructed for use in this study. The heart of the calcination reactor is a 1700W Lindberg furnace. This furnace has the ability to reach and maintain temperatures as high as 1200°C.

2.4 Slaking Reactor

A bench-scale slaking reactor (Figure 2-2) has been designed and constructed for use in this study. This reactor system is primarily comprised of a 1000 ml jacketed reaction flask, a K-Tron solids feeder, and a Brookfield EX-100 constant temperature circulator. This slaking reactor can be operated in any one of three modes: (1) batch, both in water and lime, (2) semi-batch, batch in water but with a continuous lime flow to the reactor, and (3) continuous is both water flow and lime flow. The slaking reactor can be operated in both constant temperature and variable temperature modes.

- 1. Air Cylinder
- 2. Air in
- 3. Calcium Carbonate
- 4. Sample Container
- 5. Vent
- 6. Temperature Recorder and Controller
- 7. Furnace

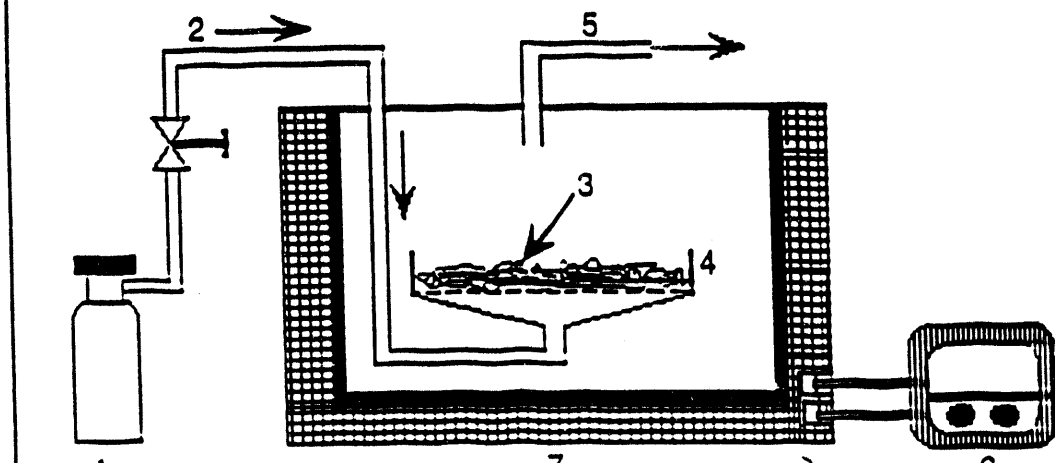


Figure 2-1. Schematic of bench-scale calcination reactor.

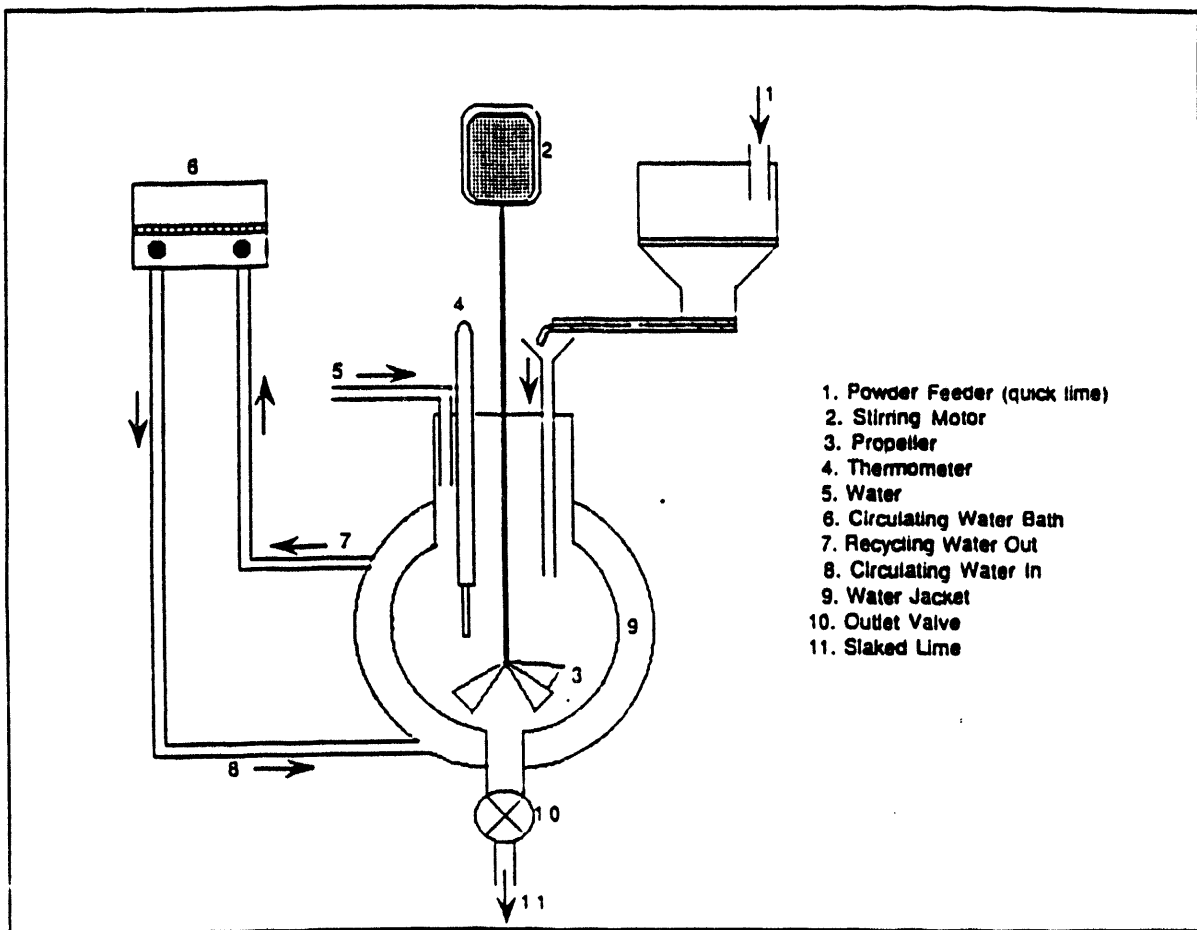


Figure 2-2. Schematic of bench-scale slaking reactor.

2.5 Calcination Reactions

Calcines from each of the limestones received during Project Year #1 were prepared using the experimental setup illustrated in Figure 2-1. In each calcination test, approximately 250 grams of powdered limestone (either -70M or -80 + 100M) was calcined at 950°C for six hours. A steady flow of air (25 cc/s) was used as a sweep gas during the calcination reaction.

2.6 Slaking Reactions

Shakedown and test runs were performed in the batch mode using a 500 ml slaking reactor. Reagent grade calcium oxide [Fisher C114-3, lot no. 896449] was used as the feed to the shakedown runs.

Project Year #2 hydrations were performed in a semi-batch mode using a 500 ml slaking reactor. The entire charge of water (500 ml) was added to the reactor vessel at the beginning of each hydration run. Calcine was added to the slaking water at a constant rate of 4 grams per minute for a period of 20 minutes. Calcine/water contacting was continued for a period of 10 minutes after the calcine addition had ceased. This procedure resulted in a final 20:1 H₂O:calcine mole ratio in the reactor. The slaking reactor was held at a temperature of 70 - 75°C for the duration of the slaking process.

3.0 PROJECT YEAR #2 ACCOMPLISHMENTS

3.1 Sorbent Preparation

Duplicate limestone characterizations (BET and mercury porosimeter) of the limestones collected during Project Year #1 and the two additional limestones (Carey and Bucyrus) collected during Project Year #2 have been completed. The collected materials have been characterized in -4+5 mesh, -70 mesh, and -80+100 mesh size fractions with the -80+100 mesh size fraction being selected for calcination and subsequent hydration testing.

Figure 3-1 shows a comparison of the BET surface areas measured for the six different feed limestones while Figure 3-2 shows a comparison of the BET surface areas of the calcines produced from the selected -80+100 mesh limestones. Only small changes in BET surface areas were observed after calcination. If any trend is observed, it is that the BET surface area of the calcitic and magnesia limestones decreases after calcination whereas the BET surface areas of the dolomitic limestones (Carey and Bucyrus) increased after calcination. It has not yet been determined whether or not these small changes in BET surface area are statistically significant.

Figure 3-1. Comparison of BET surface areas of -80+100M limestone samples.

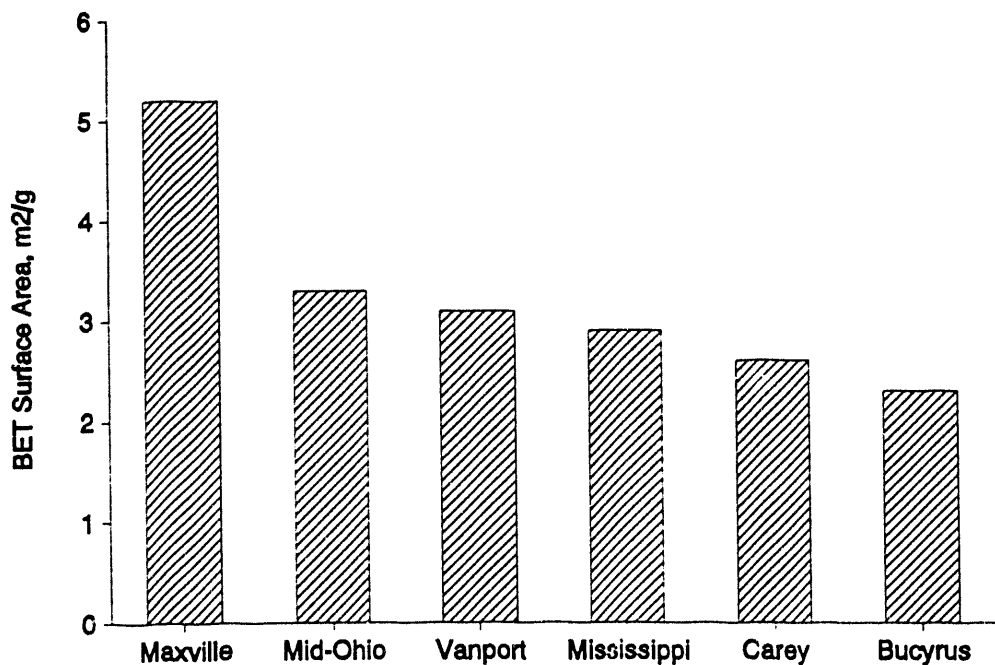


Figure 3-3 shows a comparison of the BET surface areas of the hydrates produced from the calcines made from the -80+100 mesh parent limestones. In all cases, the surface areas of the hydration products were significantly larger (by a factor of 5 to 10) than those of the parent limestones. No relationship of hydrate surface area to the surface area of the parent limestone is evident from data taken to date.

Figure 3-2. Comparison of BET surface areas of -80+100M limestone samples and their calcines.

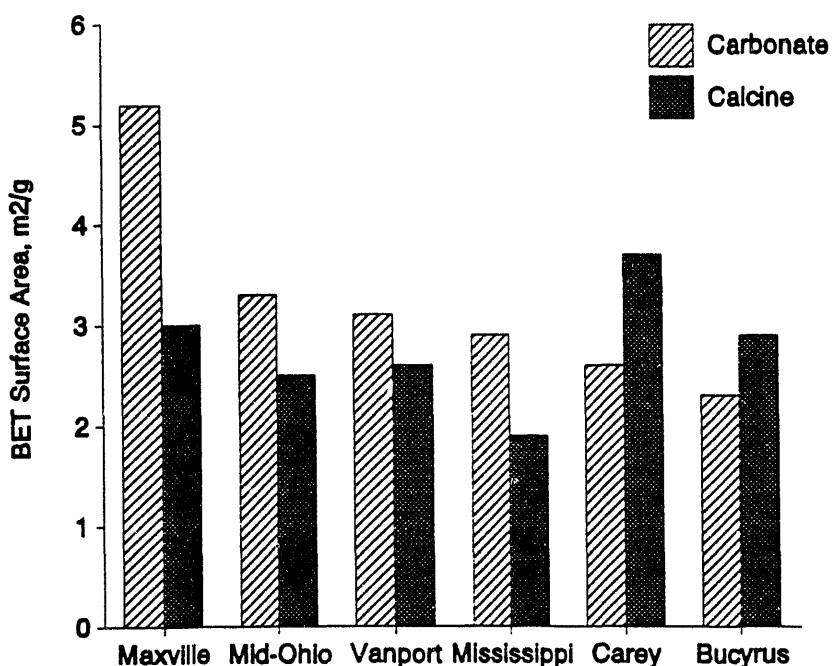
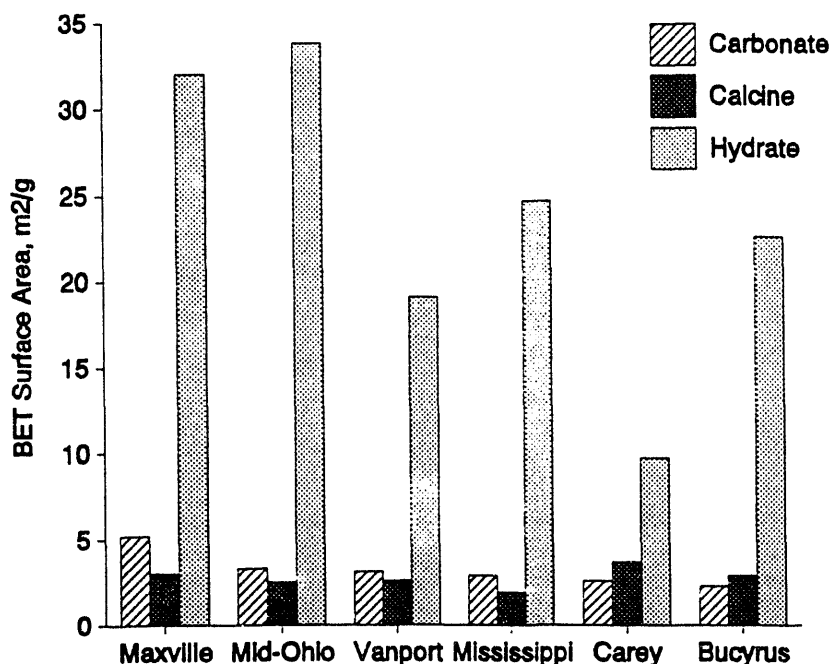


Figure 3-3. Comparison of BET surface areas of -80+100M limestone samples, their calcines, and their hydrates.



3.2 Chemical Additives

We have reviewed the additive literature and have decided to test the hypothesis set forth by Gooch et al. [1986] that additives that increase the water solubility of $\text{CaO}/\text{Ca}(\text{OH})_2$ also serve to increase the specific surface areas of slaked products made using the additive.

Sucrose, calcium chloride, and calcium nitrate were selected as the solubility enhancement additives for use in the slaking testing. Solubility data for raw $\text{CaO}/\text{Ca}(\text{OH})_2$ in aqueous solutions of sucrose, CaCl_2 , and $\text{Ca}(\text{NO}_3)_2$ are presented in Figure 3-4. Treatments with each additive were made at two levels of enhanced $\text{CaO}/\text{Ca}(\text{OH})_2$ solubility (Table 3-1). If surface area enhancement is the same for each additive at each level of treatment, a preliminary conclusion could be reached that the hypothesis is proven and that $\text{CaO}/\text{Ca}(\text{OH})_2$ solubility in the slaking water is the primary mechanism of surface area enhancement for these additives and that the specific additive used to achieve the solubility enhancement is not particularly important.

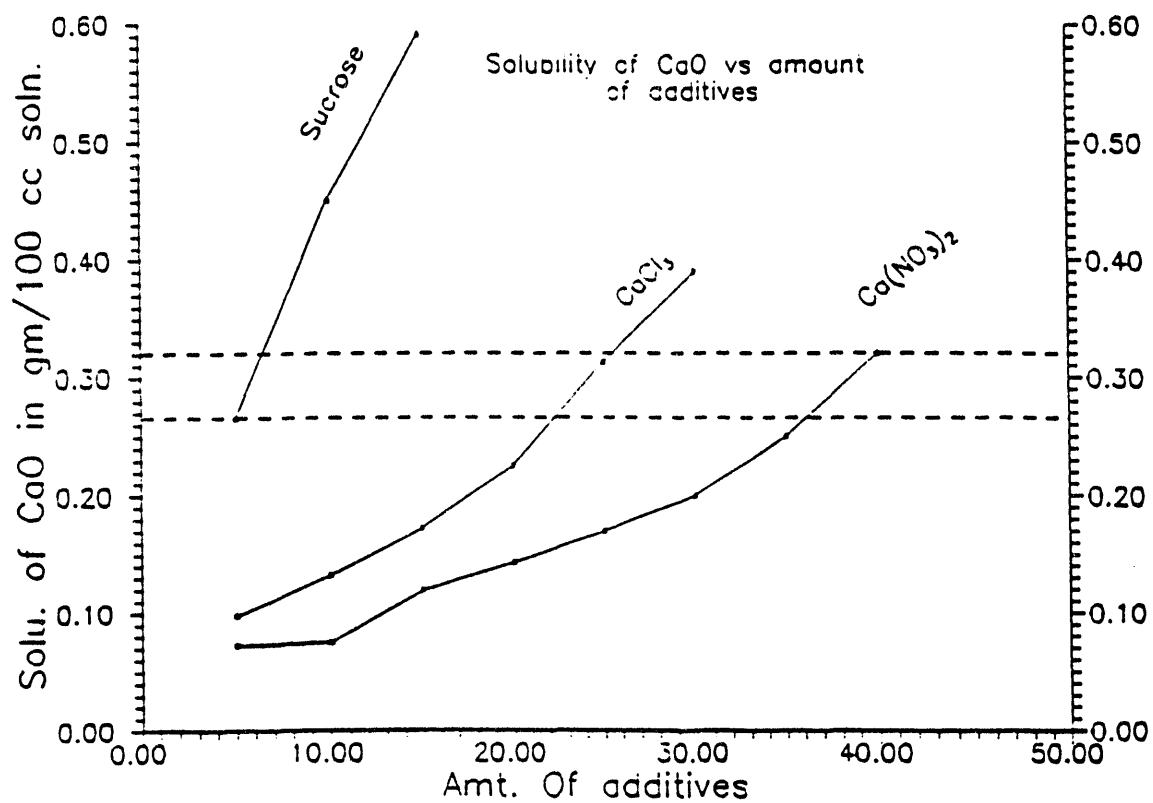
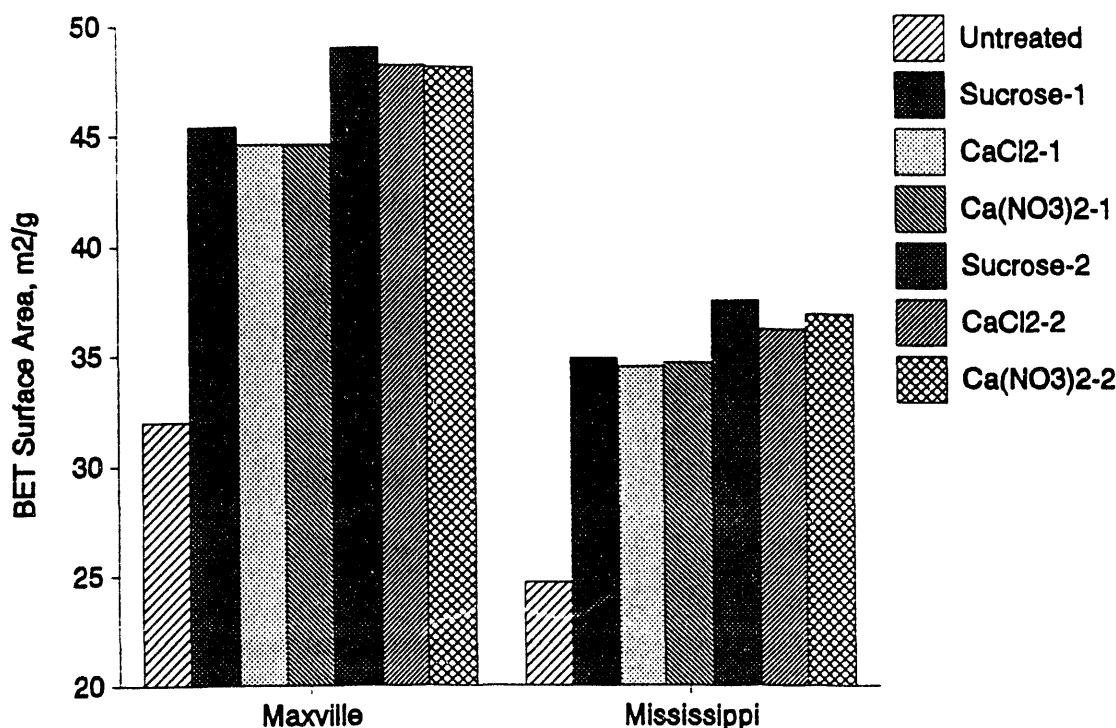


Figure 3-4. CaO solubility versus additive concentration at 70°C.

Slaking treatments of Mississippi and Maxville calcines have been performed using sucrose, CaCl_2 , and $\text{Ca}(\text{NO}_3)_2$ additives. The preliminary results of these additive tests are presented in Figure 3-5. The results obtained to date would seem to indicate that a particular degree of $\text{CaO}/\text{Ca}(\text{OH})_2$ solubility in slaking water results in a particular degree of hydrate surface area enhancement independent of the solubility enhancement additive used (as long, at least, as the additive is either sucrose, CaCl_2 , or $\text{Ca}(\text{NO}_3)_2$).

Figure 3-5. Effect of solubility additives on hydrate BET surface area.



For the low level of solubility enhancement (+267%), both Maxville and Mississippi hydrates show about a 40% increase in surface area as measured by BET analysis. The high level of solubility enhancement (+341%) yields about a 50% increase in BET surface area for both hydrates.

Table 3-7. Treatment Levels - Solubility/Slaking Tests.

Additive:

Treatment Level "A": 4.9 g/ 100 cc solution

Treatment Level "B": 6.7 g/ 100 cc solution

Additive:

Treatment Level "A": 22.4 g/ 100 cc solution

Treatment Level "B": 25.6 g/ 100 cc solution

Additive:

Treatment Level "A": 36.3 g/ 100 cc solution

Treatment Level "B": 40.0 g/ 100 cc solution

Treatment Level "A" corresponds to roughly a 267% increase in $\text{CaO}/\text{Ca}(\text{OH})_2$ solubility in the slaking water solution.

Treatment Level "B" corresponds to roughly a 341% increase in $\text{CaO}/\text{Ca}(\text{OH})_2$ solubility in the slaking water solution.

4.0 PROJECT YEAR #3 PLANS

The following items are included in the third year research plan for this project.

- Task 1. Interact with consortium project 1.5 as regards spray drying process results obtained during second and third year research using sodium-containing slurry/slaking additives. Identify the factor or factors that contribute to the SO₂ capture enhancement and synergism demonstrated in literature (Coolside) results. Chemical effects to be evaluated will include (but not be limited to): water vapor pressure depression, pH effects, and Ca(OH)₂ and SO₂ solubility enhancement.
- Task 2. Interact with consortium project 1.1 as regards additive effects and solid-state chemistry in high-temperature SO₂ capture. Slaked limes or calcines which show potential for high utilization or reactivity as indicated by results from the surface morphology analyses or low temperature reaction studies will be evaluated in the high-temperature entrained flow reactor system.
- Task 3. Begin the experimental evaluation of the function(s) of sorbent "inert" contents in enhancing the degree of sorbent utilization. Calcines and slaked limes prepared using a variety of limestone will be reviewed using scanning electron microscopy (SEM) analysis in an attempt to identify unusual surface features. These features will then be examined for elemental composition (Ca, Mg, Si, etc.) using energy dispersive x-ray analysis (EDX) in an attempt to correlate inert content with morphology.

5.0 PROJECT YEAR #3 ACCOMPLISHMENTS

5.1 Effect of Chemical Additives on Duct Injection/ Spray Drying Performance

5.1.1 Introduction/ General Description

The primary objective of this project task was the identification of the factor or factors that contribute to the SO₂ capture enhancement and synergism due to additive addition in low temperature (< 350°F) spray drying processes. The sorbent injection strategies included are: (1) injection of slurry consisting of the sorbent Ca(OH)₂ directly in to the duct, and (2) injection of dry sorbent followed by injection of water spray (Coolside process).

Additives are generally added to calcium-based sorbents in order to enhance SO₂ capture reactivity. The reasons for this increased SO₂ capture performance can be attributed to one of, or a combination of, the following chemical effects: (1) water vapor pressure depression - the addition of a nonvolatile solute (additive) lowers the vapor pressure of water and, consequently, the evaporation rate. This increases the reaction time between the wetted sorbent and SO₂, and thus enhances the SO₂ capture, (2) pH effects - the additive (base) would change the pH of the aqueous phase and contribute to enhanced SO₂ (acid) capture, and (3) Ca(OH)₂ and SO₂ solubility enhancements. This list is not meant to be exhaustive.

The in-duct SO₂ capture model formulated by the Energy and Environmental Research Corporation (EER) (1989) was selected as the basic vehicle for determining the additive effects in spray drying processes as each effect can be evaluated separately (although this does not imply that the effects are independent). Amongst the various models available for duct injection spray drying processes, the EER model was chosen because it is a comprehensive model which accounts for the following important processes occurring concurrently with evaporation:

- (1) Diffusion of SO₂ from the bulk gas phase to the droplet surface.
- (2) Absorption of SO₂ at the droplet surface.
- (3) Dissolution of SO₂ to form H₂SO₃ and ionization of H₂SO₃ to HSO₃⁻ and SO₃²⁻.
- (4) Diffusion of these liquid-phase sulfur species inward.
- (5) Dissolution of the Ca(OH)₂ particle at the sorbent surface.
- (6) Diffusion of Ca(OH)₂ from the sorbent surface to the bulk liquid phase.

The model also considers product recycle, reaction of sorbent (wet agglomerate) with SO₂ after evaporation has ceased. A sub-model which considers the scavenging of sorbent particles is included for the Coolside type process. The EER model does not, however, have the ability to deal with the effects of varying concentrations and types

of additives in its present form. One of the major tasks of this project is altering the EER model to better accommodate the additive effects.

The low temperature, dry capture model of Jozewicz and Rochelle (1984) assumed that the rate of SO_2 capture is controlled by external SO_2 mass transfer. Karlsson and Klingspor (1987) developed two models: one assumed that external SO_2 mass transfer is controlling (high slurry concentrations) and the other assumed that lime dissolution rate is rate-limiting. The model provided by Damle and Sparks (1986) assumed that liquid-phase mass transfer is fast, and that the slurry droplet could be viewed as a well-mixed reactor. Kinzey and Harriott (1986), on the contrary, assumed that sorbent dissolution is fast and considered both of external and liquid phase mass transfer of sulfur species. The diffusion of calcium species away from the droplet center has not been considered.

The EER Slurry droplet model (which is of prime interest to us) handles both the slurry injection strategy and the scavenging injection strategy. The model assumes that sorbent particles are initially uniformly distributed throughout the droplet and that they do not circulate within the droplet. As water evaporates from the droplet, the droplet surface recedes until it encounters particles which were initially near the droplet surface. As evaporation continues, the surface particles are pushed inward and an accumulation of sorbent particles at the droplet surface occurs (Figure 5-1). A particle concentration gradient is created between the particles crowded together at the surface and those particles within the droplet which are still at the initial particle concentration.

Due to this physical model of sorbent particle concentration, the instantaneous liquid-phase reaction between the sulfur and calcium species can occur at two types of reaction fronts within the slurry droplet. As the liquid-phase sulfur species diffuse into the droplet they pass individual sorbent particles which are simultaneously diffusing calcium outward. According to film theory, calcium which has dissolved at the surface of a sorbent particle will diffuse outward through a film whose thickness can be calculated. A calcium/sulfur reaction front will therefore be present at the outer edge of this film. The sulfur species in the surrounding bulk liquid phase will also diffuse inward. The distance that calcium must diffuse outward will therefore be less than that calculated by film theory and, since the rate of sulfur diffusion inward is dependent on the bulk liquid-phase concentration of the sulfur species, the distance of the reaction front from the surface of the sorbent particle will vary depending on the local concentration of the liquid-phase sulfur species. The local concentration will, of course, be a function of the spacial location within the slurry droplet.

A total of nine different equations governing droplet deceleration, droplet temperature, droplet evaporation, gas temperature, particle scavenging, particle diffusion within the droplet, liquid-phase SO_2 diffusion of calcium, and sorbent utilization must be solved simultaneously by the EER model. The major assumptions

5-3

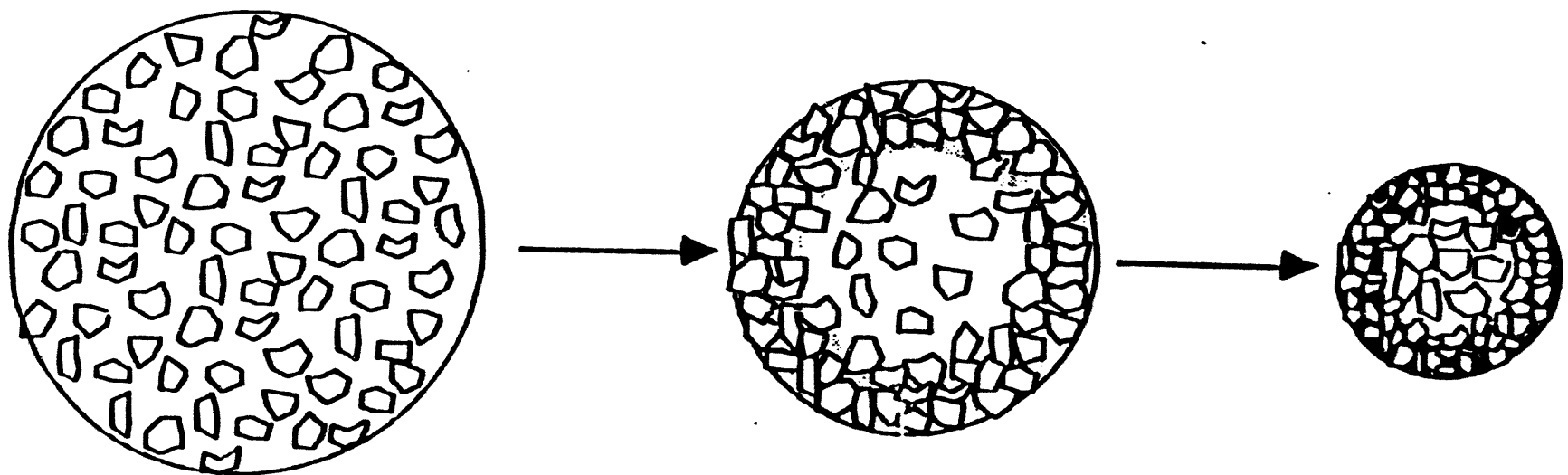


Figure 5-1. Illustration of the accumulation of sorbent and product at the droplet surface as evaporation shrinks the surface (EER, 1989).

of the EER model listed by its authors Newton et al. (1990) are as follows:

- (1) Liquid phase ionic reaction between dissolved calcium and sulfur species is instantaneous.
- (2) Water and sorbent particles do not circulate within the droplet.
- (3) Calcium sulfite is considered insoluble and precipitates as free standing crystals.
- (4) The heats of reaction and sorbent dissolution are small and can be ignored.
- (5) Thermal gradients within the droplet can be ignored.
- (6) The droplets and sorbent particles are assumed to be spherical.

The EER model which considers simultaneous humidification and SO_2 capture processes is a one-dimensional model. However, recent modelling efforts by Oberjohn et al.(1993) have indicated that a one-dimensional model is adequate for predicting SO_2 capture and droplet evaporation. The original EER model has set the lime dissolution rate constant to be rather high, implying that the resistance due to lime dissolution is negligible. However, as part of modifying the code (model) to include the effects of additives, a reasonable value has been set for the dissolution rate constant. The modified EER code (including the correlations listed below), as well as example input and output files, can be found in the Appendix.

The additives that have been tested for enhancement in sulfur-dioxide capture in spray drying processes can be classified broadly into the following categories: (1) cosorptive additives, namely, NaOH , Na_2SO_3 , Na_2CO_3 , NaHCO_3 , NaCl , NaNO_3 (sodium additives), and (2) non-cosorptive additives, namely, CaCl_2 , FeCl_3 , KCl , MgCl_2 (chloride additives). Classification of additives can be also be done in terms of basicity, chemical nature (organic or inorganic), deliquescence, etc.

Sodium additives have been considered as one of the most promising additives in duct injection processes by many researchers. Yoon et al. (1986), while conducting laboratory-scale studies on Coolside process (duct injection strategy with the lime added prior to humidification) observed that there was a relative increase of 30-114% in saturated calcium utilization, when the additive was added to lime during hydration and a 30-90% increase in saturated calcium utilization, when the additive was added to lime after hydration. NaCl was the most promising additive followed by NaNO_3 , Na_2CO_3 , Na_2SO_3 , and NaOH . NaOH and Na_2CO_3 acted as co-sorbents and the other sodium additives were converted to NaOH by reacting with hydrated lime during the process of promotion. The $\text{Na}^+/\text{Ca}^{++}$ molar ratio was between 0.05-0.2 for all the additive tests carried out in the above study. In the bench scale studies carried out by Chu and Rochelle (1989) there was a relative enhancement of 40% in SO_2 removal as compared to the base case, when 0.08M NaOH was added to the system (temp. in the system was 66°C). Although Na_2SO_3 contains twice as much sodium as NaOH contains, the results obtained with it were just about the same.

Probably, some SO_2 removal can be attributed to NaOH itself. The sorbent evaluation studies conducted by Stouffer et al.(1989) as part of the pilot plant demonstration in support of the Coolside process, clearly showed the important role played by NaOH in the enhancement of SO_2 removal. Aqueous NaOH was added to the humidification water at $\text{Na}^+/\text{Ca}^{++}$ mole ratios up to 0.2. For tests conducted with Mississippi hydrated lime with a Ca/S ratio of 2, SO_2 inlet ppm of 1620, gas inlet temperature of 300°F and an approach to saturation of 25°F, a 90% removal of SO_2 was obtained with a Na/Ca molar ratio of 0.2. The SO_2 removal without any NaOH , for the same conditions was 60%. The sorbent utilization studies conducted using a mini-pilot spray dryer by Keener et al.(1992) also illustrated the beneficial effect of sodium additives in SO_2 removal. The additive which effected the maximum increase in SO_2 removal over the base case was NaOH (16% increase), followed by NaHCO_3 (12%), NaCl (11%) and CaCl_2 (4%), for an additive concentration of 300 mg/l-slurry. The tests were performed with an approach to saturation of 28°F, Ca/S ratio of 1.0, SO_2 inlet ppm of 2500 and gas inlet temperature of 300°F.

Yoon et al.(1986) found that chloride additives (CaCl_2 , KCl , FeCl_3) were as effective as the sodium additives. Calcium chloride, when added (0.1 mole/mole $\text{Ca}(\text{OH})_2$) during the hydration of lime, increased the saturated calcium utilization by around 100%. The second best result was obtained with KCl (77% increase), followed by FeCl_3 (45%) and MgCl_2 (14%). Organic additives (glycerin, adipic acid, sugar) tested in the above study showed no significant positive effect. The effectiveness of using a hygroscopic salt like CaCl_2 as an additive was highlighted by Brown et al.(1990). In the pilot-scale tests, SO_2 removal increased from 40%(base case) to 72% when recycle was used and CaCl_2 was added(3.4%)to the humidification water. The base conditions were Ca/S ratio of 2.0, 30°F approach to adiabatic saturation, no recycle and the lime was injected upstream of humidification. With recycle alone (i.e., additive not added) the SO_2 removal was 54%. However when CaCl_2 alone was added to water(without any recycle) ,there was no significant increase in SO_2 removal performance.

In light of the above literature results, four typical additives were chosen for this study. Among the sodium additives, NaOH (cosorbent) is a strong base, Na_2CO_3 (has twice the amount of sodium compared to NaOH) is a weak base and NaCl is a neutral salt. CaCl_2 is highly hygroscopic and is a chlorine additive.

5.1.2 Chemical Effects of Additives

5.1.2.1 Vapor Pressure Depression. The addition of a non-volatile solute (additive) lowers the water vapor pressure and, consequently the evaporation rate. This increases the drying time of the droplet and thus, enhances the SO_2 capture. The dissolved solids (additives) cause the evaporation to stop before the droplet dries to completion. As a result, moisture is retained in the pores of the solid agglomerate. This core of moisture is called the equilibrium moisture content of the solid. The core diameter or the moisture content is solely determined by the concentration of the dissolved salts, the temperature and the humidity of the gas. Increasing the equilibrium moisture content increases the capture of sulfur dioxide during the post-evaporation stage of the process. According to Kinzey (1988), in typical spray drying processes, though the equilibrium moisture content represents less than 1% of the original water in the droplet, about 50% of the solid in the agglomerate remains wet.

For this purpose, the vapor pressure lowering data was obtained from the literature (Perry, 1973) for the selected additives (CaCl_2 , NaCl , Na_2CO_3 , NaOH) and the data was fit to the following (Antoine) equation:

$$P_w = a * \exp\left(A - \frac{B}{T+C}\right) \quad (5-1)$$

where P_w is the vapor pressure of water, a is an activity coefficient, T is the temperature, and A, B, C are Antoine constants. a , the activity coefficient, is represented by a polynomial of the form,

$$a = a_0 + a_1 * X_m + a_2 * X_m^2 + a_3 * X_m^3 + a_4 * X_m^4 \quad (5-2)$$

where a_0, a_1, a_2, a_3 and a_4 are fitting constants for the polynomial and X_m is the weight fraction of additive in solution. The values of the above constants for the four additives mentioned is given in Table 5-1.

Table 5-1. Regression coefficients the Antoine equation.

Additive	a_0	a_1	a_2	a_3	a_4	A	B	C
CaCl_2	0.9899	-8.68E-3	-3.68E-2	4.624E-3	-1.67E-4	18.3036	3816.44	46.13
NaCl	0.9899	-3.71E-2	1.416E-3	-1.06E-3	2.50E-5	18.5208	3935.38	41.37
Na_2CO_3	0.9899	-3.65E-2	-5.74E-3	3.09E-3	-1.05E-3	17.9918	3623.98	53.38
NaOH	0.9899	-2.33E-2	-3.11E-3	1.66E-4	-2.0E-6	18.3028	3722.23	53.44

There is an enhancement of around 3 to 7 percentage points in SO_2 capture due to the vapor pressure depression effect alone. Several sets of simulation results are represented graphically in Figure 5-2.

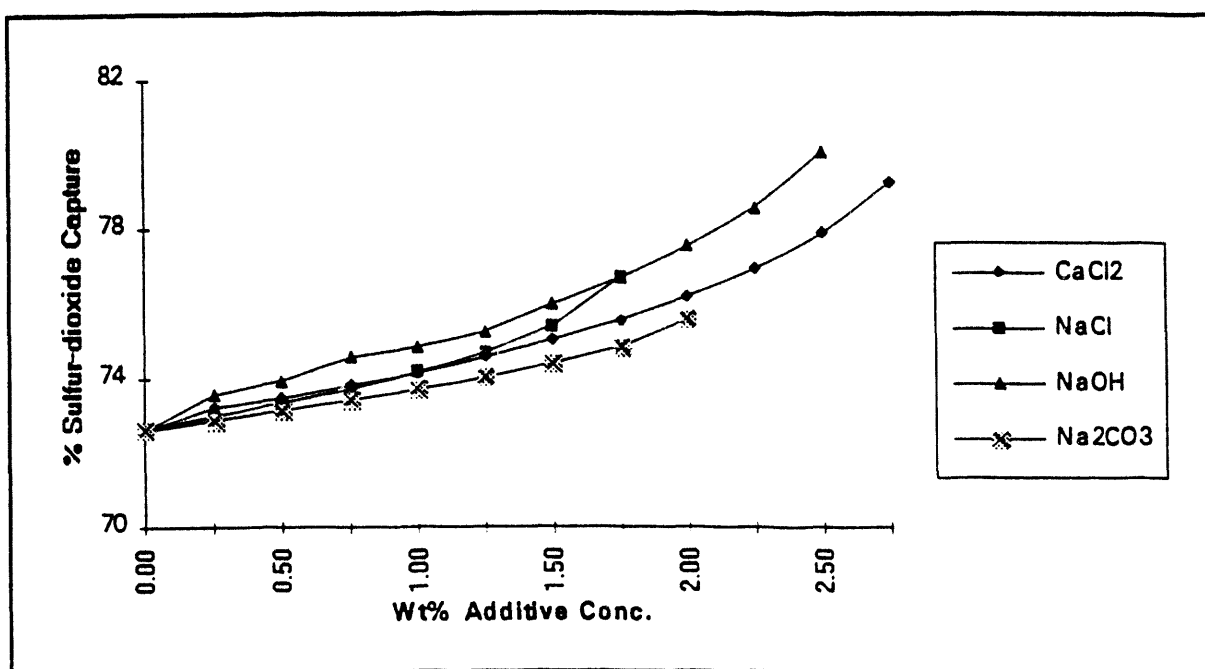


Figure 5-2. SO_2 capture efficiency versus additive concentration (vapor pressure depression effect).

5.1.2.2 $\text{Ca}(\text{OH})_2$ Solubility Enhancement. With the addition of the additive, the solubility of lime is found to increase for most of the cases studied here (the exception being NaOH). An increase in the solubility of lime enhances the diffusion of the calcium species and thus, increases calcium utilization and SO_2 capture. In the case of NaOH, the solubility of lime decreases due to the common-ion effect. The solubility data for ternary mixtures of $\text{Ca}(\text{OH})_2$ -water-additive (eg., CaCl_2) have

been obtained and as the solubility of $\text{Ca}(\text{OH})_2$ was found to be linear function of the concentration of the additive (for an additive concentration of within 10 wt%, our area of focus), the data was fit to the following equation.

$$\text{CLime} = \frac{A}{T} + BX + C \quad (5-3)$$

where CLime is the concentration of $\text{Ca}(\text{OH})_2$, X is the weight percent of the additive, and T is the temperature. A , B , and C are fitting constants. The value of the fitting constants for three of the additives studied are given in Table 5-2.

Table 5-2. Regression coefficients Equation 5-3.

Additive	A	B	C
CaCl_2	16550	1.13556	35.62
* NaOH	16550	-17.12	35.62
NaCl	16550	0.45105	35.62

The value for the dissolution rate at the sorbent surface was set arbitrarily high in the original EER model. This model deficiency needs to be corrected prior to the evaluation of effect of $\text{Ca}(\text{OH})_2$ solubility enhancement/reduction on the sulfur dioxide capture. The importance of lime dissolution rate is dealt with in the next section.

5.1.2.3 Dissolution Rate of Lime. The EER model assumes that there is no resistance to the dissolution of $\text{Ca}(\text{OH})_2$, in other words, that the dissolution of lime does not affect the rate of sulfur dioxide capture. Hence, the dissolution rate constant for lime has been set unrealistically high in the original EER model. The concentration of lime at the sorbent particle surface (C_L^*) is related to the equilibrium concentration of lime ($C_{L,e}$) by the following equation (as given in the EER model):

$$C_L^* = \frac{C_{L,e}}{1 + \frac{D_L}{\sigma \delta K_d}} \quad (5-4)$$

where D_L is the diffusivity of lime in m^2/s , δ is the film thickness in meters (when diffusion of liquid-phase sulfur species to the particle is considered), σ is the

roughness factor, and K_d is the dissolution rate constant of lime. The original model sets K_d equal to $1.0 \text{ m}^3/\text{m}^2\cdot\text{s}$ (i.e. $C_L^* = C_{L,e}$). Typical values of D_L , σ are $1.67E-9 \text{ m}^2/\text{s}$ (at a temperature of 310K) and 20, respectively. The value of δ is in the order of $10^{-7}\text{-}10^{-8}\text{m}$ (a typical droplet diameter is $50 \mu\text{m}$).

The dissolution times for an isolated $\text{Ca}(\text{OH})_2$ particle, as given by Kinzey (1988) are tabulated as follows:

Table 5-3. Dissolution times for $\text{Ca}(\text{OH})_2$ particle.

Particle size, (μm)	1	2	3	4	5
Dissolution time, (sec)	0.08	0.33	0.75	1.33	2.08

Although the residence time of a droplet is typically 2.5 - 5 seconds (in the model parameters), its drying time is usually much less. For droplets around $50\mu\text{m}$ in size, the drying time is generally between 0.3-1.2 seconds. Thus, dissolution rate becomes important for larger sorbent particles ($4\text{-}5\mu\text{m}$).

A sensitivity study was performed on the dissolution rate constant of lime to give an insight into its role in the SO_2 capture process. The upper and lower limits for the dissolution rate constant were fixed at 1.0 and $10^{-4} \text{ m}^3/\text{m}^2\cdot\text{s}$, respectively. If it is assumed that C_L^* is 80% of $C_{L,e}$ in Equation 5-1, then a typical value of K_d (dissolution rate constant) would be $3 \times 10^{-4} \text{ m}^3/\text{m}^2\cdot\text{s}$. Furthermore, typical values of the lime dissolution rate constant obtained by Ritchie et al.(1991) by using rotating discs prepared from calcium hydroxide were $10^{-5}\text{-}10^{-6} \text{ m}^3/\text{m}^2\cdot\text{s}$. However, for powdered samples, the dissolution rate constant is expected to have a two order of magnitude higher value. It can be seen from Figure 5-3 that there is a steep increase in sulfur dioxide removal until a K_d value of around $10^{-2} \text{ m}^3/\text{m}^2\cdot\text{s}$ is reached. There is not a considerable increase in SO_2 removal after this point. The dissolution rate is expected to play a major role in the Coolside processes where the sorbent is injected upstream of water spray, as the sorbent does not have a large mixing time with water before the drying of the droplet. In typical spray drying processes, the dissolution rate constant would be in the order of $10^{-2}\text{-}10^{-4} \text{ m}^3/\text{m}^2\cdot\text{s}$. The presence of CO_2 in the flue gas might reduce the dissolution rate of lime as CO_2 may react with the sorbent particles to form a layer of relatively insoluble calcium carbonate. The value for the dissolution rate constant has been set at $3 \times 10^{-4} \text{ m}^3/\text{m}^2\cdot\text{s}$ (point at which the slope changes in Figure 5-3) for all of the model simulations unless otherwise mentioned.

With the addition of additives, the dissolution rate constant would increase or decrease depending on the type of additive used. In the case of NaOH , there is a considerable decrease in the dissolution rate. Data was taken from the literature

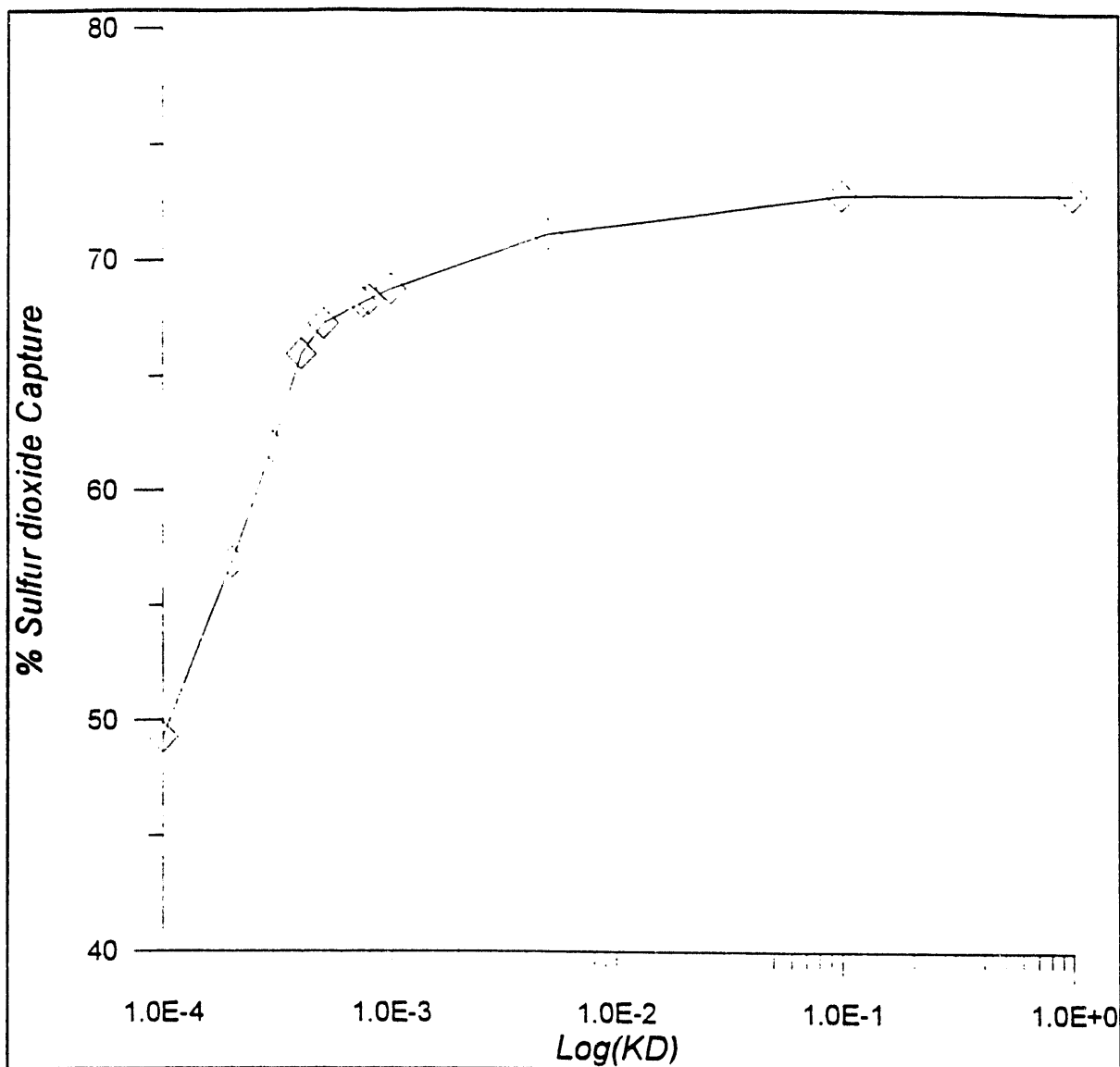


Figure 5-3. Percentage sulfur dioxide capture versus dissolution rate constant for lime (slurry injection case).

(Ritchie et al., 1991) for the reduction in the dissolution rate constant with the addition of NaOH and was regressed to obtain the following equation:

$$K_{d(\text{NaOH})} = K_d \left(\frac{x^{-0.925}}{917.37} \right) \quad (5-5)$$

where K_d is the dissolution rate constant of lime in $\text{m}^3/\text{m}^2 \cdot \text{s}$ and x is the weight percent of NaOH in water. Equation 5-5 is good only for x values between 0.08 to 5%. Figure 5-4 shows the reduction in the lime dissolution rate constant as a function of NaOH concentration.

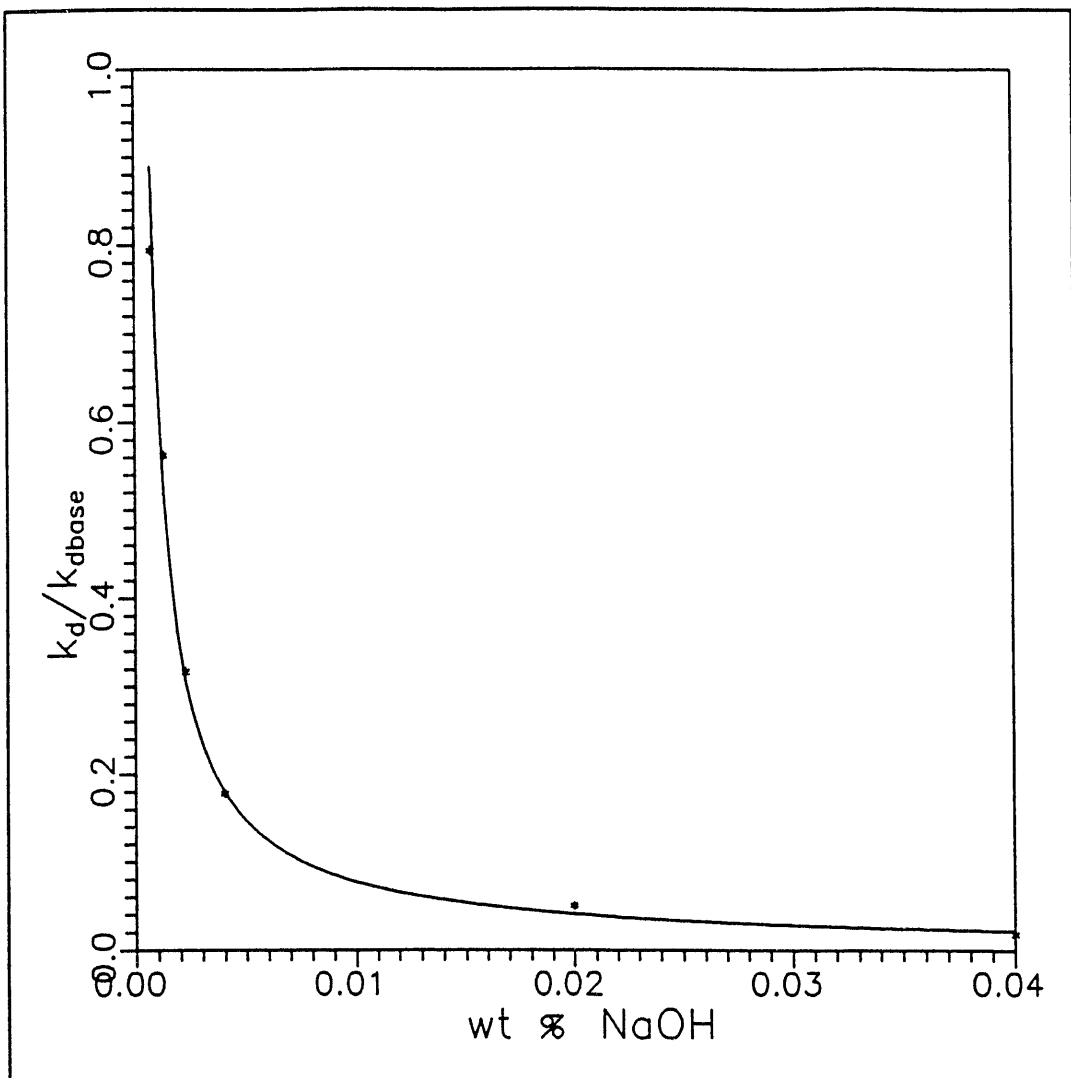


Figure 5-4. Reduction in dissolution rate constant as a function of NaOH concentration.

The effect of changes in the equilibrium solubility of lime on SO_2 removal efficiency at various dissolution rate constants is presented here. It can be seen from Figure 5-5 that with an increase in solubility of lime, the enhancement in sulfur-dioxide removal is much more for lower dissolution rates of lime. 'Clime' in Figure 5-5 refers to the equilibrium solubility of lime in water. Thus, for baseline conditions, the sulfur-dioxide removal would be around 60% (as compared to 72% with K_d being equal to $1.0 \text{ m}^3/\text{m}^2 \cdot \text{s}$).

The common process parameters in all the above simulations were as follows: inlet SO_2 (ppm) = 1500, no sorbent recycle, Ca/S ratio = 2.0, approach to saturation = 23°F , and mean droplet diameter = $50 \mu\text{m}$, sorbent particle diameter = $4 \mu\text{m}$ and

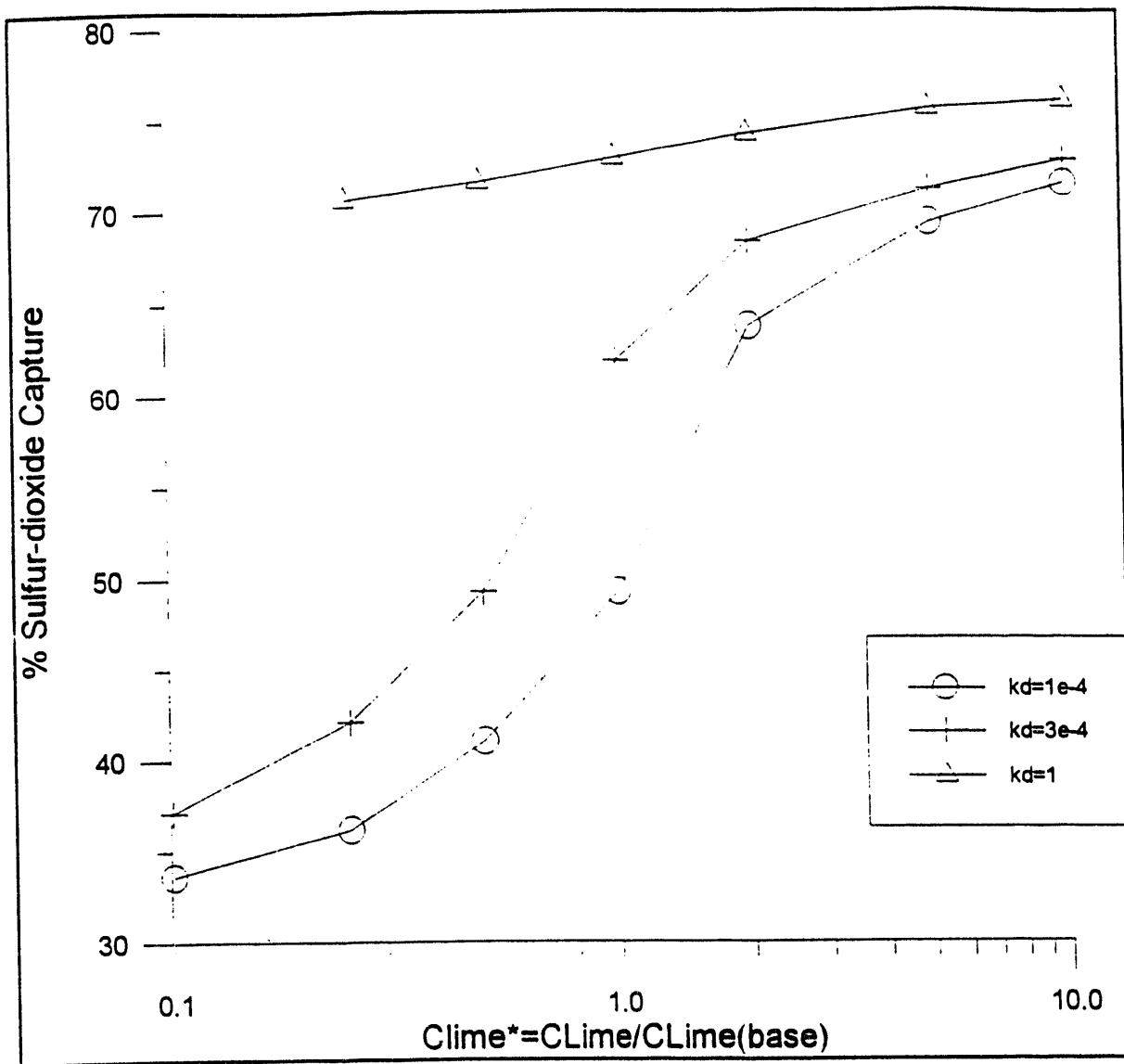


Figure 5-5. Percentage sulfur dioxide capture versus equilibrium solubility of lime at various lime dissolution rates constants.

residence time = 2.5 seconds. It should be noted that the value of dissolution rate constant in Figure 5-2 (vapor pressure depression effect) is $1.0 \text{ m}^3/\text{m}^2 \cdot \text{s}$.

5.1.2.4 pH Effects. The pH of the droplet decreases as SO_2 diffuses to sites near the $\text{Ca}(\text{OH})_2$ particles. This enhances the lime dissolution rate. On the other hand, the addition of NaOH into the system increases the pH and thus decreases the dissolution rate of lime. This has been dealt with in the previous section. However, the increase in pH of the droplet has got some beneficial effects.

SO_2 Absorption. With the addition of NaOH to the slurry, there is an enhancement in the capture of sulfur dioxide. Literature (Chang and Rochelle, 1980) values were obtained for the enhancement factors (ϕ) for SO_2 absorption as a function of concentration of NaOH. The sulfur absorption rate is given by,

$$N_{\text{SO}_2} = -\phi \left(D_1 \frac{dC_1}{dr} + D_2 \frac{dC_2}{dr} \right) \quad (5-6)$$

where D_1 and D_2 are the diffusivities of H_2SO_3 and HSO_3^- , respectively in m^2/s , C_1 and C_2 are the concentration of H_2SO_3 and HSO_3^- , respectively in moles/ m^3 .

A sensitivity study was done to determine whether the SO_2 absorption was rate controlling in the overall process. For this purpose, the mass-transfer enhancement factor was multiplied to the Equation 5-6 and the SO_2 capture was determined for various cases. It can be seen from Figure 5-6 that there is not much of an enhancement in the net SO_2 removal rate due to enhanced absorption of SO_2 into the droplet due to NaOH addition.

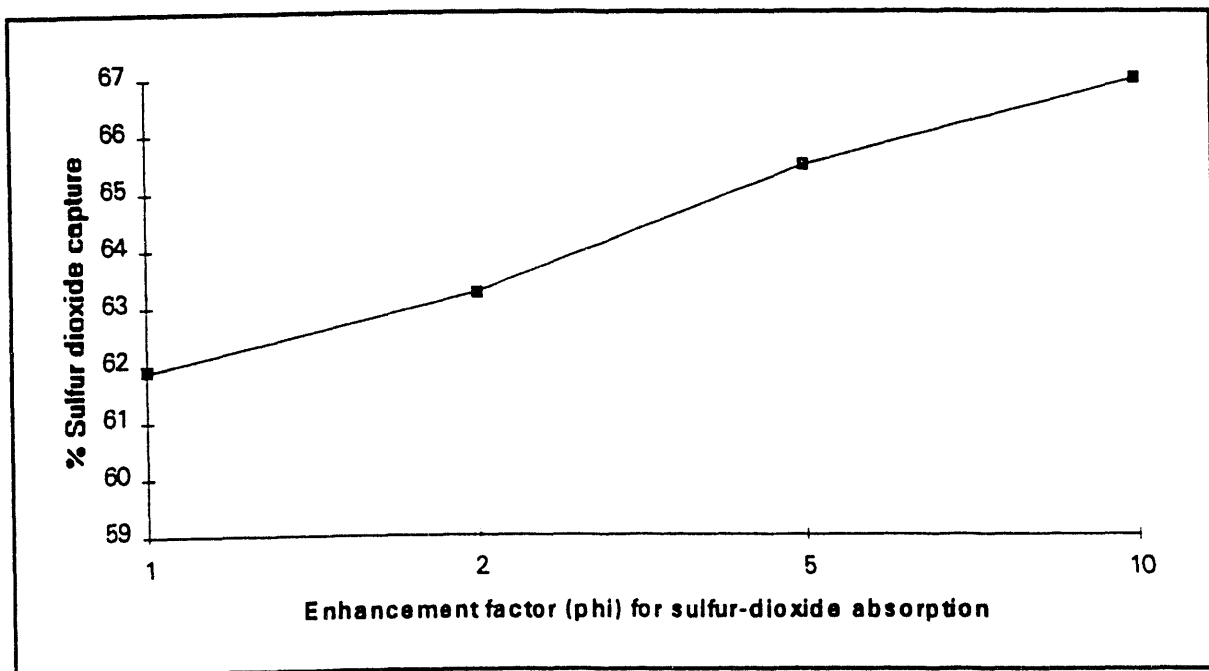


Figure 5-6. Percentage SO_2 capture versus SO_2 absorption enhancement factor.

Solubility of SO_2 . The effect of solubility of SO_2 on SO_2 capture was studied by carrying out a sensitivity study on He. The value of He constant (Rabe and Harris, 1963) for the base case as given by the model is :

$$\text{He} = \alpha * \exp \left(2.4717 - \frac{2851.1}{T_d} \right) \quad (5-7)$$

where T_d is the drop temperature (K). For different values of α , He is calculated and the corresponding SO_2 capture is determined (Figure 5-7). It can be seen that with increasing values of He, though there is a decrease in SO_2 capture as expected, this decrease is not very significant. This indicates that the solubility of SO_2 is not a limiting factor in SO_2 removal. In this particular simulation, the dissolution rate constant was kept at $3 \times 10^{-4} \text{ m}^3/\text{m}^2 \cdot \text{s}$.

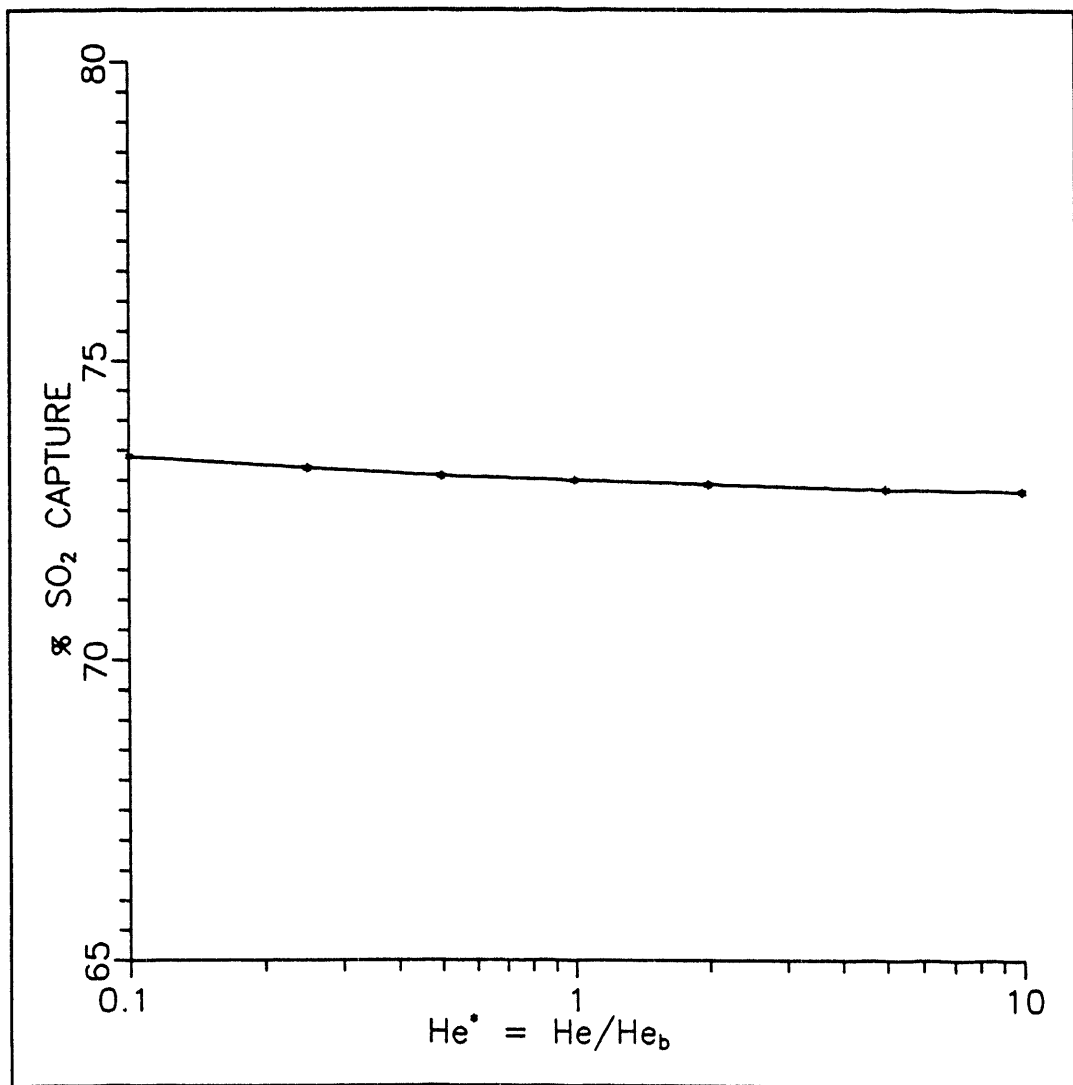


Figure 5-7. Percentage SO_2 capture efficiency versus Henry's law constant.

Thus, the liquid phase diffusional resistances are not rate limiting in the overall SO_2 removal rate. It may become significant towards the end of the droplet lifetime when the sorbent particles near the surface are consumed and the sulfur species have to diffuse inward through the product layer to react with $\text{Ca}(\text{OH})_2$.

Alkalinity of the Wet Agglomerate. The most important effect of pH would be to increase the alkalinity of the wet agglomerate. As water evaporates, the mass fraction of the additive (NaOH) increases (though some of it may react with SO_2), thereby affecting the wet agglomerate alkalinity. Thus, the dried solids reactivity towards SO_2 will increase for the case where NaOH is the additive. The increase in alkalinity in the agglomerate due to NaOH addition is much more than that in the liquid phase. SO_2 capture is drastically reduced once the evaporation has stopped; hence, any factor that would increase the reactivity of the wet solids would have a significant effect in SO_2 removal efficiency.

Once the evaporation has stopped, the moisture retained in the pores of the solid agglomerate aids in the capture of sulfur-dioxide. The chemical reaction rate constant(K_r) for the lime- SO_2 reaction in the wet agglomerate is known to be dependent on the relative humidity of the gas. Experiments performed by Damle and Sparks (1986) showed that the value of K_r under conditions of 50% relative humidity is thrice that obtained under completely dry conditions. There are no similar experimentally proven results obtained so far on the dependence of K_r on the pH of the wet agglomerate. Nevertheless, the resistance to the absorption rate of SO_2 is bound to decrease as a result of increased alkalinity of the agglomerate. This would be reflected in the increase in magnitude of the reaction constant. A sensitivity study has been performed on the effect of change in the reaction constant (K_r) i.e. the alkalinity of the wet agglomerate on the sulfur-dioxide removal efficiency. The results are depicted in Figure 5-8.

5.1.2.5 Summary of Synergistic Effects. The additive effects described in the preceding sections were evaluated independently. The combined results of the chemical effects of the additives listed for both the injection strategies are presented here. The percentage sulfur dioxide removal in the case of calcium chloride and sodium chloride is given in Figure 5-9. The baseline conditions hold good. The enhancement in sulfur dioxide capture due to these additives is primarily due to increase in droplet lifetime due to reduced evaporation. For 2 wt% CaCl_2 , the droplet lifetime increases from 0.45 sec to 0.6 sec, which is significant considering the fact that the total residence time is only 2.5 sec in the duct. Also, the equilibrium water content of the wet agglomerate increases. When compared with the vapor pressure lowering effect, the effect on SO_2 capture due to enhancement in solubility of lime in water is not very significant. As the pH of the slurry is affected marginally due to the addition of CaCl_2 , NaCl , the effect on dissolution rate of lime is also negligible. The pH of saturated $\text{Ca}(\text{OH})_2$ drops from 12.47 to 12.43 when 3 wt% NaCl is added to the slurry (Keener et al., 1992).

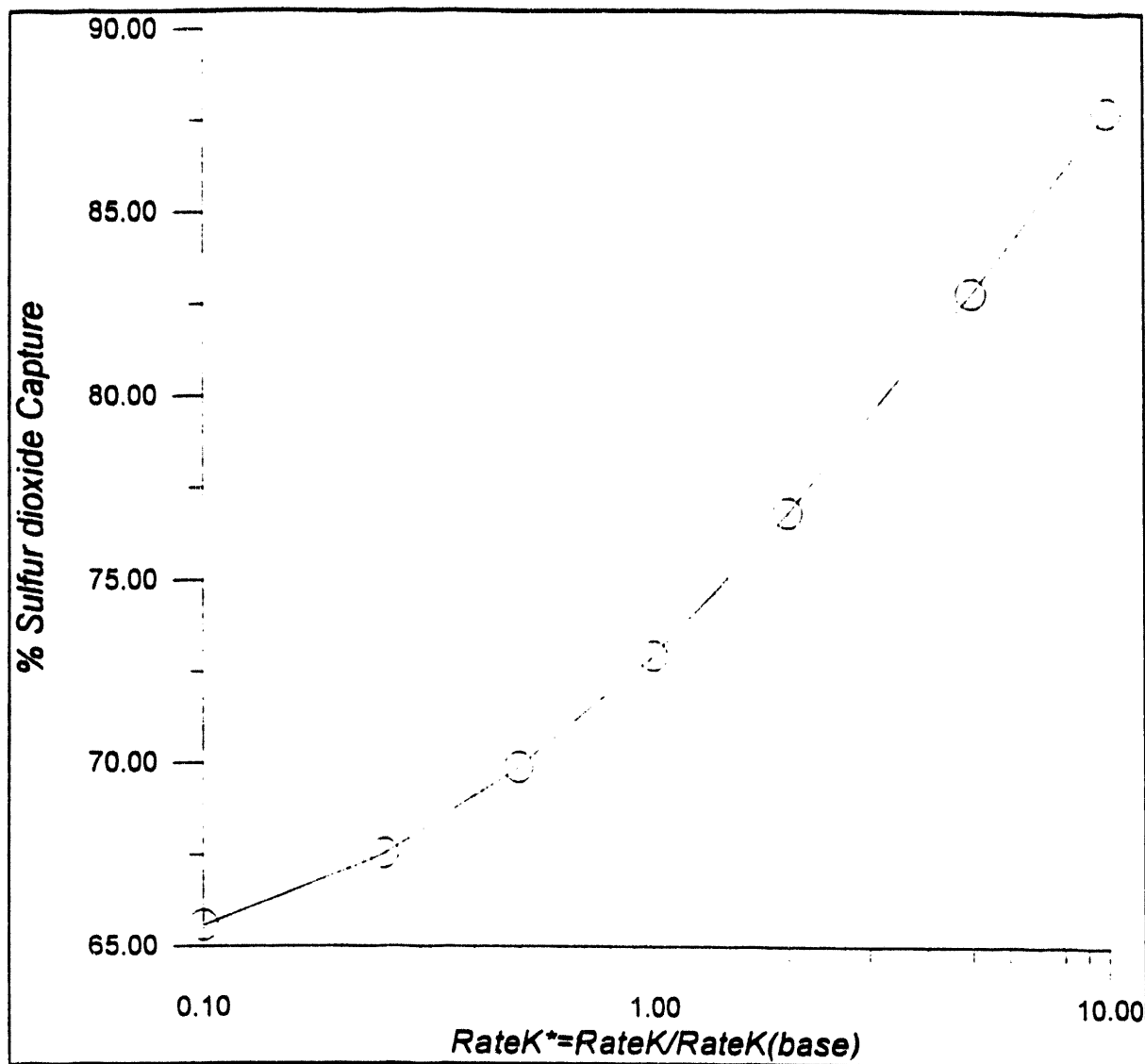


Figure 5-8. Sulfur dioxide capture efficiency as a function of solid-phase alkalinity.

Figure 5-9 indicates that the performance of CaCl_2 as an additive is slightly better than NaCl in slurry injection case. For a 3.5 wt% additive concentration (wt% of initial mass of water), the increase in SO_2 removal is 10 and 7 percentage points for CaCl_2 and NaCl respectively. For both cases, there is a steep increase in SO_2 removal initially (till around 3 and 2 wt% for CaCl_2 and NaCl respectively). After this additive concentration, the net increase in sulfur-dioxide removal over the base case is almost the same.

The effect due to change in the solubility of lime in water due to Na_2CO_3 addition could not be evaluated as data could not be obtained for this ternary system. However, the net SO_2 removal is expected to increase, with the vapor pressure

lowering effect alone contributing to around 4-5 percentage points for a typical concentration of 3 wt%.

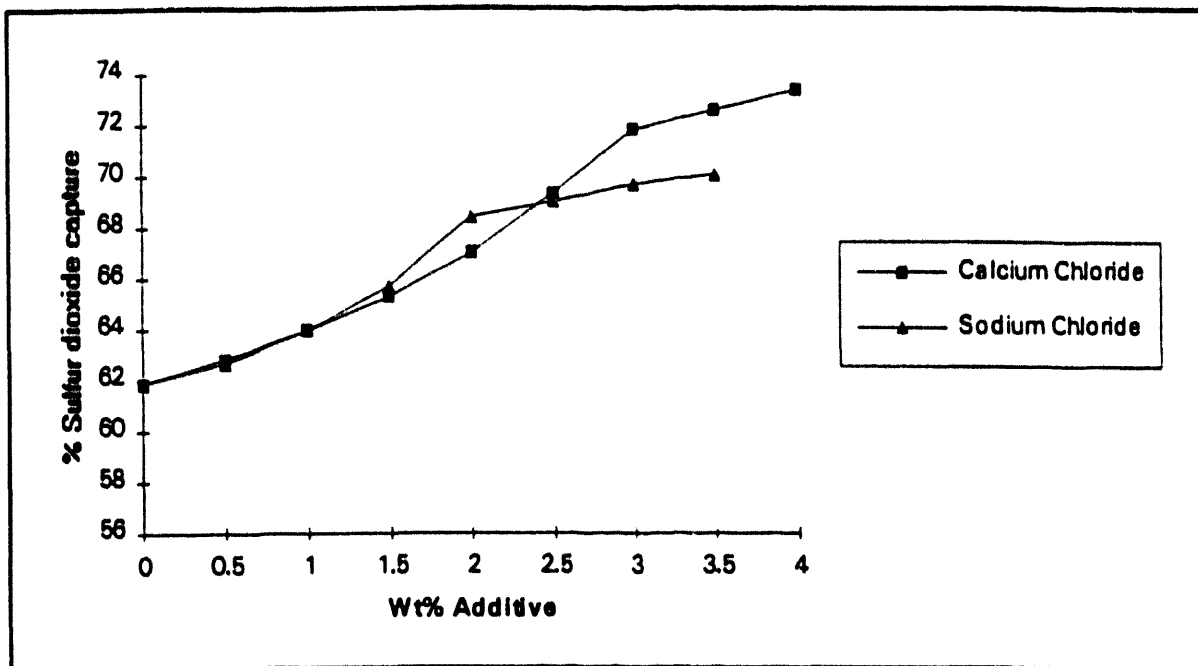


Figure 5-9. Percentage SO_2 capture efficiency versus additive concentration.

In the case of NaOH, there is significant decrease in solubility of lime in water and the lime dissolution rate which tends to counter the increase in droplet lifetime and enhancement in the liquid phase flux of SO_2 inward during the evaporation and post-evaporation stages(wet agglomerate). The enhancement in mass transfer coefficient of SO_2 in the droplet due to the increased alkalinity has a lesser impact on the SO_2 removal rate than the decrease in dissolution rate of lime due to the same reason. However, in the post-evaporation stage, when the wet agglomerate consisting of unreacted sorbent particles and reaction product($\text{CaSO}_3 \cdot 1/2 \text{H}_2\text{O}$) with equilibrium amount of moisture is formed, the alkalinity provided by NaOH is expected to result in significant removal of SO_2 . The data for this phenomena could not be obtained from literature. Also, the effective stoichiometric ratio increased marginally, considering the fact that NaOH can be treated as co-sorbent. The net increase in SO_2 removal without the effect due to increased alkalinity of the wet agglomerate is 6.5 percentage points for a NaOH concentration of 3 wt%.

For the sorbent injection followed by water spray case, the baseline SO_2 capture is 25 percentage points. This is an under-prediction of SO_2 removal considering that the reported SO_2 removal is 40 percentage points in the pilot-scale

studies conducted at Meredosia station (Charles et al., 1990) as part of the demonstration of the Coolside process. However, the droplet size distribution was not reported (Average droplet diameter in simulations is 50 μm). The importance of the droplet size is illustrated here.

It can be seen from Figure 5-10 that until a drop size of around 20 μm , there is a steep increase in percent SO_2 capture efficiency as droplet size increases. This increase is due to increase in the lifetime of the droplet. Above 20 μm , as drop size increases, the decreasing rate of external mass transfer almost encounters the increase in lifetime effect and the net increase in SO_2 capture is not significant. Also, the droplet size distribution plays an important role as a larger sized droplet will take longer time to evaporate in the presence of smaller sized droplets than it would otherwise take.

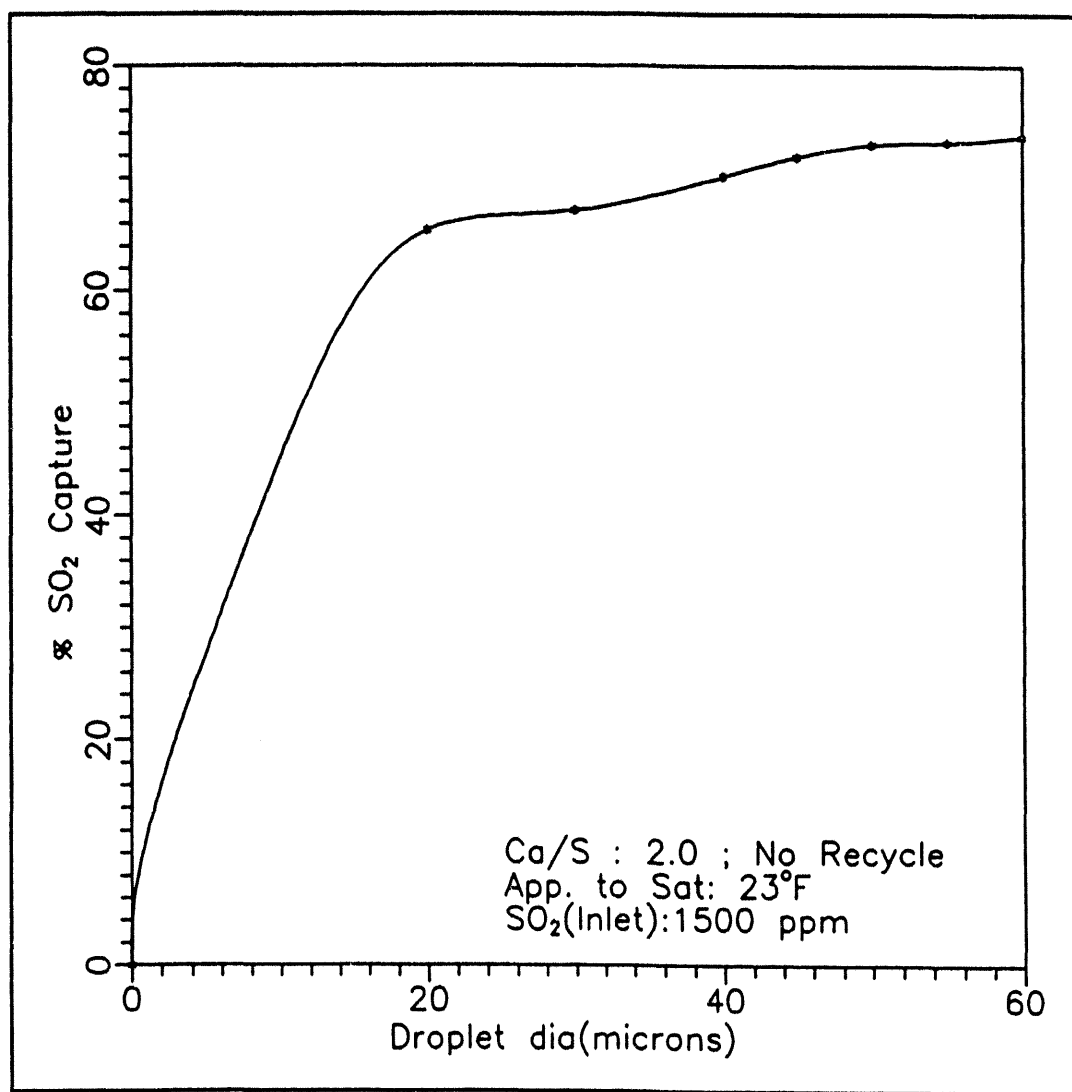


Figure 5-10. Percentage SO_2 capture efficiency versus droplet size.

There may also be an under-prediction of the number of sorbent particles scavenged by the decelerating droplet in the duct which may lead to decreased SO₂ capture. The simulations run for the various additive cases listed predicted only marginal improvement in SO₂ removal. The probable reasons for this observation should be investigated in future work.

5.1.3 Model Comparisons

Comparisons of model results for slurry injection strategy with those obtained experimentally at the University of Cincinnati (UC spray dryer tests) are provided in Table 5-4.

Table 5-4. Comparison of the enhanced EER model with UC spray dryer test results for the additive CaCl₂.

Wt % additive	CaCl ₂ (additive)	
	Model	Exptl.
0.0(Base case)	38.31	44.2
1.0	40.48	-
2.0	43.93	-
3.0	46.51	48.8

The process parameters for the comparisons provided are as follows: Ca/S ratio = 1.0, SO₂ (inlet) = 2200 ppm, no recycle, approach to saturation = 26°F. Droplet size was not reported in the experimental results (droplet size in model predictions = 50 μm). The residence time in the experiment was 10 seconds (approx). For the model simulations, the residence time was taken as 2.5 seconds. The difference in the experimental and model results could be due to the different residence times used. In fact, when the residence time was increased, the difference in the model and experimental values did come down. However, percentage SO₂ removal was predicted with a 2.5 second residence time as this is a typical value in duct injection processes.

It was intended at the initiation of this project that a more extensive comparison of the EER model with UC results of spray drying with additives be performed. As it turned out, additional UC experimental results were not available to us for model comparison and validation.

5.1.4 Conclusions and Recommendations

The summary of the chemical effects of additives for duct injection(slurry) spray drying processes are given as follows:

- (1) The lowering of water vapor pressure with the addition of additives(dissolved solids) is the primary reason for the enhancement in sulfur-dioxide removal. The droplet lifetime is increased and so is the equilibrium moisture content of the wet agglomerate.
- (2) The enhancement in lime solubility in water due to addition of certain additives like CaCl_2 , NaCl also increases the SO_2 capture, though the effect is not as significant as the first effect.
- (3) With the addition of NaOH , the decrease in solubility of lime in water due to common-ion effect and the decreased dissolution rate of lime due to increase in pH of slurry is countered by the increased absorption of SO_2 ; however, the liquid phase diffusion of SO_2 is not rate controlling throughout most periods of time except when the sorbent particles near the droplet surface are consumed. This happens only towards the end of the droplet lifetime.
- (4) The alkalinity of the wet agglomerate is increased with the addition of NaOH , leading to increased SO_2 removal in the post-evaporation stage.

Recommendations

Experiments to evaluate parameters like the dissolution rate of lime, reactivity of wet solids, equilibrium moisture content in the wet agglomerate, etc. need to be made for typical spray drying processes with and without various additives. The modified EER model can then be evaluated/validate and additional modifications could be added as needed.

5.2 Solid State Chemistry at High Temperatures

5.2.1 Introduction/ General Description

The primary aim of this task is to review the various additives that have been considered to enhance the SO_2 capture and sorbent utilization in in-furnace FGD systems. A brief literature review of high-temperature additives is presented here.

5.2.2 Literature Review

Calcium-based sorbents injected into the post-flame zone of boilers for the purpose of controlling SO_2 emissions have been subject to extensive studies. $\text{Ca}(\text{OH})_2$ (Hydrated lime) seems to be a better sorbent compared to other calcium-based sorbents like CaCO_3 and CaO . Several approaches including optimizing calcination and hydration conditions and the addition of additives are currently underway to enhance sorbent (like $\text{Ca}(\text{OH})_2$, CaCO_3) utilization. The latter approach is reviewed here.

Borgwardt (1985) showed that there was an enhancement in sorbent reactivity up to a factor of 4.6 in a differential reactor when alkali metals, or metal oxides like Cr_2O_3 were added to limestone. Cole et al. (1985) showed more modest improvements in sorbent utilization in the entrained flow reactor at temperatures of 1100°C and residence times of 0.92s. Rakes et al. (1985) showed that the enhancement in sorbent utilization by the addition of sodium compounds was greater for limestone (less reactive as compared to $\text{Ca}(\text{OH})_2$) than for hydrated dolomitic lime. Muzio et al. (1986), investigated the effect of nine additives, which included sodium, lithium, potassium, cesium and ferric compounds, added to the hydration water on sulfur dioxide capture and found that cesium had the maximum favorable effect on SO_2 capture followed by potassium, sodium, lithium and ferric additives. It was speculated that alkali crystals block the pores at room temperature but, as a result of melting and vaporization in the combustion zone, the pore structure may reopen at reaction conditions. However, the effectiveness of alkali-metal promoters like sodium was lost as these volatile promoters are deposited on the ash particles during coal-firing [Slaughter et al. (1986); Muzio et al. (1986)].

West (1984) claimed that the higher reactivity of CaO is due to the defects inherent with the crystal structure of limestone derivatives. Diffusion through product layer in a solid by solid-state mechanisms was considered to increase with increase in the concentration of lattice defects. The presence of impurities increases the lattice defects and facilitates in ionic diffusion through product layer of solids (when it occurs by solid-state mechanisms). When sulfates of lithium, sodium and potassium were added to pre-calcined and pre-sintered CaO , Borgwardt et al. (1987), found that there was a significant increase in sorbent utilization. However, if the additives were added prior to calcination there was a decrease in sorbent utilization due to increased rate

by solid-state mechanisms). When sulfates of lithium, sodium and potassium were added to pre-calcined and pre-sintered CaO, Borgwardt et al.(1987), found that there was a significant increase in sorbent utilization. However, if the additives were added prior to calcination there was a decrease in sorbent utilization due to increased rate of sintering.

Slaughter (1985) showed that both sodium and chromium react with calcium to increase the accessibility of CaO sites by particle fragmentation, creation of large cracks(or pores), and the presence of a liquid phase. Though iron is a transition metal like chromium, it did not promote an increased sulfur capture.

According to Haji-Sulaiman et al.(1987), higher impurity content(more crystal defects) of the material increased the extent of calcination. Thus, sorbents with a more open pore structure are obtained, resulting in improved sulfation efficiency by preventing early pore blockage. Shadman and Dombek (1988) consider the role of additives as structure modifiers. Experiments with bauxite,silica and kaolin suggested that the increased rate of conversion obtained with these additives were due to increase in macroscopicity.

Another class of additives that were tried were organic additives like alcohols (e.g., methanol) and sucrose. It was speculated (Gooch et al.,1986) that alcohols would increase the surface area of the sorbent by taking off the heat of hydration from the sorbent surfaces by evaporation. Sucrose, on the other hand increased the solubility of CaO in water. Experimental evidence to support these mechanisms were lacking.

Kirchgessner and Lorrain (1987) demonstrated that the organic surfactant, calcium lignosulfonate, added to $\text{Ca}(\text{OH})_2$ in the water of hydration increased the SO_2 capture by 15-20%. Lignosulfonate was originally chosen because it is known to be compatible with calcium-based systems, it is inexpensive and in some applications , has dispersant properties. Initially, the enhanced reactivity displayed by this promoted sorbent was attributed to particle size distribution(Borgwardt and Bruce,1986; Cole et al.,1986; Kirchgessner and Lorrain, 1987). But, when this modified sorbent was tried on a commercial scale, it showed no significant reduction in particle size though there was a substantial increase in SO_2 capture. A study by Kirchgessner and Jozewicz (1988) which focused on the structural changes undergone by the modified sorbent during furnace injection showed that it calcines more quickly and is more resistant to sintering than the unmodified sorbent. It hypothesized that more rapid dehydration would allow the sorbent longer period of time to react with SO_2 . Alternatively, it could be argued that a delay in sintering would allow the sorbent to retain higher specific surface areas and porosities and, therefore to remain reactive longer. Borgwardt and Bruce (1986) have shown a definite relationship between higher calcined surface areas to higher reactivity with SO_2 . The importance of porosity and pore volume distribution in the SO_2 capture has been considered (Gullett

et al., 1988).

A relatively clearer picture of the possible mechanisms due to which lignosulfonate promoted lime (lignolime) enhances the SO_2 capture over unmodified sorbent was given by Kirchgessner and Jozewicz (1989). They performed extensive studies of the changes in pore structure during sintering of CaO produced from $\text{Ca}(\text{OH})_2$ modified with 1% calcium lignosulfonate. They showed that reduced particle size is not a prerequisite to enhanced reactivity of lignolime, though it would definitely aid in increased SO_2 capture. They demonstrated that increased extent of calcination also has a role to play in enhanced reactivity with SO_2 although, the most important factor in enhanced reactivity is due to the reduction in the rate of sintering in the sorbent.

The pilot-scale testing of lignolime was carried out at the Ohio Edison Edgewater station (LIMB Extension Testing Program, 1991). Four sorbents that were taken up for evaluation of SO_2 removal efficiency were : i) calcitic limestone, ii) "type-N" atmospherically hydrated dolomite, iii) calcitic lime and, iv) calcitic lime with calcium lignosulfonate. The tests were carried over a range of Ca/S ratio and humidification conditions while burning Ohio coals with nominal sulfur content of 1.6, 3.0, 3.8 percent by weight. The highest removal efficiencies without humidification to close approach (humidifier outlet temperature : 250 - 275 °F) were obtained by using lignolime. Removal efficiencies on the order of 60% , at a stoichiometric ratio of 2.0, were achieved by burning a nominal 3.8% sulfur coal. These results are illustrated in Figure 5-11. The favorable results obtained using lignolime has made it even more necessary to better understand the mechanisms by which it causes enhanced SO_2 capture efficiency.

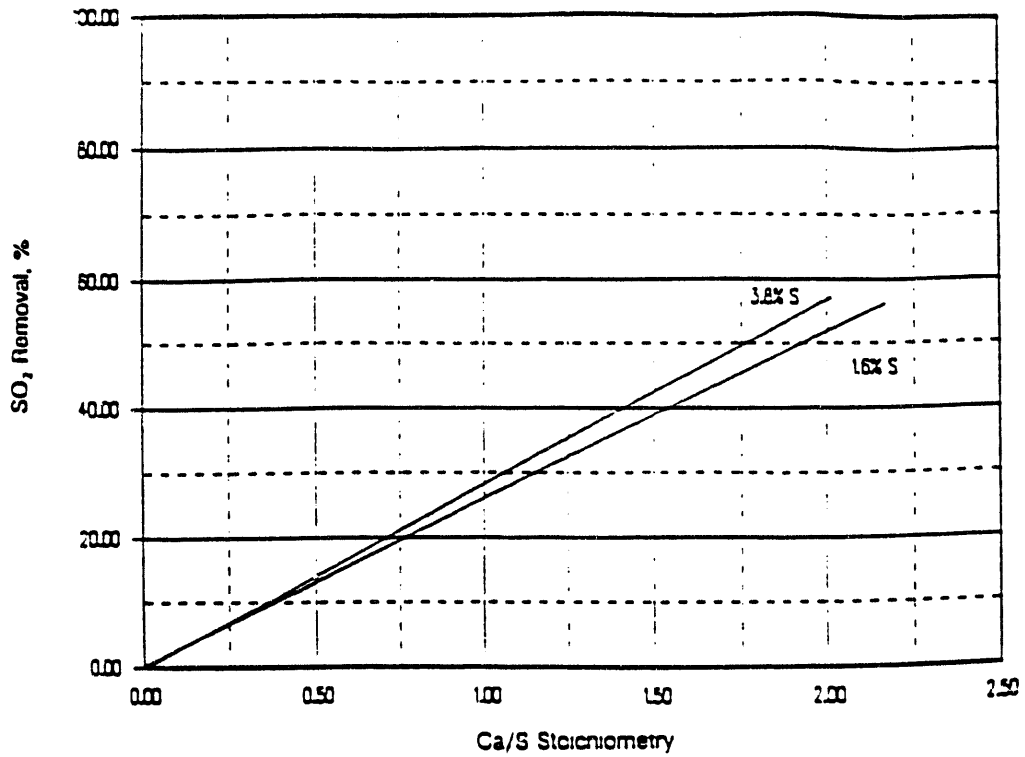


Figure a. Removal for commercial calcitic lime.

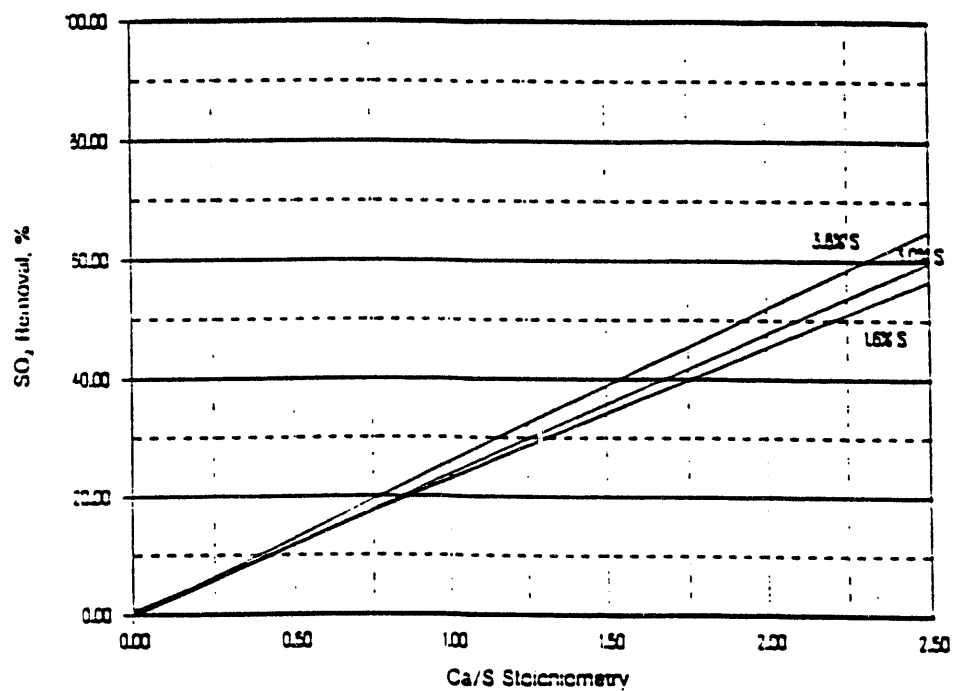


Figure b. Removal for "Type-N" dolomitic lime.

Figure 5-11a,b. Removal efficiencies for lime [LIMB Extension Testing at Edgewater, 1991].

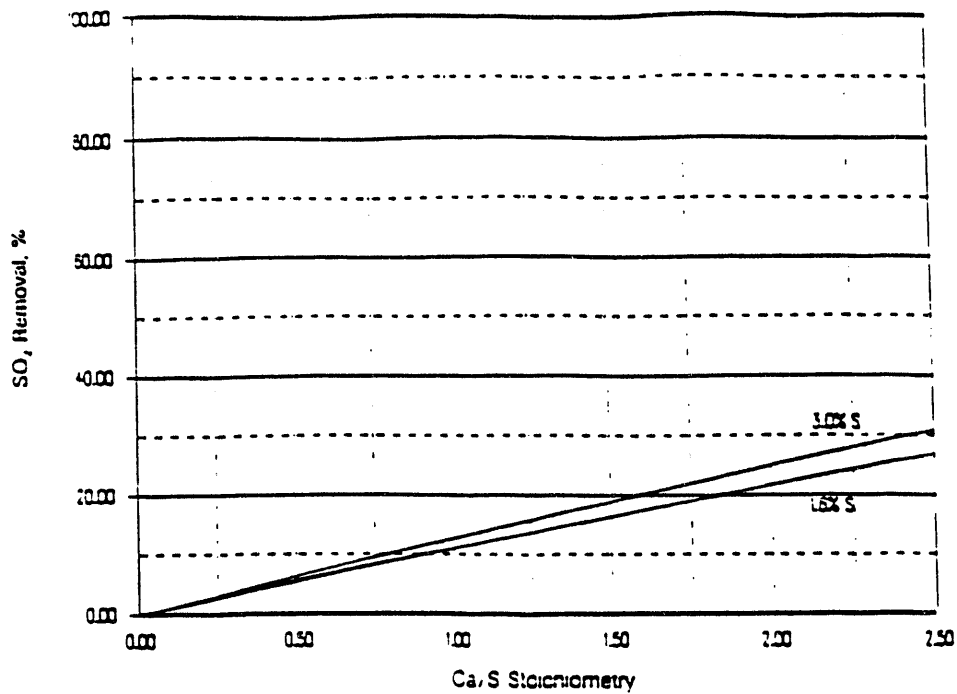


Figure c. Removal for coarse calcitic limestone.

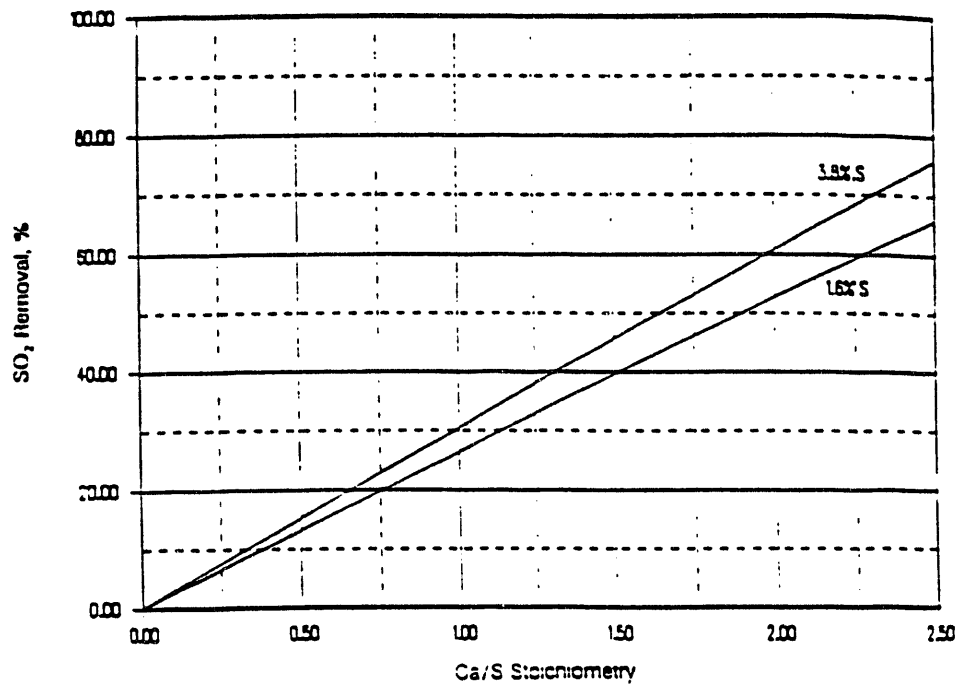


Figure b. Removal for ligno lime.

Figure 5-11c,d. Removal efficiencies for lime [LIMB Extension Testing at Edgewater, 1991].

5.3 Effect of Sorbent "Inert" Contents at Low Temperatures

5.3.1 Introduction/ General Description

The aim of this task was to evaluate the role of inerts in enhancing the sorbent utilization and sulfur-dioxide capture. Magnesium in the form of $MgCO_3$, found in many limestones in varying amounts has been considered to play one of the most significant role amongst the inerts in enhancing the degree of sorbent utilization. The role of silica (another inert in limestone) was also evaluated. For this purpose limestones of varying magnesium content were selected ranging from dolomitic (Carey) to moderate Mg limestone (Maxville). Comparison of Maxville and Bucyrus limestones would indicate the role played by other inerts (silica). The compositions of the various limestones are tabulated in Table 5-5.

Table 5-5. Composition of Limestones.

Limestone	$CaCO_3$ (wt%)	$MgCO_3$ (wt%)	$(SiO_2, Al_2O_3, Fe_2O_3)$
Maxville	70.00	12.87	16.12
Bucyrus	80.00	17.00	3.00
Carey	53.89	44.68	~1.38

5.3.2 Experimental

5.3.2.1 Overall Methodology. The overall experimental methodology for this task is listed below.

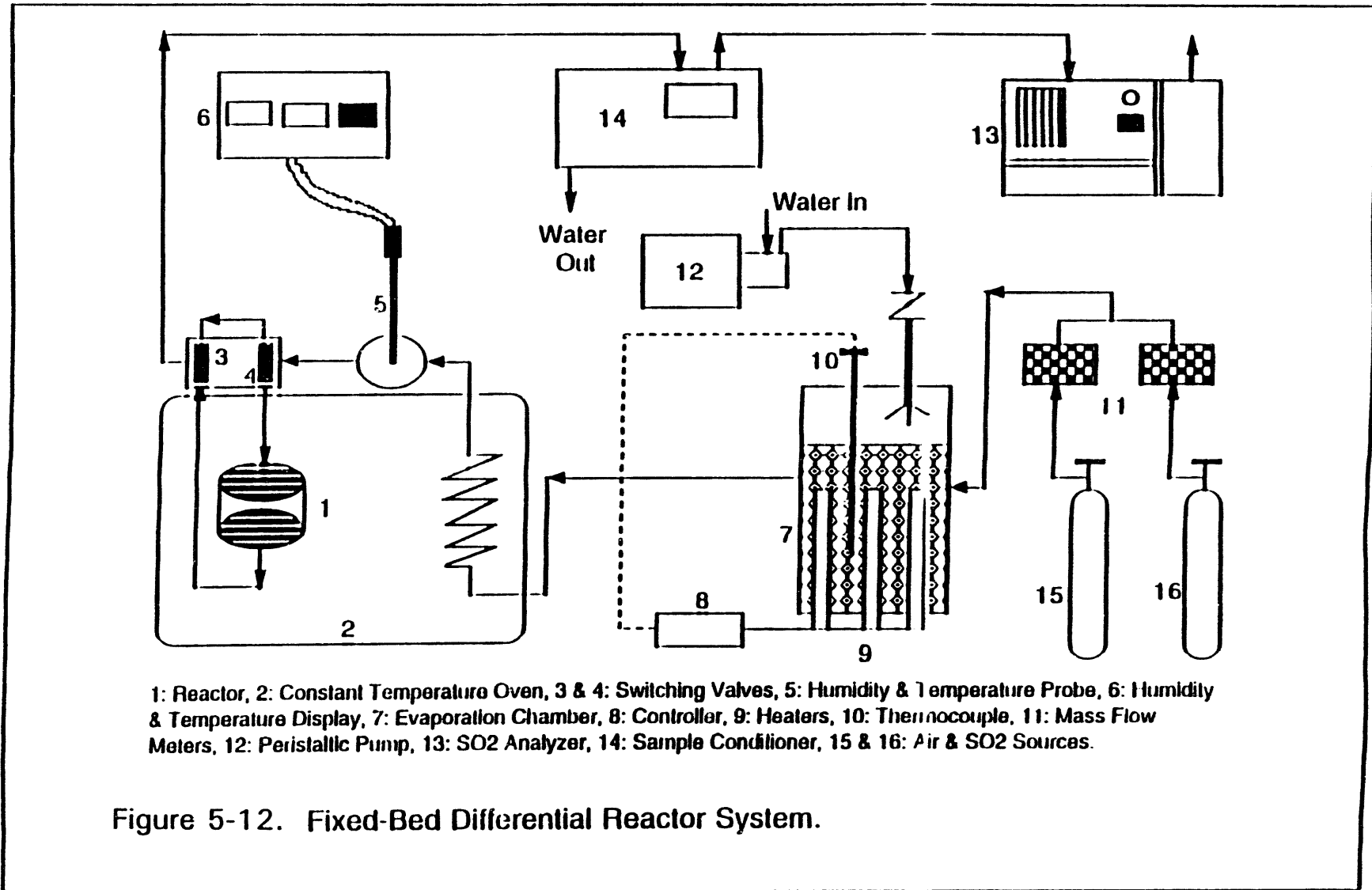
- (1) Samples of the subject limestone were prepared by crushing and sieving to a -80 + 100 mesh particle size range.
- (2) The prepared limestone samples were characterized by BET surface area analysis (to determine BET surface area) and SEM analysis (to check surface morphology including qualitative determination of crystallinity, porosity, and other surface features).
- (ii) The prepared limestone samples were calcined and characterized by BET surface area analysis.
- (iii) The calcined samples were hydrated to produce calcium hydroxide and once again characterized by BET surface area analysis. It is expected that some magnesium hydroxide may also be formed during the hydration process.

(iv) The hydrated lime samples were sulfated in a low temperature, differential reactor and the sulfated product was analyzed for sulfur content using a LECO sulfur analyzer.

5.3.2.2 *Calcination.* The calcination process was essentially a heating operation using a modified electrical furnace. A detailed diagram of the calcination apparatus is shown in Figure 2-1. A typical calcination was conducted as follows. Approximately 150 grams of prepared limestone was placed inside the calcination reactor on the wire screen. The whole set-up was held at 950°C for a predetermined time period of 6 hours. During the heating period a steady air flow rate of 25 cm³/s was maintained. As the heating proceeded, two different reactor temperatures were measured at regular intervals. At the end of the heating period, only the heating switch was turned off. The air inlet was kept open for an additional hour and then turned off. The entire set-up was allowed to cool down to approximately 100°C. The calcined product was then collected, bottled and retained for subsequent processing (hydration) and analysis. Additional details about the calcination reactor and the calcination procedure have been given by Mandal (1993).

5.3.2.3 *Hydration.* A semi-batch hydration system was used in this study. A detailed diagram of the system is shown in Figure 2-2. To perform a hydration, a total of 514 cm³ of water was added to the hydration reactor and heated to about 70°C. 80 grams of calcine (produced by the calcination process described in Section 5.3.2.2, above) was added to the hydrator to produce a final mole ration of water-to-calcine of 1:20. The calcine powder was added continuously to the hydration reactor at a rate of 4 grams per minute by a screw feeder for a total of 20 minutes. During the entire calcine addition period, the mixture was stirred continuously. The stirring was continued for 10 minutes after the end of the calcine addition. Once the hydration reaction commenced, the slurry temperature began to increase. In order to control the hydration temperature between 70 and 75°C, water at around 50 to 55°C was allowed to flow through the outer jacket of the hydration reactor. After about 30 minutes, the hydrated reaction products were withdrawn from the bottom of the reactor and dried. The dried, hydrate was then collected, bottled and retained for subsequent processing (sulfation) and analysis. Additional details about the hydration reactor and the hydration procedure have been given by Mandal (1993).

5.3.2.4 *Sulfation.* A bench-scale differential reactor system was used to collect sulfation data. This reactor used small amounts of sorbent and is particularly suited to sulfating calcium-based sorbent powders at low temperatures. The fixed-bed differential reactor system is shown in Figure 5-12. The main difference was that the reactor unit is a stainless steel filter holder (Gelman Sciences, Model No. 2220) in which about 0.8 g of hydrate particles was evenly dispersed across a filter. The reactor unit was mounted in a constant temperature electric oven. A detailed description of the reactor unit is shown in Figure 5-13. The other equipment, which included mass flow meters, evaporation chamber, and humidity and temperature



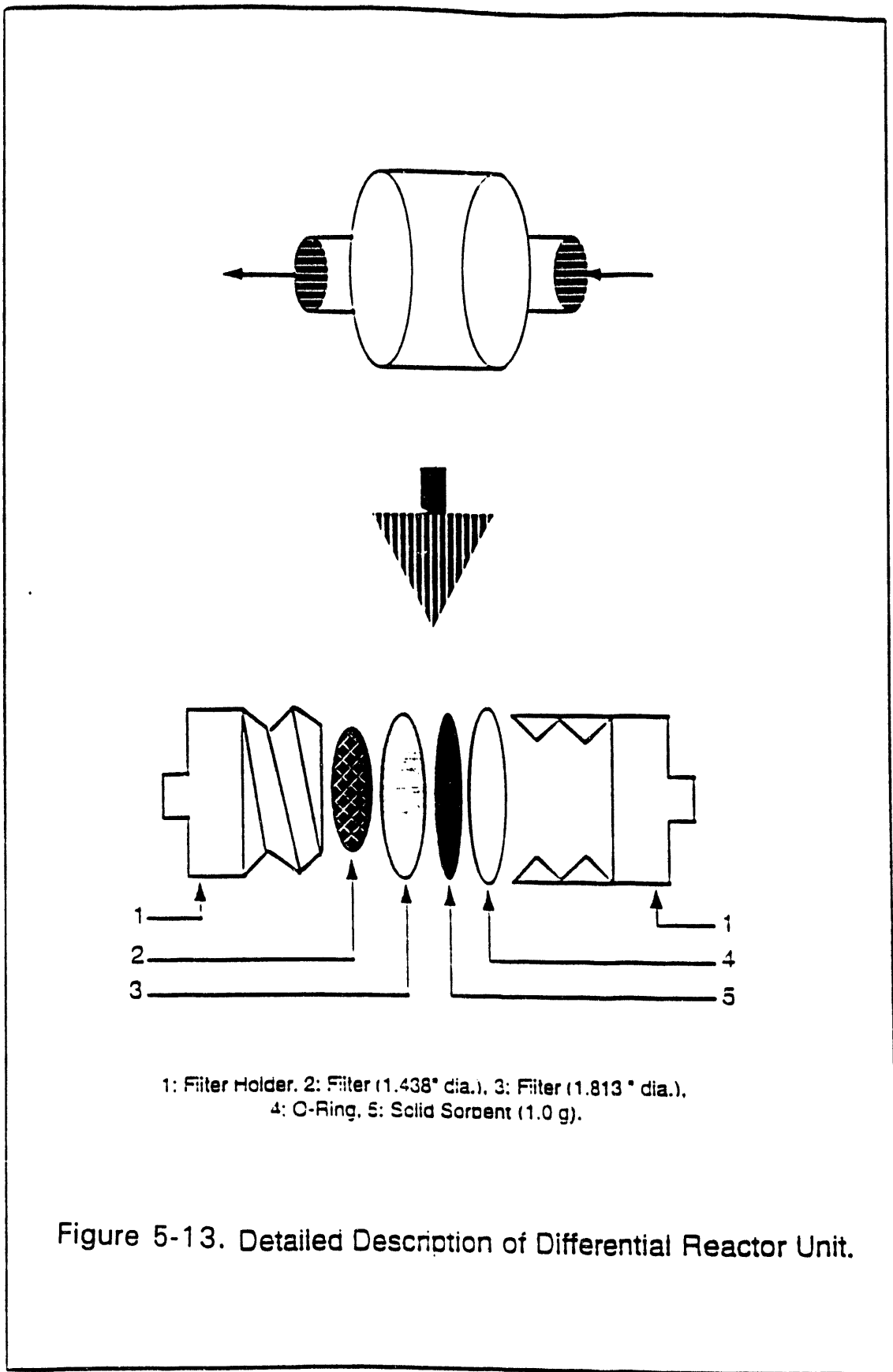


Figure 5-13. Detailed Description of Differential Reactor Unit.

devices. Initially, humidified air with the same relative humidity as the reacting SO₂ gas was passed over the hydrate sample for about 15 minutes to bring the reactor and reaction medium into thermal and humidity equilibrium with the flue gas and to allow for sorbent pre-conditioning. The reacting gas, consisting of air, SO₂ and water vapor, was mixed, passed through a coil of stainless steel tubing located inside the oven and by-passed to allow this stream to reach reaction temperature. At the start of an experimental run, the switching valves were reversed and the hydrate sample was exposed to the reacting gas for selected periods of time, which were measured using a stop watch. The run was ended by reversing the switching valves. The hydrate sample was then removed from the filter and dried at about 110°C in an electric oven. The sulfur content of the sample was obtained using a LECO SC-32 sulfur analyzer. The fixed experimental conditions are shown in Table 5-6. Additional details about the sulfation reactor and the sulfation procedure have been given by Ben-Said (1993).

Table 5-6. Fixed Experimental Conditions for Differential Reactor Runs.

Reaction Temperature	140°F
Gas Relative Humidity	90%
SO ₂ Concentration	1000 ppmdv
Superficial Gas Velocity	1.0 ft/s
Reaction Time	360 seconds
Hydrate Sample Size	0.8 g

5.3.3 Results and Discussion

Experimental results obtained at high reaction temperatures (characteristic of above the flame and economizer zones) have indicated that sorbent utilization and SO₂ capture is higher when a dolomitic (MgCO₃-CaCO₃) limestone is used to prepare sorbents instead of using a calcitic (CaCO₃) limestone. The conversion of calcium in dolomite is greater than that of calcium in limestone (Alvfors and Svedberg, 1988). A probable explanation for this observation could be that MgO, which is relatively inert towards SO₂ capture at high temperatures, will help to maintain a higher degree of porosity than that which is obtained in limestone, thus enhancing pore diffusion into the inner parts of the sorbent particle and providing a more even conversion distribution in the sorbent particle.

To evaluate the role played by the inerts in SO_2 capture and sorbent utilization at low temperatures (characteristic of after the air preheater) the experiments mentioned above were performed. The BET surface areas of the samples were measured at each stage of processing and the values are reported in Table 5-7. A comparison of the calcines of the three limestone seem to show no significant variation in BET surface area.

Table 5-7. BET surface areas (m^2/g) of raw limestones (149-177 μm) and their calcines and hydrates.

Limestone Name	Raw Limestone	Calcine	Hydrate
Maxville	4.90	3.50	27.75
Bucyrus	2.45	2.95	20.55
Carey	2.70	3.80	11.65

Upon hydration, the BET surface area of the calcine increases by a factor of 3 to 4. Table 5-7 shows that hydrates prepared from the two higher calcium limestones have BET surface areas significantly higher than the hydrate prepared from the highly dolomitic Carey limestone. The probable explanation of this phenomena is that MgO is less soluble in water than CaO . Hence, all other things equal, the hydrates formed from higher calcium calcines disintegrate (dissolve and redeposite in hydration) more than the hydrates prepared from low calcium calcines, leading to increased surface area.

Upon sulfation at high temperatures, the calcine ($\text{CaO}-\text{MgO}$) sorbent is considered to react as if the magnesium were inert. Thus, $(\text{CaO} \cdot m \text{MgO}) + \text{SO}_2 + 1/2 \text{O}_2 \rightarrow (\text{CaSO}_4 \cdot m \text{MgO})$, where m relates to the molar ratio of Mg/Ca . For a purely calcitic limestone, $m=0$. It has been shown by Levindis, et al.(1993) that the molar volume during sulfation of CaO increases by a factor of 3.1, thus plugging the pores and limiting conversion. However, the molar volume during sulfation of $(\text{CaO} \cdot 2 \text{MgO})$ increases by a factor of 2.25, thus permitting better utilization of the oxide.

The role played by inerts in low temperature dry scrubbing (monolayer of water sorbed onto the sorbent particle) processes has not been previously defined. Sulfation in the low temperature regime was performed for the hydrated limes obtained from the parent limestones listed. The percentages sulfur contents found in the sulfated products are presented in Table 5-8.

Table 5-8. Wt% Sulfur Contents of the Sulfated Products.

Parent Limestone	Wt% Sulfur in Product		
	Run#1	Run#2	Average
Maxville	18.60	17.50	18.05
Bucyrus	19.60	18.70	19.15
Carey	22.90	22.10	22.50

An XRD (X-ray diffraction) and/or EDAX analysis of both the hydrate and the sulfated product would have been instructive in determining the relative contents of oxide and hydrate (for both calcium and magnesium in the hydration product) and to forms of sulfur oxide and their hydration states in the sulfation product. Unfortunately, the instrumentation that has served us so well over the last year broke down and was not available for use. This has made the interpretation of our experimental results problematic.

The high amount of sulfur in the sulfated products indicate that magnesium as well as calcium reacts in a significant way with SO_2 in humidified dry scrubbing. The weight percent of sulfur in pure MgSO_3 and CaSO_3 is 30.8% and 26.7%, respectively. On the other end of the spectrum, the weight percent sulfur in $\text{MgSO}_4 \cdot 7\text{H}_2\text{O}$ and $\text{CaSO}_4 \cdot 2\text{H}_2\text{O}$ are 13.0% and 18.6%, respectively. The composition of the parent limestone compositions indicate that the sulfur content of the final products cannot be the ones reported in Table 5-8 if only calcium-containing species are reacted. Thus, some amounts of $\text{MgSO}_3/\text{MgSO}_4$ (in unknown states of hydration) should also have been formed. This indicates that the role played by magnesium in the low temperature reaction regime is qualitatively different from the role played in the high temperature regime. Of particular interest is the observation that the sulfation product of the highly dolomitic Carey limestone shows a significantly higher sulfur content than the sulfation products of the higher calcium content Maxville and Bucyrus stones. Without detailed compound analysis it is impossible to say whether or not this is attributable to increased utilization (of calcium and magnesium), variation in "real" inerts (silicas, clays) contents, or/and the hydration states of the sulfation products.

REFERENCES

Alvfors, P., and G. Svedberg, "Modelling of the Sulphation of Calcined Limestone and Dolomite - A Gas-Solid Reaction with Structural Changes in the Presence of Inert Solids, *Chem. Eng. Sci.*, **43**, 1183 (1988).

Bardakci, T., *Thermochim. Acta*, **76**, 287 (1984).

Beals, J.; Cannell, L.; and J. Hengel, "How FGD Reagent Quality Affects System Performance," *Power*, **128**(3), (1984).

Beittel, R.; Gooch, J.P.; Dismukes, E.B.; and L.J. Muzio, "Studies of Sorbent Calcination and SO₂-Sorbent Reactions in a Pilot-Scale Furnace," paper 16, *Proceedings: First Joint Symposium on Dry SO₂ and Simultaneous SO₂/NO_x Control Technologies*, 1, EPRI CS-4178, June 1985.

Ben-Said, L., "Reaction Kinetics and Mechanisms of Low Temperature SO₂ Removal by Dry Calcium-Based Sorbents," Ph.D. Dissertation, Ohio University, Athens, OH, 1993.

Berniere, F.; and C.R.A. Catlow, *Mass Transport in Solids*, Plenum, New York, 1983.

Bird, R.B.; Stewart, W.E.; and E.N. Lightfoot, *Transport Phenomena*, Wiley, New York, 1960.

Blythe, G.M.; Burke, J.M.; Kelly, M.E.; Rohlack, L.A.; and R.G. Rhudy, "EPRI Spray Drying Pilot Plant Status and Results," *Proceedings: Symposium on Flue Gas Desulfurization*, 2, EPA-600/9-83-0206 (NTIS PB84-110576), 1983.

Borgwardt, R.H.; and K.R. Bruce, "Effects of Specific Surface Area on the Reactivity of CaO with SO₂," *AIChE J.* **32**, 239 (1986).

Borgwardt, R.H.; and Bruce, K.R., "EPA Study of Hydroxide Reactivity in a Differential Reactor," *Proceedings: 1986 Joint Symposium on Dry SO₂ and Simultaneous SO₂/NO_x Control Technologies*, 1, EPRI CS-4966, December 1986.

Borgwardt, R.H.; Bruce, K.R.; and J. Blake, "An Investigation of Product-Layer Diffusivity for CaO Sulfation," *Industrial & Engineering Chemistry*, **26**(10), 1993 (1987).

Bortz, S.J.; and P. Flament, "Recent IFRF Fundamental and Pilot Scale Studies on the Direct Sorbent Injection Process," paper 17, *Proceedings: First Joint Symposium on Dry SO₂ and Simultaneous SO₂/NO_x Control Technologies*, 1, EPRI CS-4178, June 1985.

Brown, C.A.; Blythe, G.M.; Humphries, L.R.; Robends, R.F.; Runzan, R.A.; and R.G. Rhudy, "Results From the TVA 10-MW Spray Dryer/ESP Evaluation," *EPA/EPRI First Combined FGD and Dry SO₂ Control Symposium*, St. Louis, MO., October, 25-28, 1988.

Brown, C.A.; Maibodi, M.; and L.M. McGuire, "1.7 MW Pilot Results for the Duct Injection FGD Process using Hydrated Lime Upstream of an ESP," session 4-B, pg-305-324, *Proceedings: 1991 SO₂ Control Symposium*, 1, EPRI, December 1991.

Bruce, K.R.; Gullett, B.K.; and L.O. Beach, "Comparative SO₂ Reactivity of CaO Derived from CaCO₃ and Ca(OH)₂," *AIChE J.*, 35(1), 37 (1989).

Chan, P.K.; and G.T. Rochelle, "Limestone Dissolution: Effects of pH, CO₂, and Buffers Modeled by Mass Transfer," *Flue Gas Desulfurization*, J.L. Hudson and G.T. Rochelle, eds., ACS Symp. Ser. 188, Washington, 75-97 (1982).

Chang, J.C.S.; and T.G. Brna, "Enhancement of Wet Limestone Flue Gas Desulfurization by Organic Acid/Salt Additives," paper 6b, *Tenth Symposium on Flue Gas Desulfurization*, Atlanta, GA, November 18-21, 1986.

Chang, C.S.; and Rochelle, G.T., "SO₂ Absorption into NaOH and Na₂SO₃ Aqueous Solutions," *Ind. Eng. Chem. Fund.*, 24, 7 (1985)

Cole, J.A.; Kramlich, J.C.; Seeker, W.R.; and M.P. Heap, "Activation and Reactivity of Calcareous Sorbents Toward Sulfur Dioxide," *Environ. Sci. Technol.*, 19, 1065 (1985).

Cole, J.A.; Kramlich, J.C.; Seeker, W.R.; Silcox, G.D.; Newton, G.H.; Harrison, D.J.; and D.W. Pershing, "Fundamental Studies of Sorbent Reactivity in Isothermal Reactors," paper 16, *Proceedings: 1986 Joint Symposium on Dry SO₂, and Simultaneous SO₂/NO_x Control Technologies*, 1, EPRI CS-4966, December 1986.

Damle, A.S.; and L.E. Sparks, "Modelling of SO₂ Removal in Spray-Dryer Flue Gas Desulfurization System," *Proc. AIChE Meeting*, New Orleans, 1986.

Dharmarajan, N.N., "Stirred Mill Proves Its Worth for Lime-Slaking Duties," *Power*, 129(10), October, 1985.

Energy and Environmental Research Corporation, "In-Duct Slurry Droplet Process Model," Topical Report No.3, prepared for the U.S.D.O.E., Contract No. DE-AC22-88PC8873, November 1989.

Gooch, J.P.; Dismukes, E.B.; Beittel, R.; Thompson, J.L.; and S.L. Rakes, "Sorbent Development and Production Studies," paper 11, *Proceedings: 1986 Joint Symposium on Dry SO₂ and Simultaneous SO₂/NO_x Control Technologies*, Vol. 1, EPRI CS-4966, December 1986.

Gooch, J.P.; Dismukes, E.B.; Dahlin, R.S.; and M.G. Faulkner, "Scaleup Tests and Supporting Research For the Development of Duct Injection Technology, Draft Topical Report No. 1 - Literature Review," U.S. DOE, Pittsburgh, PA., March 31, (1989).

Goots, T.R.; Depero, M.J.; Purdon, T.J.; and P.S. Nolan, "Results from LIMB Extension Testing at the Ohio Edison Edgewater Station," *Proceedings: 1991 SO₂ Control Symposium*, 1, EPRI TR-101054, November 1992.

Gullett, B.K.; and K.R. Bruce, "Pore Distribution Changes of Calcium-Based Sorbents Reacting with Sulfur Dioxide," *AIChE J.*, 33(10), 1719 (1987).

Gullett, B.K.; and K.R. Bruce, "Effect of CaO Sorbent Physical Parameters Upon Sulfation," paper 5A-7, *EPA/EPRI First Combined FGD and Dry SO₂ Control Symposium*, St. Louis, MO, 1988.

Haji-Sulaiman; Scaroni, A.W.; and S. Yavuzkurt, "Sorbent Performance During Fluidized Bed Combustion," *Proceedings: 4th Annual Pittsburgh Coal Conference*, 129, 1987.

Huang, H.S.; Farber, P.S.; Livengood, C.D.; Yeh, J.T.; Markussen, J.M.; and C. J. Drummond, "Simultaneous NO_x and SO₂ Removal in a Spray Dryer System," *AIChE 1987 Spring National Meeting*, Houston, TX., March 29-April 2, 1987.

Jarvis, J.B.; Farmer, R.W.; and D.A. Stewart, "Description and Mechanism of Limestone FGD Operating Problems Due to Aluminum/Fluoride Chemistry," pp 7/79-7/83, *Proceedings: Tenth Symposium on Flue Gas Desulfurization*, 1, EPRI CS-5167, May 1987.

Jozewicz, W.; and G.T. Rochelle, "Fly Ash Recycle in Dry Scrubbing," *Environmental Progress*, 5(4), 218 (1986).

Karlsson, H.T.; Klingspor, J.; Linne, M.; and I. Bjerle, "Activated Wet-Dry Scrubbing of SO₂," *Journal of Air Pollution Control Association*, 33(1), 23 (1983).

Keener, T.C., "Simultaneous Removal of Sulfur Oxides and Particulate Matter From Stoker-Fired Boiler Flue Gas With A Pilot Plant Fabric Filter Collector," *Master's Thesis, University of Tennessee*, Knoxville, August, 1977.

Keener, T.C.; Khang, S.J.; and J. Wang, "Sorbent Utilization Studies Using A Mini-Pilot Spray Dryer," Final Report, prepared for the O.C.D.O, Contract No. OCRC/91-1.5, October 1992.

Kelly, M.E.; Kilgroe, J.D.; and T.G. Brna, "Current Status of Dry SO₂ Control Systems," *Proceedings: Symposium on Flue Gas Desulfurization*, 2, EPRI, Palo Alto, CA., March, 1983.

Kinzey, M., "Modelling the Gas and Liquid phase Resistances in the Dry Scrubbing Process for Sulfur Dioxide Removal," Masters Thesis, Cornell University, 1988.

Kirchgessner, D.A.; Gullett, B.K.; and J.M. Lorrain, "Physical Parameters Governing the Reactivity if Ca(OH)₂ with SO₂," paper 8, *Proceedings: 1986 Joint Symposium on Dry SO₂ and Simultaneous SO₂/NO_x Control Technologies*, 1, EPRI CS-4966, December 1986.

Kirchgessner, D.A.; and J.M. Lorrain, "Lignosulfonate-Modified Calcium Hydroxide for Sulfur Dioxide Control," *Ind. Eng. Chem. Res.*, 26(11), 2397 (1987).

Kirchgessner, D.A.; and W. Jozewicz, "Structural Changes in Surfactant-Modified Sorbents During Furnace Injection," *AIChE J.*, 35(3), 500 (1989).

Kirchgessner, D.A.; and W. Jozewicz, " Enhancement of Reactivity in Surfactant-Modified Sorbents for Sulfur Dioxide Control," *Ind. Eng. Chem. Res.*, 28, 413 (1989).

Levindis, A.Y.; Zhu, W.; Wise, D.L.; and G.A. Simons, "Effectiveness of Calcium Magnesium Acetate as an SO_x sorbent in Coal Combustion," *AIChE J.*, 39, 761 (1993).

Linke, W., *Solubilities: Inorganic and Metal-organic*, Van Nostrand, NJ, 1958.

Mandal, D.K., "Production of Improved Calcium-Based Sorbents for Sulfur Dioxide Capture," Masters Thesis, Ohio University, Athens, OH, 1993.

McCarthy, J.M.; Chen, S.L.; Kramlich, J.C.; Seeker, W.R.; and D.W. Pershing, "Reactivity of Atmospheric and Pressure Hydrated Sorbents for SO₂ Control," paper 10, *Proceedings: 1986 Joint Symposium on Dry SO₂ and Simultaneous SO₂/NO_x Control Technologies*, 1, EPRI CS-4966, December 1986.

Muzio, L.J.; Boni, A.A.; Offen, G.R.; and R. Beittel, "The Effectiveness of Additives for Enhancing SO₂ Removal with Calcium Based Sorbents," paper 13, *Proceedings: 1986 Joint Symposium on Dry SO₂ and Simultaneous SO₂/NO_x Control Technologies*, 1, EPRI CS-4966, December 1986.

Newton, G.H.; Kramlich, J.; and R. Payne, "Modelling the SO₂-Slurry Droplet Reaction," *AIChE J.*, **36**, 1865 (1990).

Overmoe, B.J.; Chen, S.L.; Ho, L.; Seeker, W.R.; Heap, M.P.; and D.W. Pershing, "Boiler Simulator Studies on Sorbent Utilization for SO₂ Control," paper 15, *Proceedings: First Joint Symposium on Dry SO₂ and Simultaneous SO₂/NO_x Control Technologies*, 1, EPRI CS-4178, June 1985.

Perry, R.H., ed., *Chemical Engineer's Handbook*, 5th ed., McGraw-Hill, NY, 1973.

Rabe, A.E.; and J.F. Harris, "Vapor-Liquid Equilibrium Data for the Binary System, Sulfur Dioxide and Water," *J. Chem. Eng. Data*, **8**, 333 (1963).

Reinauer, T.V.; Monat, J.P.; and M. Mutsakis, "Reducing Plant Pollution Exposure: Dry FGD on an Industrial Boiler," *Chemical Engineering Progress*, **79**(3), March, (1983).

Ritchie, I.; Giles, D.; Xu, B.A., "Kinetics and Mecahnism of Lime Slaking," *Proc. Australasian Chemical Engineering Conference*, Auckland, NZ, August 1990.

Rochelle, G.T.; and C.J. King, "The Effect of Additives on Mass Transfer in CaCO₃ and CaO Slurry Scrubbing of SO₂ from Waste Gases," *Ind. Eng. Chem. Fundamentals*, **16**(1), 67 (1977).

Rochelle, G.T.; Weems, W.T.; Smith, R.J.; and M.W. Hsiang, "Buffer Additives for Lime/Limestone Slurry Scrubbing," in *Flue Gas Desulfurization*, J.L. Hudson and G.T. Rochelle, eds., *ACS Symp. Ser. 188*, pp243-265, Washington, (1982).

Ruiz-Alsop, R.N.; and G.T. Rochelle, "Effect of Deliquescent Salt Additives on the Reaction of Sulfur Dioxide with Dry Ca(OH)₂," *ACS Div. Fuel Chem. Prepr.*, **30**(2), 88 (1985).

Shadman, F.; and P.E. Dombek, "Enhancement of SO₂ Sorption on Lime by Structure Modifiers," *Can. J. Chem. Eng.*, **66**, 930 (1988).

Silcox, G. D.; et al. "Status and Evaluation of Calcitic SO₂ Captures: Analysis of Facilities Performance," Vol 1, **EPA 600/7-87-014**, June, (1987).

Slaughter, D.M.; Chen, S.L.; and W.R. Seeker, "Enhanced Sulfur Capture by Promoted Calcium-Based Sorbents," paper 12, *Proceedings: 1986 Joint Symposium on Dry SO₂ and Simultaneous SO₂/NO_x Control Technologies*, 1, EPRI CS-4966, December 1986.

Snow, G.C.; Lorrain, J.M.; and S.L. Rakes, "Pilot Scale Furnace Evaluation of Hydrated Sorbents for SO₂ Capture," paper 6, *Proceedings: 1986 Joint Symposium on Dry SO₂ and Simultaneous SO₂/NO_x Control Technologies*, 1, EPRI CS-4966, December 1986.

Stouffer, M.R.; Rosenhoover, W.A.; and H. Yoon, "Pilot Plant Process and Sorbent Evaluation Studies for 105 MWe Coolside Process Demonstration," Topical Report, prepared for U.S.D.O.E., Contract No. DE-FC22-87PC79798, 1989.

Teixeira, D.P.; Lott, T.A.; and L.J. Muzio, "Dry Sorbent SO₂ Control for New Power Plants Burning Low Sulfur Western Coals," paper 7, *Proceedings: 1986 Joint Symposium on Dry SO₂ and Simultaneous SO₂/NO_x Control Technologies*, 1, EPRI CS-4966, December 1986.

Wang, S.C.; and D.A. Burbank, "Adipic Acid-Enhanced Lime/Limestone Test Results at the EPA Alkali Scrubbing Test Facility," *Flue Gas Desulfurization*, J.L. Hudson and G.T. Rochelle, eds., *ACS SYMP. Ser. 188*, pp267-306, Washington, (1982).

Weber, G.F.; Collings, M.E.; and M.H. Bobman, "Enhanced Utilization of Furnace Injected Calcium-Based Sorbents," paper 9, *Proceedings: 1986 Joint Symposium on Dry SO₂ and Simultaneous SO₂/NO_x Control Technologies*, 1, EPRI CS-4966, December 1986.

West, A.R., *Solid State Chemistry and Its Applications*, Wiley, New York, 1984.

Yoon, H.; Withum, J.A.; Rosenhoover, W.A.; and F.P. Burke, "Sorbent Improvement and Computer Modeling Studies for Coolside Desulfurization," paper 33, *Proceedings: 1986 Joint Symposium on Dry SO₂ and Simultaneous SO₂/NO_x Control Technologies*, 2, EPRI CS-4966, December 1986.

APPENDIX

EER ONE-DIMENSIONAL DUCT INJECTION MODEL

(with modifications to handle the additives:

NaOH, Na₂CO₃, NaCl, and CaCl₂)

Table A-1. Sample Input File.

15	Sorbent surface area (m ² /g)
4.0	Sorbent particle size (microns)
ALURRY	Slurry (s), Dry (d), or scavenging (any letter)
2.00	Calcium to Sulfur ratio
2.00	Ash Diameter
700	Ash mass flowrate (g/sec)
40	% Sorbent recycled
40	% Utilization of sorbent in recycle
.091	Water mole fraction in duct gases
.1011	CO ₂ mole fraction in duct gases
144.65	Gas mass flowrate (Kg/sec)
30	Duct Length (m)
14.25	Duct cross-sectional area (m ²)
H	Direction of gas flow, up, down, or horizontal
437.8	Gas temperature
295	Drop temperature, initial
1	Pressure (atm)
1800	ppm SO ₂
2.0	Additive(% of initial mass of water)
1	Type of additive
added(1-cac12,2-nacl,3-na2co3,4-naoh)	
1	r1 (Diss rate const.)
1	phin (enhancement factor for mass transfer)
1	s1 (solubility of lime)
5450	Water spray rate (g/sec)
60	Velocity of spray, initial
N	Allows droplets to have varying initial velocities
1	Number of drop sizes in distribution (15 maximum)
50,1.0	Drop size (microns), weight fraction (sum=1)
1	Number of positions where drop variables will be
printed	
0.01	Distance to " " " " "
"	

Table A-2. Samples Output File.

Input file=t2.dat

Sorbent Diameter = 4.00 microns
 Sorbent Surf Area= 15.00 m²/g
 Ca/S = 2.00
 Slurry Conc. = 16.64 % Wt. (sorbent only, calculated)
 SO₂ Concentration= 1500.00 ppm
 Additive = 0.00% initial mass of water
 Additive flow = 0.00g/s
 Type of additive = CaCl₂
 Ave. Ash Diameter= 10.00 microns
 Ash Mass Rate = 700.00 g/sec
 Gas Mass Rate = 144.65 Kg/sec
 Gas Temperature = 437.80 K
 Gas Humidity = 9.10 %
 Gas CO₂ Conc. = 10.11 %
 Duct Area = 14.25 m²
 Duct Length = 30.00 m
 Water Mass Rate = 5450.00 g/sec
 Water Velocity = 60.00 m/sec
 Gas flow direction is horizontal

Drop Size Distribution:

Drop Diameter (Microns)	Weight Fraction
50.0	1.000

Dist	Time	Frac	Unevap	%Util	%SO ₂	Cap	Gas	Temp	App/Sat	#Wet	Humidity
0.01	0.001	1.005		0.03	0.051	435.9	118.5			1	.0908

At 0.013 meters the individual drop parameters are:

Drop Diam	Frac Water	%Water	Drop Temp	Drop Time	Drop Vel	% Util	%Ash
50.09	1.005	83.34	308.5	0.000	57.47	0.03	0.1

Dist	Time	Frac	Unevap	%Util	%SO ₂	Cap	Gas	Temp	App/Sat	#Wet	Humidity
0.02	0.002	1.007		0.04	0.089	435.2	117.8			1	.0907
0.03	0.003	1.008		0.07	0.138	434.6	117.3			1	.0907
0.04	0.003	1.008		0.09	0.189	434.2	116.8			1	.0907
0.05	0.004	1.006		0.12	0.243	433.9	116.5			1	.0908
0.06	0.005	1.005		0.15	0.299	433.6	116.2			1	.0909
0.07	0.006	1.003		0.18	0.357	433.3	115.9			1	.0910
0.08	0.007	1.000		0.21	0.418	433.0	115.6			1	.0911
0.09	0.008	0.997		0.25	0.494	432.7	115.2			1	.0913
0.10	0.008	0.995		0.28	0.560	432.5	114.9			1	.0914
0.20	0.017	0.963		0.61	1.221	429.4	111.5			1	.0932
0.30	0.025	0.922		0.94	1.883	425.6	107.2			1	.0955
0.40	0.033	0.876		1.4	2.80	421.3	102.4			1	.0981
0.50	0.042	0.831		2.0	3.91	417.2	97.8			1	.1006
0.60	0.050	0.793		2.6	5.13	413.8	94.0			1	.1026
0.70	0.059	0.758		3.2	6.41	410.7	90.5			1	.1045
0.80	0.067	0.725		3.9	7.75	407.7	87.2			1	.1064
0.90	0.076	0.692		4.6	9.18	404.8	84.0			1	.1081
1.00	0.084	0.661		5.4	10.76	402.1	81.0			1	.1098
2.00	0.173	0.412	13.8	27.67	380.4	57.0				1	.1231
3.00	0.264	0.243	20.2	40.40	366.2	41.4				1	.1318
4.00	0.358	0.129	24.9	49.74	356.7	31.1				1	.1376
5.00	0.453	0.050	28.2	56.43	350.2	24.0				1	.1416
6.01	0.548	0.039	28.8	57.59	349.3	23.0			0		.1422
7.01	0.644	0.039	28.9	57.84	349.3	23.0			0		.1422
8.01	0.740	0.039	29.0	58.08	349.3	23.0			0		.1422
9.01	0.836	0.039	29.2	58.31	349.3	23.0			0		.1422
9.99	0.930	0.039	29.3	58.52	349.3	23.0			0		.1422
10.01	0.932	0.039	29.3	58.53	349.3	23.0			0		.1422
12.51	1.172	0.039	29.5	59.04	349.3	23.0			0		.1422
15.01	1.411	0.039	29.8	59.52	349.3	23.0			0		.1422

Table A-3. Subroutine CA.

```
SUBROUTINE CA(J,R,R0,dCdR,dCdREMT0,dCdR0,VRR,ER,IRWARN)

C This subroutine calculates concentration from the second-order
C differential equation of C with respect to R using a
C 4th order Runge-Kutta method.

IMPLICIT REAL (K)
REAL dR(15,50),KDISSOC,NPart(15,50)
REAL ShellFlux(15,50),SolFrac(15,50),DropDiam(15)
REAL *8 R,xdR,ddR,R0,Rmin,Rmax,Z,XS8,YS8CALC,Cld
REAL *8 dCdR,Cmax,Cmin,CStart,Cdum,CCa(200)
REAL *8 CCa0(15),Cold(15),dCdRgoal,dCdR0Old,C,CCa0Old
INTEGER NStart(15),Mevap(15),NShell(15),MStart(15),IFlux(15)

COMMON/DR/dR
COMMON/SO2/DSO2,CMTSO2,HE,KDISSOC,DH2SO3,DHSO3,YS8
COMMON/NT/NStart
COMMON/DROP/DropDiam
COMMON/MEVAP/Mevap
COMMON/ICE/ICEASE
COMMON/SHEL/ShellFlux
COMMON/LIME/Dlime,CLimeEq
COMMON/CCA0/CCa0
COMMON/NS/NSHELL
COMMON/MOLD/Mold
COMMON/CLEDUM/CLEdum
COMMON/NPDR/NPart
COMMON/IF/IFlux
COMMON/SOL/SolFrac
common/dis/dis
common/pz/ipz

C      C a l c u l a t e      c a l c i u m
profile.*****
C Calculate flux of Ca from each shell (flux/pi).

IMAX=50*NShell(J)
ITotal=0
CLEdum=CLimeEq
IF(CCa0(J).GE.CLimeEq) CCa0(J)=.99*CLimeEq
MStart(J)=MStart(J)-1
if(dis.ge.9999.and.j.ne.0.and.dis.lt.9998) THEN
print *,,' R0 reset in Flx',' NShell=',NSHELL(j),' ,
CLE=','CLIMEEQ
print *,,'ccao(j)=' ,ccao(J)
Print *,,' before ms>ns check',' ms=' ,mstart(J) ,
ns=' ,nstart(J)
endif
IF(MStart(J).LE.0.OR.MStart(J).GT.NStart(J)) MStart(J)=1
if(dis.ge.9999.and.j.ne.0.and.dis.lt.9998) print *,
```

```

&           ' after ms>ns check'
&           ' ms=' ,mstart (J) , ' ns=' ,nstart (J)
Mold=0
MINUS=0
10  ICa=0
Cmin=0
Cmax=CLimeEq
IF(MStart(J).NE.1) CCa0(J)=.99*CLimeEq
CCa0old=0
if(dis.ge.9999.and.j.ne.0.and.dis.lt.9998)print*, '      mstart
reset'
if(dis.ge.9999.and.j.ne.0.and.dis.lt.9998)print*, ,
&           ' nst=' ,nstart (J) ,
&           ' mst=' ,mstart (J) , ' R0=' ,r0, ' D/2=' ,dropdiam(J)/2
199 ICa=ICa+1
ITotal=ITotal+1

IF(ICa.EQ.55.OR.ITotal.EQ.IMAX) THEN
  IF(R0.EQ.DropDiam(J)/2.AND.Cmax-Cmin.LT..00000001*CMIN)
THEN
  IRWARN=1
  RETURN
ENDIF
*,'*****'
P          R          I          N          T
*,'*****'
PRINT  *, '***Calcium    profile    diverged.      Program
terminated***'
P          R          I          N          T
*,'*****'
ICEASE=1
PRINT 4,'ICa=' ,ICa,' ITot=',' ITot,' MStart=' ,MStart(J) ,
&           ' NStart=' ,NStart(J) , ' IMAX=' ,IMAX
4   FORMAT(1X,A,I2,A,I4,2(A,I2),A,I4)
  RETURN
ENDIF
dCdR=0
C=CCa0(J)
R=0
RR=0
IN=15./ (NStart(J) -MStart(J) +1)+.99999999
IF(IN.LT.2) IN=2
NCa=IN* (NStart(J) -MStart(J) +1)
if(dis.ge.9999.and.j.ne.0.and.dis.lt.9998) print *, ,
&           ' ms=' ,mstart (J) ,
&           ' nst=' ,nstart (J) , ' in=' ,in, ' NCa=' ,nca

DO 100,MM=1,MStart(J)-1
R=R+dR(J,MM)
100 RR=RR+dR(J,MM)

101 M=MStart(J)-1
ICOUNT=0
DO 200,L=1,NCa

```

```

ICOUNT=ICOUNT+1
IF(L/FLOAT(IN)-INT(L/IN).LT..01) ICOUNT=0
IF(ICOUNT.EQ.1) THEN
  IF(IFlux(J).EQ.1.AND.SolFrac(J,M).GT..7) THEN
    ShellFlux(J,M)=-4*R**2*(dCdR*Dlime-ER*C/55334)
  ELSEIF(L.NE.1) THEN
    ShellFlux(J,M)=-4*R**2*dCdR*Dlime
  ENDIF
  if(dis.ge.9999.and.j.ne.0.and.dis.lt.9998) print 98,'m=',m,
  &           ' shlfIx=',
  &           shellflux(j,m),' ER=',er,' nst=',nstart(J)
98  format(1x,a,i2,a,e12.4,A,F6.3,A,i2,E12.4)
  M=M+1
  IF(M.NE.NStart(J)) THEN
    xdR=dR(J,M)/IN
  ELSE
    xdR=(R0-RR)/IN
  ENDIF
  RR=RR+dR(J,M)
  VRR=RR**3-(RR-dR(J,M))**3
ENDIF

K11=xdR*dCdR
K12=xdR*CaDif(C,dCdR,R,J,M,VRR,ER)
K21=xdR*(dCdR+K12/2)
K22=xdR*CaDif(C+K11/2,dCdR+K12/2,R+xdR/2,J,M,VRR,ER)
K31=xdR*(dCdR+K22/2)
K32=xdR*CaDif(C+K21/2,dCdR+K22/2,R+xdR/2,J,M,VRR,ER)
K41=xdR*(dCdR+K32)
K42=xdR*CaDif(C+K31,dCdR+K32,R+xdR,J,M,VRR,ER)

Cld=C
C=C+(K11+2*K21+2*K31+K41)/6
CCa(L)=C
IF(C.LT.-2000.OR.C.GT.0.AND.Cld.LE.0.AND.L.NE.1) THEN
  Cmin=CCa0(J)
  if(dis.ge.9999.and.j.ne.0.and.dis.le.9998) print *, 'cmin set
1'
  CCa0(J)=(.94-ICa/400)*(Cmax-Cmin)+Cmax
  if(dis.ge.9999.and.j.ne.0.and.dis.le.9998) then
    print *, 'cca0 reset because c>0 and cld<0'
    print *, 'L=',l,' C=',c,' Cold=',CLD
    print *, 'ica=',ica,' cmin=',cmin,' cmax=',cmax
    print *, 'c=',c,' cca0old=',cca0old
    print *, 'dCdR=',dCDR,' cca0=',cca0(J),' z=',z
    print 3,'IN=',in,' NCa=',nca,' m=',m,' L=',l,' RR=',rr
  endif
  GO TO 199
ENDIF
IF(C.GT.Cld.AND.dCdR.GT.0)THEN
  Cmax=CCa0(J)
  CCa0(J)=(.94-ICa/400)*(Cmax-Cmin)+Cmin
  if(dis.ge.9999.and.j.ne.0.and.dis.le.9998) then
    print *, 'cca0 reset because c>cld'

```

```

print *, 'L=', l, ' C=', c, ' Cold=', CLD
print *, 'ica=', ica, ' cmin=', cmin, ' cmax=', cmax
print *, 'c=', c, ' cca0old=', cca0old
print *, 'dCdR=', dCdR, ' cca0=', cca0(J), ' z=', z
print 3, 'IN=', in, ' NCa=', nca, ' m=', m, ' L=', l, ' RR=', rr
endif
GO TO 199
ENDIF
IF(C.LT.0.AND.L.LT.NCa.AND.R0.EQ.DropDiam(J)/2) THEN
  Cmin=CCa0(J)
  if(dis.ge.9999.and.j.ne.0.and.dis.le.9998) print *, 'cmin set
2'
  CCa0(J)=(.6-ICa/400)*(Cmax-Cmin)+Cmin
  if(dis.ge.9999.and.j.ne.0.and.dis.le.9998) then
    print *, 'cca0 reset because c<-10 and r0=D/2'
    print *, 'ica=', ica, ' cmin=', cmin, ' cmax=', cmax
    print *, 'c=', c, ' cca0old=', cca0old
    print *, 'cold=', cold(J), ' cca0=', cca0(J), ' z=', z
  endif
  GO TO 199
ENDIF
dCdR=dCdR+(K12+2*K22+2*K32+K42)/6
if(dis.ge.9999.and.j.ne.0.and.dis.le.9998) then
  print *, 'L=', l, ' C=', c, ' dCdR=', dcdR
endif
200 R=R+xdR

C Calculate new CCa0(J) based on setting C(R0) = 0 when R0 isn't at
the
C drop surface or setting flux at the drop surface equal to the
maximum
C rate of external mass transfer.

Z=CCa0(J)
IF(ABS(R0-DropDiam(J)/2).GT..0001*DropDiam(J)/2) THEN
  IF(ABS(C).LT.1E-2) GO TO 201
  IF(Cmax-Cmin.LT..0000000000000001*CMIN.AND.Mstart(J).NE.
  &      Nstart(J)) THEN
    MStart(J)=MStart(J)+1
    MINUS=1
  if(dis.ge.9999.and.j.ne.0.and.dis.le.9998) then
    print *, 'mstart reset to ms+1, cmax-cmin too small, goal
c=0'
  endif
  GO TO 10
ENDIF

  IF(C.GT.CLimeEQ.OR.C.GT.0.AND.CCa0(J).LT.Cmax.AND.C.LT.Cld)
  &      THEN
    Cmax=CCa0(J)
  ELSEIF(C.LT.0.AND.CCa0(J).GT.Cmin) THEN
    Cmin=CCa0(J)
  if(dis.ge.9999.and.j.ne.0.and.dis.le.9998) print *, 'cmin set
3'

```

```

ENDIF

CCa0(J)=CCa0(J)-C/(C-COLD(J))*(CCa0(J)-CCa0old)
if(dis.ge.9999.and.j.ne.0.and.dis.le.9998) then
print *, 'ica=', ica, ' cmin=', cmin, ' cmax=', cmax
print *, 'c=', c, ' cca0old=', cca0old
print *, 'cold=', cold(J), ' cca0=', cca0(J), ' z=', z
print 3, 'IN=', in, ' NCa=', nca, ' m=', m, ' L=', l, ' RR=', rr
3 format(4(a,i3),a,e12.4)
endif
COLD(J)=C
ELSEIF(ABS(R0-DropDiam(J)/2).LT..0001*DropDiam(J)/2) THEN
dCdRgoal=-dCdREMT0+dCdR0*C
IF(ABS(dCdR-dCdRgoal).LT.ABS(.001*dCdR)) GO TO 201
IF(Cmax-Cmin.LT..00000000000001*CMIN.AND.Mstart(J).NE.
& NStart(J)) THEN
MStart(J)=MStart(J)+1
MINUS=1
if(dis.ge.9999.and.j.ne.0.and.dis.le.9998) then
print *, 'mstart reset to ms+1, cmax-cmin too small, goal
dCdR=0'
endif
GO TO 10
ENDIF

IF(C.GT.CLimEQ.OR.dCdR.GT.dCdRgoal.AND.CCa0(J) .
& LT.Cmax.and.dCdR.LT.0) THEN
Cmax=CCa0(J)
ELSEIF(C.LT.0.AND.CCa0(J).GT.CCa0old.OR.dCdR.LT.dCdRgoal.
& AND.CCa0(J).GT.Cmin) THEN
Cmin=CCa0(J)
if(dis.ge.9999.and.j.ne.0.and.dis.le.9998) print *, 'cmin set
4'
ENDIF
Z2=CCa0(J)
CCa0(J)=CCa0(J)-(dCdR-dCdRgoal)/(dCdR-dCdR0old)*(CCa0(J) -
& COLD(J))
if(dis.ge.9999.and.j.ne.0.and.dis.le.9998) then
print *, 'ica=', ica, ' cmin=', cmin, ' cmax=', cmax
print *, 'dcdr=', dcdr, ' dcdrgoal=', dcdrgoal, ' dcdr0old=', dcdr0old
print *, 'cold=', cold(J), ' cca0=', cca0(J), ' z=', z
print 3, 'IN=', in, ' NCa=', nca, ' m=', m, ' L=', l, ' RR=', rr
endif
dCdR0old=dCdR
COLD(J)=Z2
ENDIF

150 IF(ICa.GE.15.and.ICa.LT.25.OR.ICa.GE.35.AND.ICa.LT.45) THEN
IF(IIC.EQ.0) THEN
CCa0(J)=(.33+ICa/400.)*(Cmax-Cmin)+Cmin
IIC=1
ELSE
CCa0(J)=(.67+ICa/400.)*(Cmax-Cmin)+Cmin
IIC=0

```

```

        ENDIF
    ENDIF
    IF(CCao(J) .LE. Cmin) CCao(J) = (.4+ICa/126.)*(Cmax-Cmin)+Cmin
    IF(CCao(J) .GE. Cmax) CCao(J) = (.7+ICa/170.)*(Cmax-Cmin)+Cmin
    IF(CCao(J) .EQ. CCaoold) CCao(J) = (.5-ICa/400.)*(Cmax-Cmin)+Cmin
    IF(CCao(J) .EQ. Z) CCao(J) = (.6-ICa/400.)*(Cmax-Cmin)+Cmin

    IF(ICa.EQ.49) THEN
        DO 550,MM=M,MStart(J),-1
        IF(ShellFlux(J,MM).LT.0) THEN
            MStart(J)=MStart(J)+1
            MINUS=1
            if(dis.ge.9999.and.j.ne.0.and.dis.le.9998) then
            print *, 'shellflux <0 at ICa=49, mstart reset, ms=',mstart(J),
            & ' dis=',dis
            endif
            GO TO 10
        ENDIF
    550    CONTINUE
    ENDIF

    CCaoold=Z
    GO TO 199

201    CONTINUE
    if(dis.ge.9999.and.j.ne.0.and.dis.le.9998) then
    print *, 'ica=',ica,' cmin=',cmin,' cmax=',cmax
    print *, 'dcdr=',dcdr,' dcdrgoal=',dcdrgoal,' dcdrold=',dcdrold
    print *, 'cold=',cold(J),' cca0=',cca0(J),' z=',z
    print 3,'IN=',in,' NCa=',nca,' m=',m,' L=',l,' RR=',rr
    endif
    IF(IFlux(J).EQ.1.AND.SolFrac(J,M).GT..7) THEN
        ShellFlux(J,M)=-4*R0**2*(dCdR*Dlime-ER*C/55334)
    ELSE
        ShellFlux(J,M)=-4*R0**2*dCdR*Dlime
    ENDIF
    if(dis.ge.9999.and.j.ne.0.and.dis.lt.9998) print 98,'m=',m,
    & ' shlflx=',
    & shellflux(j,m),' ER=',er
    if(dis.ge.9999.and.j.ne.0.and.dis.lt.9998) print *,
    & ' wet shlflx=',shellflux(
    & j,m),' emtflux=',4*r0**2*cmtso2*ys8

C Find shell where calculated flux is negative (due to evaporation)
and
C begin again at next larger shell. If one isn't found, begin
again at
C the next smaller shell until a negative flux is found (MINUS is
than
C set to 1) and calculate final profile.

    DO 300,MM=NStart(J),MStart(J),-1
    IF(ShellFlux(J,MM).LT.0) THEN
        MStart(J)=MM+1

```

```

    IF(MStart(J).GT.NStart(J)) MStart(J)=NStart(J)
    if(dis.ge.9999.and.j.ne.0.and.dis.lt.9998) print *, 
    &'shlflx<0, ms+1='
    & ,mstart(J), ' ****
    MINUS=1
    GO TO 10
  ENDIF
300  CONTINUE
  IF(MStart(J).NE.1.AND.MINUS.EQ.0) THEN
    MStart(J)=MStart(J)-1
    if(dis.ge.9999.and.j.ne.0.and.dis.lt.9998) print *, 
    & 'minus=0, ms-1=',mstart(J)
    GO TO 10
  ENDIF
  if(dis.ge.9999.and.j.ne.0.and.dis.lt.9998) print *

```

R=0
 RR=0
 DO 110,MM=1,MStart(J)-1
 ShellFlux(J,MM)=0
 R=R+dR(J,MM)
 110 RR=RR+dR(J,MM)

M=MStart(J)-1
 ICOUNT=0
 IF(IPZ.EQ.1) PRINT *, 'R=', ZZZ, 'L=', NZZ, ' Ca=', CCa0(J)
 & , ' dCdR=', ZZZ
 DO 210, L=1, NCa
 ICOUNT=ICOUNT+1
 IF(L/FLOAT(IN)-INT(L/IN).LT..01) ICOUNT=0
 IF(ICOUNT.EQ.1) THEN
 M=M+1
 IF(M.NE.NStart(J)) THEN
 xdR=dR(J,M)/IN
 ELSE
 xdR=(R0-RR)/IN
 ENDIF
 RR=RR+dR(J,M)
 ENDIF
 R=R+xdR
 IF(IPZ.EQ.1) PRINT *, 'R=', r, 'L=', l, ' Ca=', CCa(L)
 & , ' dCdR=', dcdr

210 CONTINUE
 RETURN
 END

Table A-4. Function CaDif.

```
FUNCTION CaDif(C,dCdR,R,J,M,VRR,ER)

C Second order differential equation governing diffusion of SO2
C the droplet or agglomerate.

REAL W(7,15),WPD(15,50),NPART(15,50),KDISSOC
REAL SolFrac(15,50)
REAL *8 R,C,dCdR
INTEGER Mevap(15),IFlux(15)

COMMON/DUM/W,WPD
COMMON/SA/RoughK
COMMON/LIME/Dlime,ClimeEq
COMMON/AG/DissRate,RateK,Dprod,WETRATE
COMMON/NPDR/NPart
COMMON/E/SD,PDO,SP,PDD
COMMON/MEVAP/Mevap
COMMON/SOL/SolFrac
COMMON/MOLD/Mold
COMMON/CLEDUM/CLEdum
COMMON/IF/IFlux
common/dis/dis

IF(M.NE.Mold) Rough=1+EXP(Roughk* ( (WPD(J,M)/PDO)**3-.8))

C Liquid phase mass transfer.

IF(WPD(J,M).GT.0) THEN

  IF(M.NE.Mold.OR.J.NE.Jold) THEN
    EP=NPart(J,M)/1.33333333/VRR
    Delta=(1/SolFrac(J,M)**.333333-1)
    IF(Delta.GT.1) Delta=1
    Delta=Delta*WPD(J,M)/2
    CC=EP/(1-SolFrac(J,M))/(Dlime/Rough/DissRate/WPD(J,M)**2+
    & (2/WPD(J,M)-1/(WPD(J,M)/2+Delta))/4)
  ENDIF

  ELSE
    CC=0
  ENDIF

  A=CC
  B=0
  IF(R.NE.0) THEN
    B=2*Dlime/R
    IF(IFlux(J).EQ.1.AND.SolFrac(J,M).GT..7) A=A+2*ER/55334/R
  ENDIF
  IF(IFlux(J).EQ.1.AND.SolFrac(J,M).GT..7) B=B-ER/55334
```

```
CaDif=-CC*CLEdum+A*C-B*dCdR

if(dis.ge.9999.and.dis.lt.9998) then
print *, 'j=',j,' m=',m,' solfrac(j,m)=',solfrac(j,m)
print *, 'Rough=',rough,' ep=',ep,' delta=',delta
print *, 'cc=',cc,' a=',a,' b=',b
print *, 'CaDif=',cadif
endif

Mold=M
Jold=J
RETURN
END
```

Table A-5. Subroutine CHK.

```
SUBROUTINE CHK(HMIN,Dist,VAR)

C Assign appropriate step size values to each drop size.

REAL *8 HMIN,Dist
REAL DropDiam(15),VAR(7,15)
INTEGER ISTOP(15)

COMMON/I/ISTOP
COMMON/IMIN/IMIN
COMMON/RKPR/NW,NE
COMMON/PRNT/GV
COMMON/DROP/DropDiam

IF(ISTOP(NW).EQ.1) THEN
  HMIN=2D-2
  GO TO 101
ENDIF

DO 100,I=1,NW

IF(ISTOP(I).EQ.1) GO TO 100
IF(DropDiam(I).LE.9E-6) THEN
  HMIN=1D-3
ELSEIF(DropDiam(I).LE.12E-6) THEN
  HMIN=2D-3
ELSEIF(DropDiam(I).LE.24E-6) THEN
  HMIN=1D-2
ELSEIF(DropDiam(I).LE.42E-6) THEN
  HMIN=2D-2
ELSEIF(DropDiam(I).LE.64E-6) THEN
  HMIN=1D-1
ELSEIF(DropDiam(I).LE.84E-6) THEN
  HMIN=2D-1
ELSE
  HMIN=5D-1
ENDIF
IF(VAR(5,I).GE.1) HMIN=HMIN/10
IF(GV.LT.8.1.AND.VAR(4,I).LT.8) HMIN=HMIN/INT(16/VAR(4,I))
IF(GV.LT.1) HMIN=HMIN*3
IF(GV.GT.23) HMIN=HMIN*INT(VAR(4,I)/12)
GO TO 101
100 CONTINUE

101 IF(Dist.LT.2D-1-1D-5.AND.HMIN.GT.1D-2) HMIN=1D-2
IF(Dist.GT..1-1D-5.AND.Dist.LE.1-1D-4.AND.HMIN.GT.1D-1) HMIN=1D-1
IF(Dist.GT.1.AND.HMIN.GT.2D-1) HMIN=2D-1

RETURN
```



```

C      RateK=.01
C      Dprod=1E-6
C      DissRate =1.0e-3

C Initialize variables and print output headings.

IJJ=0
CALL INITIAL(III,PSDPt,DuctLength,VAR,PD,IJJ)
IF(IJJ.EQ.1) GO TO 866

CLOSE(UNIT=24)

C Initialize operational variables.

J=1
ID=0
Dist=0
IPSD=0
ICHK=0
IHED=0
IF(Slu.NE.'D') ICHK=1
IPRNT=0
IWARN=0
ICEASE=0
PRNTSTP=.01

C Determine the inital step size.

H=1D-4
IF(Slu.NE.'D') CALL CHK(H,Dist,VAR)

C Perform numerical calculations.

50      CONTINUE
IF(Slu.EQ.'A'.AND.IHED.EQ.0.AND.ABS(VAR(4,NW)-GV).LT.1) THEN
  PRINT *
  CALL PRINT(Dist,VAR,PD,ID,1)
  IHED=1
  CALL HEADING
ENDIF

CALL RUNGKUTT(VAR,PD,Dist,H,IWARN)
IF(ICEASE.EQ.1) GO TO 867
Dist=Dist+H
dis=dist

C For dry sorbent/condensation case change step size when
condensation
C      has ceased.

C Change frequency of printout with distance and adjust step size.

```

```

IF(Slu.EQ.'D'.AND.IDRY.EQ.1.AND.ICHK.EQ.0) THEN
  H=1D-3
  ICHK=1
ENDIF

IF(Dist.GT..1-1D-5.AND.ICHK.EQ.1) THEN
  PRNTSTP=.1
  IF(Slu.EQ.'D'.AND.IDRY.EQ.1) THEN
    H=5D-3
  ELSEIF(Slu.NE.'D') THEN
    CALL CHK(H,Dist,VAR)
  ENDIF
  ICHK=2
ELSEIF(Dist.GT.1-1D-4.AND.ICHK.EQ.2) THEN
  PRNTSTP=1
  ICHK=3
ELSEIF(Dist.GE.9.99.AND.ICHK.EQ.3) THEN
  ICHK=4
  PRNTSTP=2.5
ELSEIF(Dist.GE.39.99.AND.ICHK.EQ.4) THEN
  ICHK=5
  PRNTSTP=5
ELSEIF(Dist.GE.59.99.AND.ICHK.EQ.5) THEN
  PRNTSTP=10
ENDIF

```

C Print results if spray has evaporated.

```

IF(IWARN.NE.0) THEN
IF(IWARN.EQ.4) THEN
PRINT *
PRINT *, 'Spray has evaporated, final results:'
PRINT 77, 'At distance=', Dist, ':'
PRINT *
CALL HEADING
77   FORMAT(A13,F7.3,A1)
GO TO 867

```

C If program is diverging cease program execution.

```

ELSEIF(IWARN.EQ.5) THEN
  PRINT *, 'IWARN=', IWARN
  GO TO 867
ELSE

PRINT 1
PRINT *, 'PROGRAM HAS DIVERGED, FINAL OUTPUT:'
  PRINT *, 'Step Size=', H, ' meters'
  print *, 'iwarn= ', iwarn
PRINT *
CALL HEADING
  CALL PRINT (Dist,VAR,PD,ID,0)
PRINT 1
GO TO 867

```

```
ENDIF
ENDIF
1      FORMAT(1X,80('*'))
```

C Print drop variables at specified distances.

```
ipz=0
IF(Dist.GT.DuctLength) GO TO 867
IF(INT(Dist/PSDpt(J)).NE.IPSD) THEN
  CALL PRINT (Dist,VAR,PD,ID,0)
  J=J+1
  IPSD=Dist/PSDpt(J)
  IPRNT=Dist/PRNTSTP+1D-5
  CALL HEADING
ipz=2
  GO TO 50
ENDIF
IPSD=Dist/PSDpt(J)
```

C Print results at varing distances.

```
IF(INT(Dist/PRNTSTP+1D-5).NE.IPRNT) THEN
  CALL PRINT(Dist,VAR,PD,ID,1)
ENDIF
IPRNT=Dist/PRNTSTP+1D-5

GO TO 50

867      CALL PRINT (Dist,VAR,PD,ID,0)
866      CONTINUE
10       format(F7.5)

400      CLOSE(UNIT=2)
        STOP
END
```

Table A-7. Subroutine DELR(J).

```
SUBROUTINE DELR(J)

C Calculate size of radial differential shells.

REAL DropDiam(15),dR(15,50)
REAL VolPart(15,50)
INTEGER NSHELL(15),Mevap(15),ISTOP(15)

COMMON/DROP/DropDiam
COMMON/DR/dR
COMMON/NS/NSHELL
COMMON/MEVAP/Mevap
COMMON/VL/VolPart
COMMON/I/ISTOP
common/dis/dis

IF(Mevap(J).EQ.0) RETURN

C In each shell, calculate the volume of solids (VolPart), the
minimum
C delta radius (delR) which is based on a close packing of 75%
solid
C spheres.

R=DropDiam(J)/2
DO 10,M=NSHELL(J),1,-1

C If the shell has stopped evaporating set dR to the close packing
value.

IF(M.GT.Mevap(J)) THEN

  IF(R**3.GT.VolPart(J,M)/3.14159) THEN
    dR(J,M)=R-(R**3-VolPart(J,M)/3.14159)**.3333333
  ELSE
    Mevap(J)=0
    ISTOP(J)=1
    R=0
    DO 201,L=1,NShell(J)
      dR(J,L)=(R**3+VolPart(J,L)/3.14159)**.3333333-R
  201  R=R+dR(J,L)
    DropDiam(J)=2*R
    RETURN
  ENDIF

C If the shell is the evaporating shell calculate dR and the close
C packing dR and, if dR is less than delRmin set equal to delRmin.

ELSEIF(M.EQ.Mevap(J)) THEN
```

```

dR (J, M) =R- (M-1) *dR (J, 1)
IF (R**3.GT.VolPart (J, M) /3.14159) THEN
  delRmin=R- (R**3-VolPart (J, M) /3.14159) **.3333333
ELSE
  Mevap (J) =0
  R=0
  DC 200, L=1, NShell (J)
  dR (J, L) =(R**3+VolPart (J, L) /3.14159) **.3333333-R
200  R=R+dR (J, L)
  DropDiam (J) =2*R
  RETURN
ENDIF

IF (dR (J, M) .LE. delRmin) THEN
  dR (J, M) =delRmin
  Mevap (J) =Mevap (J) -1
ENDIF

ELSEIF (M.LT.Mevap (J) ) THEN
  RETURN
ENDIF

10  R=R-dR (J, M)

RETURN
END

```

Table A-8. Function DIFF.

```
FUNCTION DIFF(C,dCdR,R,dR,J,M,VRR,ILERT,ER)

C Second order differential equation governing diffusion of SO2
C the droplet or agglomerate.

REAL W(7,15),WPD(15,50),NPART(15,50),RWCore(15),KDISSOC
REAL Rdry0(15,50),SolFrac(15,50)
REAL *8 R,dR,dCdR
INTEGER Mevap(15),IFlux(15)

COMMON/DUM/W,WPD
COMMON/SA/RoughK
COMMON/SO2/DSO2,CMTSO2,HE,KDISSOC,DH2SO3,DHSO3,YS8
COMMON/AG/DissRate,RateK,Dprod,WETRATE
COMMON/LIME/Dlime,ClimeEq
COMMON/NPDR/NPart
COMMON/E/SD,PDO,SP,PDD
COMMON/MEVAP/Mevap
COMMON/RW/RWCore
COMMON/RD/Rdry0
COMMON/A/ALPHA
COMMON/SOL/SolFrac
COMMON/MOLD/Mold
COMMON/IF/IFlux
common/dis/dis

IF(M.NE.Mold) Rough=1+EXP(Roughk* ((WPD(J,M)/PDO)**3-.8))
IF(ILERT.EQ.0) THEN

C Liquid phase mass transfer.

A=2*DHSO3/KDISSOC*C+DH2SO3
B=2*DHSO3/KDISSOC*dCdR
IF(R.NE.0) B=B+2*A/R
IF(IFlux(J).EQ.1.AND.SolFrac(J,M).GT..7)
B=B+(1+2*C/KDISSOC)*
& ER/55334

IF(IFlux(J).EQ.1.AND.SolFrac(J,M).GT..7) THEN
  EVTERM=(C+C**2/KDISSOC)*ER*2/R/55334
ELSE
  EVTERM=0
ENDIF

IF(WPD(J,M).GT.0) THEN
  IF(M.NE.Mold.OR.J.NE.Jold) THEN
    U=4*Dlime*ClimeEq
    V=4*Dlime/Rough/DissRate/WPD(J,M)**2
    EP=NPart(J,M)/VRR/1.33333
    DUM2=1/Rough/DissRate/WPD(J,M)**2
  ENDIF
```

```

        dmoldt=CLimeEq/(DUM2+(2/WPD(J,M)-1/(WPD(J,M)/2+
&           Del(C,WPD(J,M),U,V,J,M)))/4/DLime)
        DIFF=(dmoldt*EP/(1-SolFrac(J,M))-EVTERM-B*dCdR)/A
    ELSE
        DIFF=(-EVTERM-B*dCdR)/A
    ENDIF

    ELSE

C Gas phase mass transfer through dried agglomerate.

    Deff=DSO2*(1-SolFrac(J,M))
    IF(Rdry0(J,M).EQ.0) THEN
        Rdry0(J,M)=WPD(J,M)/2
        B=0
    ELSE

        Rratio=1/(ALPHA*(2*Rdry0(J,M)/WPD(J,M))**3+1-ALPHA)**.33333333
        B=12.5664*NPart(J,M)/((R+dR)**3-R**3)*
        &           (WPD(J,M)/2)**2/Deff/(1/Ratek/Rough+WPD(J,M)/2/
        &           Dprod*(1-Rratio))
    ENDIF
    DIFF=B*C-2/R*dCdR

    ENDIF

    Mold=M
    Jold=J
    RETURN
END

FUNCTION DEL(C,PD,U,V,J,M)

REAL KDISSOC,SolFrac(15,50)
COMMON/SOL/SolFrac
COMMON/SO2/DSO2,CMTSO2,HE,KDISSOC,DH2SO3,DHSO3,YS8

Delta=(1/SolFrac(J,M)**.333333-1)
IF(Delta.GT.1) Delta=1
Delta=Delta*PD/2
IF(C.GT.0) THEN
    T=DHSO3*C+2*DHSO3*C**2/KDISSOC
    Del=(U+T)/(2*T/PD+T*V+U/(PD/2+Delta))-PD/2
ELSE
    Del=Delta
ENDIF

RETURN
END

```

Table A-9. Function ETA.

```
FUNCTION ETA(U,D,SD,PD)
C Calculate collision efficiency.

IMPLICIT REAL (N)

COMMON/PRNT/GV
COMMON/ET/ReG,VisG

PSI=SD*PD**2*(U-GV)/18/VisG/D

IF(PSI.LT.1./24) THEN
  NIP=0
ELSE
  NIP=4*PSI**2/(2*PSI+.5)**2
ENDIF

IF(PSI.LE..607) THEN
  NIV=0
ELSE
  NIV=1/(1+.75* ALOG(4*PSI)/(2*PSI-1.214))**2
ENDIF

IF(ReG.LE.1) THEN
  NI=NIV
ELSE
  NI=(NIV+NIP*ReG/60)/(1+ReG/60)
ENDIF

R=1+PD/D
NCV=R*R-3./2*R+1./2/R

IF(ReG.LE.1) THEN
  NCP=0
ELSE
  NCP=R**2-1/R
ENDIF

IF((U-GV).EQ.0) THEN
  NC=0
ELSE
  NC=(NCV+NCP*ReG/60)/(1+ReG/60)
ENDIF

ETA=1-(1-NI)*(1-NC)

RETURN
END
```

Table A-10. Subroutine FLX.

SUBROUTINE FLX(J,ER,SMF)

C This subroutine calculates concentration from the second-order
C differential equation of C with respect to R using a
C 4th order Runge-Kutta method.

```
IMPLICIT REAL (K)
REAL dR(15,50),KDISSOC,RWCore(15),dRSO2(15)
REAL C0(15),ShellFlux(15,50),CD0(15)
REAL DropDiam(15),W(7,15),WPD(15,50),NPart(15,50)
REAL MolWt,SolFrac(15,50)
REAL *8 R,xdR,Rold1(15),R0,Rmin,Rmax,Z,XS8,YS8CALC
REAL *8 YS8OLD(15),dCDR
REAL CP(0:55)
INTEGER NSHELL(15),NStart(15),Mevap(15),IFlux(15)

COMMON/DUM/W,WPD
COMMON/DR/dR
COMMON/SO2/DSO2,CMTSO2,HE,KDISSOC,DH2SO3,DHSO3,YS8
COMMON/NS/NSHELL
COMMON/NT/NStart
COMMON/RW/RWCore
COMMON/DROP/DropDiam
COMMON/MEVAP/Mevap
COMMON/NPDR/NPart
COMMON/VOL/VolMol,CaUt
COMMON/MOL/MolWt
COMMON/C0/C0
COMMON/SS/dRSO2
COMMON/ROLD/Rold1
COMMON/ICE/ICEASE
COMMON/SHEL/ShellFlux
COMMON/MOLD/Mold
COMMON/LIME/Dlime,ClimeEq
COMMON/CCA0/CCa0
COMMON/IF/IFlux
COMMON/SOL/SolFrac
COMMON/P/CD0,SMF0
common/dis/dis
common/pz/ipz
common/cas/cas
```

```
DO 113,M=1,NShell(J)
113 IF(WPD(J,1).GT.0) GO TO 114
      RETURN
```

C SO₂ concentration profiles are calculated using a separate set of
C radial shells. The term droplet radial shell will refer to the
radial
C shells used throughout the rest of the program and the term L
shells

C will refer to the radial shells used in this subroutine to calculate
C the SO₂ concentration profile.

```
114 IF(C0(J).EQ.0) THEN
      IDIV2=0
    ELSE
      IDIV2=1
    ENDIF

    ISC=1
    XS8=YS8
    Rmin=0
    Rmax=DropDiam(J)/2
    R0=Rmax-dRSO2(J)
    IF (dRSO2(J).EQ.0.AND.WPD(J,NShell(J)).EQ.0)
R0=DropDiam(J)*.4998
    Mold=0
    IF(R0.LT.0.OR.C0(J).GT.0.AND.C0(J).LE.1E-6) C0(J)=2E-6
    dCdREMT0=CMTSO2*YS8/Dlime
    dCdR0=0
    IF(IFlux(J).EQ.1) dCdR0=ER/Dlime/55334
    Cmin=0
    CSMAX=SQRT(YS8*KDISSOC/HE)
    Cmax=CSMAX
    IF(C0(J).NE.0) THEN
      CP(0)=C0(J)
    ELSE
      CP(0)=0
    ENDIF
    IDC=0
    IDiverge=0

10  IDiverge=IDiverge+1
    IF(R0.LT.0) R0=0
    if(dis.ge.9999.and.j.ne.0.and.dis.lt.1.751)THEN
      if(c0(j).ne.0) print *, 'c0=',c0(J)
      print *, 'j=',j,' r0=',z,' rmin=',rmin,' rmax=',rmax
      z=r0
      print *, 'R0 new=',r0
      print *, 'ys8=',ys8,'ys8c=',ys8calc,' idiverge=',idiverge
      & , ' idiv2=',idiv2,' mevap=',mevap(j)
      do 761,i=0,11
761  print *, 'cp(1,1,1)=',cp(1)
C      print *, 'L, sorbent diameters= , dR= , '
C      & , ' Npart= , SHLFLUX='
C      do 9,l=NSTART(J),nshe1l(J)
C9      print *,l,wpd(j,l),dr(j,l),NPart(j,l),SHELLflux(j,l)
      PRINT *
      endif
      IF(IDiverge.EQ.45) THEN
        P          R          I          N          T
      *,*****SECANT METHOD HAS DIVERGED. PROGRAM
```

TERMINATED***'

C Find initial radial shell position. Calculate VRR, the volume of the

C droplet radial shell/Pi.

R_R is the radius of the outer edge of the droplet radial shell.

C R is the inner edge of L shell.

```

IF(C0(J).NE.0.AND.DropDiam(J)/2.EQ.RWCore(J)) THEN
  M=1
  NStart(J)=1
  R=0
  CP(0)=C0(J)
  VRR=dR(J,1)**3
  RR=dR(J,1)
ELSE
  RR=0
  CP(0)=0
  DO 15,M=1,NShell(J)
    RR=RR+dR(J,M)
C Do not remove the following if statement.
  if(dis.ge.9999.and.j.ne.0.and.dis.lt.1.751)print*, 'm=',m,
rr=',,
  &           rr,' r0=',r0
  IF(RR.GE..9999999*R0) THEN
    NStart(J)=M
    GO TO 16
  ENDIF
  CONTINUE
15

```

1.5 CONTINUE

ENDIE

IF(C0(J),EQ,0) THEN

IF (C0 (S) .EQ. 0) THEN
 R0 = (Rmin+Rmax)/2

```

      R0= (RMIN+RMAX)/2
if(dis.ge.9999.and.j.ne.0.and.dis.lt.1.751)THEN
  print *, 'RR and M not found (R0>RR)'
  print*, 'RR=', rr, ' new R0=', r0, ' R=', dropdiam(J)/2, ' RWc=',
&           rwcore(J)
  print *, 'm=', m
  print *
endif

```

```

        GO TO 10
ENDIF
if(c0(J).eq.0) then
print *, ' should not be reached!!!!!! after initial M, M=',m
print *, 'ns=',nshell(J), ' r0=',r0,' RR=',rr,
D/2=',dropdiam(J)/2
print *, 'ys8=',ys8,' ys8c=',ys8calc
print *, 'rmin=',rmin,' rmax=',rmax,' rold1=',rold1(J)
print *
endif

C      C a l c u l a t e      c a l c i u m
profile.*****  

16  IF(C0(J).EQ.0) THEN
    CALL CA(J,R,R0,dCdR,dCdREMT0,dCdR0,VRR,ER,IRWARN)
    IF(IRWARN.EQ.1) THEN
        IRWARN=0
        R0=.999*R0
        GO TO 10
    ENDIF
    IF(ICEASE.EQ.1) RETURN
    dCdR=-Dlime/DHSO3*dCdR
    R=R0
    ELSE
        dCdR=0
    ENDIF
    if(dis.ge.9999.and.j.ne.0.and.dis.lt.1.751)THEN
        print *, 'At R0 in FLX, dCdR= ',DCDR,' CP=',CP(0)
    endif

    IF(ShellFlux(J,NStart(J)).LT..99*ShellFlux(J,NStart(J)-1).AND.
    & NStart(J).NE.1) THEN
        Rmax=R0
        R0=(.5+.17*ISC+IDiverge/400.)*(Rmax-Rmin)+Rmin
        ISC=-ISC
        if(dis.ge.9999.and.j.ne.0.and.dis.lt.1.751)THEN
            print *, 'shf(j,ns)<shf(j,ns-1) in caflux'
        endif
        GO TO 10
    ENDIF

    IF(ABS(R0-DropDiam(J)/2).LT..00005*DropDiam(J)/2) THEN
        R0=RWCore(J)
        xs=0
        GO TO 30
    ENDIF

C      C a l c u l a t e      s u l f u r
profile.*****  

        IN=15./ (NShell(J)-NStart(J)+1)+.99999999
        IF(IN.LT.2) IN=2
        LL=IN*(NShell(J)-NStart(J)+1)

```

```

ILERT=0
Mold=0
if(dis.ge.9999.and.j.ne.0.and.dis.lt.1.751)print*,
&'before loop, m=',m,' ll=',ll
DO 20,L=1,LL
if(dis.ge.9999.and.j.ne.0.and.dis.lt.1.751)print *, 'in loop,
m='
& ,m,' L=',l

ICOUNT=ICOUNT+1
IF(L/FLOAT(IN)-INT(L/IN).LT..01) ICOUNT=0
IF(ICOUNT.EQ.1.AND.L.NE.1) THEN
  ShellFlux(J,M)=4*R**2*dCdR*(2*DHSO3*CP(L-1)/KDISSOC+DHSO3)
  IF(IFlux(J).EQ.1.AND.SolFrac(J,M).GT..7) ShellFlux(J,M)=
  & ShellFlux(J,M)+CP(L-1)*ER/55334*4*R**2

if(dis.ge.9999.and.j.ne.0.and.dis.lt.1.751)print*, 'shellflux(j, '
& ,m,')=' ,shellflux(j,m)
M=M+1
IF(M.NE.NStart(J)) THEN
  xdR=dR(J,M)/IN
ELSE
  xdR=(RR-R0)/IN
ENDIF
RR=RR+dR(J,M)
VRR=RR**3-(RR-dR(J,M))**3
ELSEIF(L.EQ.1) THEN
  xdR=(RR-R0)/IN
ENDIF

C Perform Runge-Kutta.

if(dis.ge.9999.and.j.ne.0.and.dis.lt.1.751)THEN
  print*, 'cp(l-1)=' ,cp(l-1), ' dcdr=' ,dcdr, ' r=' ,r, ' xdr=' ,xdr
  print *, 'vrr=' ,vrr, ' er=' ,er
endif
18 K11=xdR*dCdR
K12=xdR*DIFF(CP(L-1),dCdR,R,xdR,J,M,VRR,ILERT,ER)
K21=xdR*(dCdR+K12/2)

K22=xdR*DIFF(CP(L-1)+K11/2,dCdR+K12/2,R+xdR/2,xdR,J,M,VRR,ILERT
& ,ER)
K31=xdR*(dCdR+K22/2)

K32=xdR*DIFF(CP(L-1)+K21/2,dCdR+K22/2,R+xdR/2,xdR,J,M,VRR,ILERT
& ,ER)
K41=xdR*(dCdR+K32)
K42=xdR*DIFF(CP(L-1)+K31,dCdR+K32,R+xdR,xdR,J,M,VRR,ILERT,ER)


```

```

C For the case when a radial shell has not been encountered
(INSEC=0).
C For the case when a radial shell has been encountered (INSEC=1),
C up to the outer radius of the droplet radial shell.

```

C For the case after a radial shell has been encountered (INSEC=2),
C up to the outer radius of the L shell.

```
CP(L)=CP(L-1)+(K11+2*K21+2*K31+K41)/6
dCdR=dCdR+(K12+2*K22+2*K32+K42)/6
if(ipz.eq.1.or.dis.ge.9999.and.j.ne.0.and.dis.lt.1.751)
&print *, 'm=',m,' r=',r+xdr,' c=',cp(l),' dCdR=',dcdr
98 format(1x,a,i2,a,e12.4)
```

C If ShellFlux wasn't calculated above, (for C0.NE.0) calculate here.

```
IF(C0(J).NE.0.OR.L.EQ.LL) THEN

ShellFlux(J,M)=4*(R+xdr)**2*dCdR*(2*DHSO3*CP(L)/KDISSOC+DHSO3)
  IF(IFlux(J).EQ.1.AND.SolFrac(J,M).GT..7) ShellFlux(J,M)=
  &      ShellFlux(J,M)+CP1*ER/55334*4*(R+xdr)**2
  if(dis.ge.9999.and.j.ne.0.and.dis.lt.1.751)print *,
  &'shellflux(j,'',m,'')=',shellflux(j,m)
  ENDIF
c  IF(dCdR.LT.0) ShellFlux(J,M)=0
```

C If CP is decreasing or becoming to big, assign new Rmin value.

```
23  IF(L.EQ.LL.AND.CP(L).LT.CP(L-1).AND.C0(J).EQ.0.AND.WPD(J,M)
  &      .EQ.0.) THEN
    Rmax=R0
    if(dis.ge.9999.and.j.ne.0.and.dis.lt.1.751)print *,
    &      ' cp<cp(l-1) at L=LL, Rmin=R0'
    R0=.25*(Rmax-Rmin)+Rmin
    GO TO 10
  ELSEIF(CP(L).LT.CP(L-1).AND.C0(J).EQ.0) THEN
    if(dis.ge.9999.and.j.ne.0.and.dis.lt.1.751) print *,
    &      ' cp>cp(l-1), Rmin=R0'
    Rmin=R0
    R0=.3*(Rmax-Rmin)+Rmin
    GO TO 10
  ELSEIF(CP(L).GT.2*CSMAX.AND.C0(J).EQ.0) THEN
    if(dis.ge.9999.and.j.ne.0.and.dis.lt.1.751) print *,
    &      ' cp>2*csmax ('',csmax,''), Rmin=R0'
    Rmin=R0
    R0=.7*(Rmax-Rmin)+Rmin
    GO TO 10
  ELSEIF(C0(J).NE.0.AND.C0(J).LT.1E-10) THEN
    GO TO 307
  ELSEIF(CP(L).LT..85*CP(L-1).AND.C0(J).NE.0) THEN
    Cmax=C0(J)
    C0(J)=.67*(Cmax-Cmin)+Cmin
    GO TO 10
  ELSEIF(CP(L).GT.1.2*CSMAX.AND.C0(J).NE.0) THEN
    Cmax=C0(J)
    C0(J)=.25*(Cmax-Cmin)+Cmin
    GO TO 10
  ENDIF
```

20 R=R+xdR

C Check to see if the calculated ambient concentration equals the
C actual ambient concentration of SO2. If not, correct the
C guessed concentration using the secant method.

```
IF (ILERT.EQ.0) THEN
  XS=HE*CP(LL)**2/KDISSOC
  AA=dCdR*(2*DHSO3*CP(LL)/KDISSOC+DHSO3)+(CP(LL)+CP(LL)**2/
& KDISSOC)*ER/55334
ELSE
  XS=CP(LL)
  AA=dCdR
ENDIF

YS8CALC=(XS*(CMTSO2-ER-AA)+AA)/CMTSO2

IF (DABS(XS8-YS8CALC).LT..001*XS8.OR.
& Rmax-Rmin.LT.1D-5*Rmin.AND.IDiverge.GT.20.OR.
& IDiverge.GT.25.AND.IDIV2.EQ.2.AND.R0.LT.2D-8) GO TO 30
```

C Calculate new C0 for the case where SO2 diffuses to the droplet center.

307 IF(C0(J).NE.0) THEN

C Switch to the case where SO2 drops to zero at some point not at the
C center.

```
IF(C0(J).LT.1E-10) THEN
  R0=.7*(Rmax-Rmin)+Rmin
  Rold1(J)=.001*DropDiam(J)
  YS8OLD(J)=YS8CALC
  C0(J)=0
  CP(0)=0
  IDC=0
  IDIV2=IDIV2+1
  IDIVERGE=0
  GO TO 10
ENDIF
```

C Reassign new Cmin or Cmax value.

```
IF(C0(J).LT.Cmax.AND.YS8CALC.GT.YS8) THEN
  Cmax=C0(J)
ELSEIF(C0(J).GT.Cmin.AND.YS8CALC.LT.YS8) THEN
  Cmin=C0(J)
ENDIF

IF(YS8CALC.GT.1) THEN
  C0(J)=C0(J)/2
  Cold1=0
  YS8OLD(J)=0
ELSE
```

```

Z=C0(J)
IF(C0(J).EQ.Cold1) THEN
  C0(J)=C0(J)*.99
ELSE
  C0(J)=C0(J)-(YS8-YS8CALC)/(YS8OLD(J)-YS8CALC)*
& (C0(J)-Cold1)
  IF(C0(J).EQ.0) C0(J)=1D-5
  IF(C0(J).GT.Cmax) THEN
    C0(J)=.7*(Cmax-Cmin)+Cmin
  ELSEIF(C0(J).LT.Cmin) THEN
    C0(J)=.3*(Cmax-Cmin)+Cmin
  ENDIF
  Cold1=Z
  ENDIF
ENDIF
CP(0)=C0(J)

```

C For the case where sulfur drops to zero away from the droplet center.

```
ELSE
```

C Reassign new Rmin or Rmax value.

```

IF(R0.LT.Rmax.AND.YS8CALC.LT.YS8) THEN
if(dis.ge.9999.and.j.ne.0.and.dis.lt.1.751)print*,'
& 'R0<Rmax,YS8C<YS8,Rmax=R0'
  Rmax=R0
ELSEIF(R0.GT.Rmin.AND.YS8CALC.GT.YS8) THEN
if(dis.ge.9999.and.j.ne.0.and.dis.lt.1.751)print*,'
& 'R0>Rmin,YS8C>YS8,Rmin=R0'
  Rmin=R0
ENDIF

```

C Switch to sulfur diffusion to the center if necessary.

```

IF(Rmax-Rmin.LT..002*DropDiam(J)/2.AND.R0.LT.DropDiam(J)/50
&
.AND.IDiverge.GT.20.AND.Rold1(J).LT.DropDiam(J)/50.AND.IDIV2
& .LT.2) THEN
  C0(J)=CP(1)*2
  Cold1=CP(1)
  IDIVERGE=0
  R0=0
  IDIV2=IDIV2+1
  IDC=0
  GO TO 10
ENDIF

```

C Calculate new R0.

```

IF(IDiverge.GE.10.and.IDiverge.LT.15.OR.IDiverge.GE.30.AND.
& IDiverge.LT.35) THEN
  IF(IIC.EQ.0) THEN

```

```

      R0=(.33+IDiverge/400.)*(Rmax-Rmin)+Rmin
      IIC=1
    ELSE
      R0=(.67+IDiverge/400.)*(Rmax-Rmin)+Rmin
      IIC=0
    ENDIF
  ELSE
    Z=R0
    R0=R0-(XS8-YS8CALC)/(YS8OLD(J)-YS8CALC)*(R0-Rold1(J))
    IF(IDIVERGE.EQ.1) THEN
      R0=DropDiam(J)/2-1.005*(DropDiam(J)/2-Z)
    ENDIF
    IF(R0.GT.DropDiam(J)/2) THEN
      IF(Rold1(J).EQ.0) THEN
        R0=(Rmin+Rmax)/2
      ELSE
        R0=.8*(Rmax-Rmin)+Rmin
      ENDIF
    ELSEIF(R0.GT.Rmax) THEN
      R0=.7*(Rmax-Rmin)+Rmin
    ELSEIF(R0.LT.Rmin) THEN
      R0=.3*(Rmax-Rmin)+Rmin
    ENDIF
    IF(R0.EQ.Z) R0=.67*(R0-Rmin)+Rmin
    IF(R0.EQ.Z) R0=.33*(Rmax-R0)+R0
    Rold1(J)=Z
  ENDIF
ENDIF
YS8OLD(J)=YS8CALC
GO TO 10

30  dRSO2(J)=RWCore(J)-R0
SHOLD=SHELLFLUX(J,NSHELL(J))
IF(Rmax-Rmin.LT.1D-5*Rmin.AND.YS8CALC.LT..98*YS8) THEN
  print *, 'converged by rmax-rmin<1d-5'
  &      ,'*rmin, ys8=',ys8,' ys8c=',ys8calc,' xs8=',xs8
  IF(ICease.EQ.0) ICease=10
  ICease=ICease-1
ENDIF
ShellFlux(J,NShell(J))=SHOLD

if(dis.ge.9999.and.j.ne.0.and.dis.lt.2.411.or.ipz.eq.1) then
sulfnc=6*volmol*dropdiam(J)**2/pd0**3/w(2,j)*(cmtso2*
&      (ys8-xs)+xs*er)*100*cas*SMF/SMFO
axemt=6*volmol*dropdiam(J)**2/pd0**3/w(2,j)*cmtso2*
&      ys8*100*cas*SMF/SMFO
RD=R0/DROPDIAM(j)**2
print *, 'J=',j,' NStart(J)=',nstart(J)
print *, ' Dist=',dis,' dRSO2=',dRSO2(J), ' R0=',r0
print *, ' D=',DropDiam(j), ' 2*R0/D=',RD
print *, ' ys8=',ys8,' ys8calc=',ys8calc,' XS=',XS
print *, ' emt cap=',sulfnc,' max emt=',axemt,' CMTSO2=',CMTSO2
print *, ' iflux(j)=',iflux(J),' Dlime=',dlime,' ER=',er
print *, '           L sorbent diameters      Solfrac '

```

```
&,'          Npart      ShellFlux'
if(r0.eq.0) print *,zzz,' r=',zzz,' cp=',c0(j)
do 6,l=1,nshell(J)
6  print *,l,wpd(j,l),solfrac(j,l),NPart(j,l),SHELLflux(j,l)
if(dis.gt.99) then
r=dropdiam(J)/2
do 7,l=11,1
7  print *,l,' r=',r,' cp=',cp(l)
r=r-ddr
endif
endif
1  FORMAT(1X,3(A,E9.3),2(A,I2),1(A,E9.3),A,F5.0,A,I2)
RETURN
END
```

Table A-11. Function FNC.

```
FUNCTION FNC(IT,I,J,M)

C Calculate the values of the differential equations.
C W(1,1)=Gas Temperature
C W(2,J)=Number of sorbent particles in a drop
C W(3,J)=Number of ash particles in a drop
C W(4,J)=Individual Drop Velocity
C W(5,J)=Mass water remaining in drop
C W(6,J)=Individual Drop Temperature
C WPD(J,M)=Sorbent diameter in drop, function of radial position

      REAL CD0(15),DropNFLux(15),DropDiam(15)
      REAL W(7,15),WPD(15,50)
      INTEGER ISTOP(15),IVSTOP(15)
      CHARACTER *1 Slu

      COMMON/DUM/W,WPD
      COMMON/FN/DropNFLux,DuctArea,AirMassFlux,WVMFlux0
      COMMON/DROP/DropDiam
      COMMON/I/ISTOP
      COMMON/C/IVSTOP
      COMMON/E/SD,P0,SP,PDD
      COMMON/P/CD0,SMF0
      COMMON/PRNT/GV
      COMMON/VOL/VolMol,CaUt
      COMMON/Y/SO2MF0
      COMMON/CAS/CaS
      COMMON/DIR/IDir
      COMMON/SLU/Slu
      COMMON/T0/T0
      COMMON/IDRY/IDRY
      COMMON/DV/DelV0
      COMMON/ICE/ICEASE
      COMMON/ASH/ASHFLUX0,DASH,ASHFLUX
      common/dis/dis

      GO TO (1,2,3,4,5,6,7),I

C Calculate physical constants, size of differential shells, and
flux
C of SO2 through the droplet (or agglomerate).

1
IF(W(5,J).LT..002.OR.W(6,J).GE..99*W(1,1).AND.W(5,J).LT..03)THEN
  IF(Slu.NE.'D') ISTOP(J)=1
ENDIF
IF(ABS(W(4,J)-GV).LT..49) IVSTOP(J)=1

CALL PHY (IT,I,J,Q,ER,ERate,CpW,WVMFlux,HtCapG,SMF,
& DropDens,Re,DenG,HTVAP,HtCapW)
```

```

IF(Slu.NE.'D'.AND.SO2MF0.NE.0.AND.CaS.NE.0.AND.ISTOP(J).NE.1.AND
&.IT.EQ.1.AND.W(2,J).NE.0) THEN
  IF(W(4,J)-GV.LE..4*DelV0.AND.Slu.NE.'S') THEN
    CALL FLX(J,-ER,SMF)
  ELSEIF(Slu.EQ.'S') THEN
    CALL FLX(J,-ER,SMF)
  ENDIF
  IF(ICEASE.EQ.1) RETURN
ENDIF

```

C Calculate the gas temperature diff. eqn.

```

IF(ISTOP(J).EQ.1.OR.IDRY.EQ.1) THEN
  FNC=0
  RETURN
ENDIF

FNC=-DropNFlux(J)/W(4,J)*(Q/T0+ERate*CpW*(W(1,1)-W(6,J)))
&           /(AirMassFlux+WVMFlux)/HtCapG

RETURN

```

C Calculate the sorbent capture diff. eqn. for an individual drop.

```

2  IF(IVSTOP(J).EQ.1.OR.Slu.EQ.'S'.OR.Slu.EQ.'D') THEN
    FNC=0
  ELSE
    FNC=1.5*DropDiam(J)**2*SMF*ETA(W(4,J),DropDiam(J),SD,PDD)
    &           /PDD**3/SD/(1-SP)/W(4,J)/GV*ABS((W(4,J)-GV))
  ENDIF
  FNC1=FNC

RETURN

```

C Calculate the ash capture diff. eqn. for an individual drop.

```

3  IF(IVSTOP(J).EQ.1.OR.Slu.EQ.'D'.OR.W(4,J)-GV.LT..5) THEN
    FNC=0
  ELSE

FNC=1.5*DropDiam(J)**2*ASHFLUX*ETA(W(4,J),DropDiam(J),SD,DASH)
  &           /DASH**3/SD/W(4,J)/GV*ABS((W(4,J)-GV))
  ENDIF
  FNC2=FNC

RETURN

```

C Calculate individual drop deceleration diff. eqn.

```

4  IF(IVSTOP(J).EQ.1.OR.Slu.EQ.'D') THEN
    FNC=0
  ELSE

```

```

FNC=-.75*DenG/DropDens/DropDiam(J)/W(4,J)*(W(4,J)-GV)**2*27/
& Re**.84-IDir*9.8*(DropDens-DenG)/DropDens/W(4,J)
&
-3.14159/6*SD*(1-SP)*PDD**3/W(5,J)/CD0(J)*(W(4,J)-GV)*FNC1
& -3.14159/6*SD*DASH**3/W(5,J)/CD0(J)*(W(4,J)-GV)*FNC2
ENDIF

RETURN

C Calculate the drop water mass diff. eqn.

5 IF(ISTOP(J).EQ.1) THEN
  FNC=0
ELSE
  FNC=-ERate*18/W(4,J)/CD0(J)
C IF(Slu.EQ.'D') FNC=FNC-14.137*(1-SP)*WPD(1,1)**2
C & /VolMol*FNC4/CD0(J)
ENDIF

RETURN

C Calculate the individual drop temperature diff. eqn.

6 IF(ISTOP(J).EQ.0) THEN

FNC=6/3.14159/DropDiam(J)**3*(Q-ERate*HTVAP)/HtCapW/DropDens/
& W(4,J)
C FNC=FNC-444*W(4,J)**2*W(2,J)*(1-SP)/VolMol/DropDiam(J)**3
CC & /DropDens/HtCapW*FNC4
  FNC=FNC/T0
ELSE
  FNC=0
ENDIF

RETURN

C Calculate the sorbent utilization rate.

7 FNC=0
IF(W(2,J).EQ.0.OR.SO2MF0.EQ.0) RETURN

C Solve sulfur capture differential equation module.

CALL SULF(J,M,FNC,ER)

FNC4=FNC

RETURN
END

```

Table A-12. Subroutine HEADING.

```
SUBROUTINE HEADING()

COMMON/CAS/Cas
COMMON/SLU/Slu
COMMON/Y/SO2MF0
COMMON/IHED/IHED

CHARACTER *1 Slu

C Print results heading.

IF(CaS.EQ.0.OR.SO2MF0.EQ.0) THEN
PRINT 200,'Dist','Time','Frac Unevap'
& , 'Gas Temp','App/Sat',' #Wet','Humidity'
ELSEIF(Slu.EQ.'D') THEN
PRINT 100,'Dist','Time','Mole Conden','%Util','%SO2 Cap'
ELSEIF(Slu.NE.'S'.AND.IHED.EQ.0) THEN
PRINT 100,'Dist','Time','Frac Unevap','%Scav','%SO2 Cap'
& , 'Gas Temp','App/Sat',' #Wet','Humidity'
ELSE
PRINT 100,'Dist','Time','Frac Unevap','%Util','%SO2 Cap'
& , 'Gas Temp','App/Sat',' #Wet','Humidity'
ENDIF
100 FORMAT(3X,A4,2X,A4,2X,A11,2X,A5,3X,A8,1X,A8,1X,A7,2X,A5,2X,A8)
200 FORMAT(3X,A4,6X,A4,4X,A11,5X,A8,4X,A7,5X,A5,5X,A8)

RETURN
END
```

Table A-13. Subroutine INITIAL.

SUBROUTINE INITIAL(III, PSDPt, DuctLength, VAR, PD, IJJ)

C Read input data and initialize variables.

```

R E A
DropDiam(15),WF(15),CDO(15),DropNFLux(15),MolWt,NASH(15,50)
R E A
VAR(7,15),NPartOld(15),dR(15,50),NPart(15,50),Rdry0(15,50)
  REAL PSDPt(100),MWG0,DTime(15),DsSolids(15),PD(15,50),Tave(15)
  REAL CO(15),Rold1(15),dRSO2(15),ShellFlux(15,50),NPold(15)
  REAL NASHOLD(15)
  REAL *8 CCa0(15)
    REAL SOR,add
REAL r1
INTEGER ISTOP(15),IVSTOP(15),Iold(15),NSHELL(15)
INTEGER Mevap(15),NStart(15)
  INTEGER type
CHARACTER*1 DIR,Slu,LAVE
CHARACTER*4 SorbType
CHARACTER*80 FILEIN

COMMON/FILE/FILEIN
COMMON/RKPR/NW,NE
COMMON/FN/DropNFLux,DuctArea,AirMassFlux,WVMFlux0
COMMON/DROP/DropDiam
COMMON/PP/P
COMMON/E/SD,PD0,SP,PDD
COMMON/P/CDO,SMF0
COMMON/I/ISTOP
COMMON/C/IVSTOP
COMMON/WF/WF
COMMON/PRNT/GV
COMMON/Iold/Iold
COMMON/VOL/Volmol,CaUt
COMMON/MOL/MolWt
COMMON/IMIN/IMIN
COMMON/DIR/IDir
COMMON/Y/SO2MF0
COMMON/T/Time
COMMON/CO2/CO2,MWG0
COMMON/SLU/Slu
COMMON/CAS/CaS
COMMON/DTIME/DTime
COMMON/DAVE/DAVE
COMMON/SA/RoughK
COMMON/T0/T0
COMMON/IDRY/IDRY
COMMON/IC/ICOUNT
COMMON/NP/NPartOld
COMMON/NPOLD/NPold

```

```

COMMON/DS/DsSolids
COMMON/NS/NSHELL
COMMON/DR/dR
COMMON/NPDR/NPart
COMMON/MEVAP/Mevap
COMMON/RD/Rdry0
COMMON/A/ALPHA
COMMON/NT/NStart
COMMON/AG/DissRate,RateK,Dprod
COMMON/C0/C0
COMMON/ROLD/Rold1
COMMON/SS/dRSO2
COMMON/SHEL/ShellFlux
COMMON/TAVE/Tave,NSTEPS
COMMON/DV/DelV0
COMMON/CCA0/CCa0
COMMON/NASH/NASH
COMMON/ASH/ASHFLUX0,DASH,ASHFLUX
COMMON/NAOLD/NASHOLD
COMMON/UT0/UT0,EFFCAS,PDR0
COMMON/PRE/PRECYCLE
    COMMON/add/add
    COMMON/typ/type
common/r1/r1
common/phin/phin
common/s1/s1

```

C Input case data. Variables are:

```

C SorbType = Has no real use now. Enter as CHYD
C SurfArea = Surface area of sorbent in m2/g. Default value of 15
used
C      if 0 entered.
C CaUt = Fraction of calcium initially utilized by sulfur. For use
when
C      boiler injection is followed by a scavenging spray.
C PD(I,M) = Sorbent Particle Diameter in microns.
C Slu = Indicates whether sorbent is present in the spray as a
slurry(S)
C      as a Dry particle injected into a prehumidified duct (D),
or as
C      a particle which will be scavenged by a spray (any letter
but D
C      or S).
C CaS = Calcium to sulfur molar ratio.
C SP = Sorbent porosity. Usually entered as 0 for hydrated lime.
C DHum = Molar fraction of water in initially in the duct gases.
C CO20 = Molar fraction of CO2 initially in the duct gases (wet
basis).
C GasMassRate = Mass flowrate of gases initially in the duct. In
Kg/sec.
C Duct Length = Length of duct in meters.
C DuctArea = Cross sectional area of duct in sq. meters.
C DIR = Direction of flow in duct. Entered as Up, Down, or
Horizontal.

```

```

C T0 = Intial temperature of duct gases in degrees Kelvin.
C DropTemp = Initial temperature of drops in degrees Kelvin.
C P = Pressure of duct in atmospheres.
C PPM = ppm SO2 in duct gases.
C add =amt. of additive(as % of mass of water)
C type= type of additive
C WMR0 = Rate of spray into duct in grams/sec.
C WaterVel = Velocity of spray in meters/sec.
C DAVE = Allows the velocity of different sized drops to be entered
C independently. Entered either as Yes or No.
C NW = The number of drop sizes contained in the spray size
distribution.
C DropDiam(I) = Diameter of drop in microns.
C WF(I) = Weight Fraction of each size of drops in the total spray.
Sum
C           of WF(I) should equal 1.

SorbType='CHYD'
READ(24,*) SurfArea
CaUt=0
READ(24,*) PDO
READ(24,1) Slu
READ(24,*) CaS
SP=0
READ(24,*) DASH
IF(DASH.LE.0) DASH=10
READ(24,*) AshLoad
READ(24,*) PRECYCLE
READ(24,*) ReUt
READ(24,*) DHum
READ(24,*) CO20
READ(24,*) GasMassRate
READ(24,*) DuctLength
READ(24,*) DuctArea
READ(24,1) DIR
READ(24,*) T0
READ(24,*) DropTemp
READ(24,*) P
READ(24,*) PPM
  READ(24,*) add
  READ(24,*) type
READ(24,*) rl
READ(24,*) phin
READ(24,*) sl
  IF(Slu.EQ.'d') Slu='D'
  IF(Slu.NE.'D') THEN
    READ(24,*) WMR0
    READ(24,*) WaterVel
    READ(24,1) DAVE
    READ(24,*) NW
    IF(Slu.EQ.'D') THEN
  ELSE
    WMR0=1
    WaterVel=1

```

```

DAVE='N'
NNW=NW
NW=1
ENDIF
1      FORMAT(A1)
2      FORMAT(A4)
IF(CAS.EQ.0) PPM=0
IF(Slu.NE.'D'.AND.WMR0.EQ.0) THEN
  PRINT *, 'Spray Rate = 0. Program Terminated.'
  IJJ=1
  RETURN
ENDIF

```

C Change letter variables to capitals.

```

IF(Slu.EQ.'s') Slu='S'
IF(Slu.NE.'S'.AND.Slu.NE.'D') Slu='A'
IF(DIR.EQ.'u') DIR='U'
IF(DIR.EQ.'d') DIR='D'
IF(DAVE.EQ.'n') DAVE='N'
IF(DAVE.EQ.'y') DAVE='Y'

```

C Read drop size distribution.

```

IF(Slu.EQ.'D') THEN
  NN=NNW
ELSE
  NN=NW
ENDIF
DO 10,I=1,NN
  IF(DAVE.EQ.'N') THEN
    READ(24,*) DropDiam(I),WF(I)
  ELSEIF(DAVE.EQ.'Y') THEN
    READ(24,*) DropDiam(I),WF(I),VAR(4,I)
  ELSE
    PRINT  *, '*DAVE(Y,N) OR Slu(S,A,D) VARIABLES INPUT
IMPROPERLY'
    RETURN
  ENDIF

  IF(Slu.EQ.'D') THEN
    NW=1
    WF(1)=1
    DropDiam(1)=PD0
    IF(PRECYCLE.NE.0) THEN
      ALPHA=1.5519
      DropDiam(2)=(ALPHA*PD0**3*ReUt/100+PD0**3*(1-ReUt/100))
      &           **.333333333*1E-6
      NW=2
    ENDIF
  ENDIF

```

C Initialize drop variables and convert sizes from microns to meters.

```

ISTOP(I)=0
Iold(I)=0
DTime(I)=0
10     DropDiam(I)=DropDiam(I)*1E-6
PDO=PDO*1E-6
DASH=DASH*1E-6
PRECYCLE=PRECYCLE/100
ReUt=ReUt/100

C Read distances where drop variables are to be printed out.

      READ(24,*) NPSD
      DO 20,I=1,NPSD
20      READ(24,*) PSDPt(I)
      PSDPt(NPSD+1)=DuctLength+1

C Order drcp size distribution from small to large drops.

      IF(Slu.NE.'D') THEN
      DO 15,I=1,NW
      DO 16,J=I+1,NW
      IF(DropDiam(I).GT.DropDiam(J)) THEN
      DUM=WF(I)
      WF(I)=WF(J)
      WF(J)=DUM
      DUM=DropDiam(I)
      DropDiam(I)=DropDiam(J)
      DropDiam(J)=DUM
      IF(DAVE.EQ.'Y') THEN
      DUM=VAR(4,I)
      VAR(4,I)=VAR(4,J)
      VAR(4,J)=DUM
      ENDIF
      ENDIF
16      CONTINUE
15      CONTINUE
      ENDIF

C Assign a numerical value for the drop velocity calculations.

      IF(DIR.EQ.'U') THEN
      IDir=1
      ELSEIF(DIR.EQ.'D') THEN
      IDir=-1
      ELSE
      IDir=0
      ENDIF

C Initialize:
C Number of differential Equations to be solved,
C IDRY, stores when a dry sorbent particle injected into a
prehumidified
C      duct has reached the duct temperature
C ICOUNT, a counting variable used in the runge kutta routine,

```

```

C Slurry Concentration,
C Time for the duct gases, and
C IMIN, the smallest drop not evaporated.
C NSTEPS, the number of times Rungekutt is called, used to
calculate
C           a running average drop temperature which is used to
determine
C           when a slurry droplet has dried.

```

```

NE=7
IDRY=0
ICOUNT=5
SluConc=0
Time=0
IMIN=1
NSTEPS=0

```

```

C Calculate value of following variables and constants:
C CO2, the dry CO2 molar fraction,
C MWG0, the molecular weight of the duct gas,
C Y0, the initial molar fraction of SO2 in the duct gases,
C SMF0, the sorbent mass flux in the duct,
C MolWt, the molecular weight of the sorbent,
C SD, the sorbent density, gm/m3,
C VolMol, the molar volume of the sorbent.
C RoughK, roughness factor to account for the loss of BET surface
area
C           as the reaction proceeds.
C ASat, approach to saturation for dry sorbent/condensation case.

```

```

IF(SurfArea.EQ.0) SurfArea=15
CO2=CO20/(1-DHum)
MWG0=(1-CO2)*29+CO2*44
Y0=PPM*1E-6
SMF0=GasMassRate*1000/(MWG0*(1-DHum)+DHum*18)*Y0*CaS
IF(SorbType.EQ.'DHYD'.OR.SorbType.EQ.'CHYD') THEN
  MolWt=74
  SD=2.2E6
  SMF0=SMF0*74
  SMF0=SMF0 + WMR0*add/100
ELSE
  MolWt=56
  SD=3.3E6*(1-CaUt)+CaUt*2.96E6
  SMF0=SMF0*56*((1-CaUt)+CaUt*136/56)
ENDIF
Volmol=MolWt/SD
RoughK=5* ALOG(SurfArea/6*SD*PD0-1)
ALPHA=5.22E-5/VolMol
IF(PPM.NE.0) THEN
  ReAsh=AshLoad/(AshLoad+SMF0*(1-ReUt)+SMF0*ReUt*129/74)
  RECYCLE=SMF0*(1/(1-PRECYCLE)-1)*(1-ReUt)
C  EFFCAS=(SMF0+RECYCLE)/SMF0*CaS
  if(type.eq.4) then
    EFFCAS=(SMF0+RECYCLE)/SMF0*CaS + WMR0*add/100*0.5/SMF0*CaS

```

```

else
  EFFCAS= (SMF0+RECYCLE) /SMF0*CaS
endif
  UT0=PRECYCLE*ReUt
  ASHREMASS=RECYCLE* (1+ReUt / (1-ReUt) *129/74) * (ReAsh / (1-ReAsh) )
  ASHFLUX0=(AshLoad+ASHREMASS) /DuctArea
ENDIF

IF(Slu.EQ.'D'.AND.PRECYCLE.NE.0) THEN
  WF(1)=SMF0/(SMF0+RECYCLE/(1-ReUt))
  WF(2)=RECYCLE/(1-ReUt)/(SMF0+RECYCLE/(1-ReUt))
ENDIF

IF(Slu.EQ.'D') THEN
  TSat=46.13+3816.44/(18.3036-ALOG(DHum*P*760))
  ASat=T0-TSat
ENDIF

C Calculate value of following variables:
C GasFlowRate, the duct flow rate, m3/sec,
C GV, the duct gas velocity.
C DropDen0, the initial density of the drop, gm/m3,
C dry AirMassFlux, gm/m2,
C WVMFlux0, the initial water vapor mass flux, gm/m2, and
C SO2MF0, the initial molar flux of SO2.

GasFlowRate=GasMassRate*8.206E-2*T0/P/((1-DHum-CO20)*29+
&           DHum*18+CO20*44)
GV=GasFlowRate/DuctArea
IF(WaterVel.LT.GV) WaterVel=GV
IF(WaterVel.EQ.GV) THEN
  DelV0=1
ELSE
  DelV0=WaterVel-GV
ENDIF
IF(Slu.NE.'D') DropDen0=1E6
DUM=GasFlowRate*P/8.206E-5/T0/DuctArea
AirMassFlux=DUM*MWG0*(1-DHum-PPM*1E-6)
WVMFlux0=DHum*18*DUM
SO2MF0=DUM*PPM*1E-6

C For the slurry spray case calculate:
C SluConc, the slurry concentration including recycle,
C VolFrac, the fraction of the slurry drop occupied by sorbent
including
C   recycle,
C WVFRAC, the volume fraction of water in drop, and
C ASHVFRAC, the volume fraction of ash from recycled ash in drop.

CASO3=0
SluConc=0
VolFrac=0
ASHVFRAC=0
SolidFrac=0

```

```

WVFrac=1
  SOR=WMR0*add/100
  IF(Slu.EQ.'S'.AND.PPM.NE.0) THEN
    SOR=WMR0*add/100
  C      SOR=0.0

  C      EFFCAS=(SMF0+RECYCLE+SOR)/SMF0*CaS
  C      CASO3=RECYCLE*ReUt/(1-ReUt)*129/74
  C      SluConc=(SMF0+SOR+RECYCLE)/(SMF0+SOR+WMR0+RECYCLE+
  &          ASHREMASS+CASO3)
  C      VolFrac=(SMF0+SOR+RECYCLE)/SD
  C      &
/((SMF0+SOR+RECYCLE+ASHREMASS+CASO3)/SD+WMR0/DropDen0)
  WVFrac=WMR0/DropDen0
  &
/((SMF0+SOR+RECYCLE+ASHREMASS+CASO3)/SD+WMR0/DropDen0)
  ASHVfrac=ASHREMASS/SD
  &
/((SMF0+SOR+RECYCLE+ASHREMASS+CASO3)/SD+WMR0/DropDen0)
  SolidFrac=(SMF0+SOR+RECYCLE+ASHREMASS+CASO3)
  &          /(SMF0+SOR+RECYCLE+ASHREMASS+CASO3+WMR0)

  ELSEIF(Slu.EQ.'A') THEN
  WVFrac=1
  ENDIF

C Calculate average sorbent diameter of fresh and recycled sorbent.

  IF(Slu.NE.'D') THEN
    PDD=PD0*(1-PRECYCLE*ReUt)**.3333333
  ELSE
    PDD=PD0
  ENDIF

C Initialize the independent drop variables:
C VAR(1,I)=Gas Temperature,
C VAR(2,I)=Number of sorbent particles in a drop,
C VAR(3,I)=Number of ash particles in a droplet
C VAR(4,I)=Individual Drop Velocity,
C VAR(5,I)=Mass water remaining in drop,
C VAR(6,I)=Individual Drop temperature,

C and the dependent drop variables:
C DropNflux(I), the number flux of drops of each size, #/m2,
C CDO(I), the initial mass of water in a drop,
C IVSTOP(I), to remember when a drop has decelerated.
C DsSolids(I), mass of dissolved solids in a drop.
C NShell(I), number of radial shells considered in a drop.
C NStart(I), radial shell from where the initial SO2 concentration
will
C      be solved.
C Tave, running average drop temperature which is used to determine
C      when a slurry droplet has dried.

```

```

VAR(1,1)=1
DO 30,I=1,NW

IF(Slu.NE.'D') THEN
  NSHELL(I)=DropDiam(I)/PDD/2+.9
  IF(NSHELL(I).GT.49) NSHELL(I)=49
  IF(NSHELL(I).LT.2) NSHELL(I)=2
  Mevap(I)=NSHELL(I)
  delR=DropDiam(I)/NSHELL(I)/2
  Tave(I)=0
  DO 31,M=1,NSHELL(I)
    Rdry0(I,M)=0
    PD(I,M)=PDD
    dR(I,M)=delR
    ShellFlux(I,M)=0
    IF(Slu.EQ.'S') THEN
      NPart(I,M)=8.*((M*delR)**3-((M-1)*delR)**3)
      NASH(I,M)=NPart(I,M)*ASHVFrac/DASH**3
      NPart(I,M)=NPart(I,M)*VolFrac/PDD**3/(1-SP)
    ELSE
      NPart(I,M)=0
      NASH(I,M)=0
    ENDIF
31      CONTINUE
  ELSE
    NSHELL(I)=1
    Mevap(I)=1
    dR(I,1)=DropDiam(1)/2
    PD(I,1)=PDD
    IF ( P R E C Y C L E . N E . 0 . A N D . I . E Q . 2 )
    PD(I,1)=PD0*(1-ReUt)**.333333333
    PDR0=PD0*(1-ReUt)**.333333333
    NPart(I,1)=1
  ENDIF

  IF(Slu.NE.'D') THEN
    DropNFLux(I)=6./3.14159*WMR0*WF(I)/DropDen0/
    &           DropDiam(I)**3/DuctArea/WVFrac
  ELSE
    IF(I.EQ.1) THEN
      DropNFLux(I)=6./3.14159*SMF0/SD/(1-SP)/PDD**3/DuctArea
    ELSE
      DropNFLux(I)=DropNFLux(1)*PRECYCLE/(1-PRECYCLE)
    ENDIF
  ENDIF

  IF(Slu.EQ.'S') THEN
    CD0(I)=3.14159*DropDiam(I)**3/6*DropDen0*WVFrac
    DsSolids(I)=add/100*CD0(I)
    VAR(5,I)=1
    VAR(2,I)=DropDiam(I)**3*VolFrac/PDD**3
  ELSEIF(Slu.EQ.'D') THEN
    CD0(I)=3.14159*PD0**3/6*SD*(1-SP)
    VAR(5,I)=1E-10
  ENDIF

```

```

C   DsSolids(I)=500E-6*CD0(I)*1E-10
    DsSolids(I)=add/100*CD0(I)*1E-10
    VAR(2,I)=1
  ELSE
    CD0(I)=3.14159*DropDiam(I)**3/6*DropDen0
    DsSolids(I)=add/100*CD0(I)
    VAR(5,I)=1
    VAR(2,I)=0
  ENDIF
  IF(Slu.NE.'S') THEN
    VAR(3,I)=0
    NASHOLD(I)=0
  ELSE
    VAR(3,I)=DropDiam(I)**3*ASHVFrac/DASH**3
    NASHOLD(I)=VAR(3,I)
  ENDIF
  NPold(I)=VAR(2,I)
  NPartOld(I)=VAR(2,I)

  IF(Slu.EQ.'D') THEN
    VAR(4,1)=GV
  ELSEIF(DAVE.EQ.'N') THEN
    VAR(4,I)=WaterVel
  ENDIF

  IF(VAR(4,I)-GV.LT..05) THEN
    VAR(4,I)=GV
    IVSTOP(I)=1
  ELSE
    IVSTOP(I)=0
  ENDIF

  VAR(6,I)=DropTemp/T0

```

30 CONTINUE

C Calculate the approximate starting shell for the SO2 profile calculations

```

IF(Slu.NE.'D'.AND.SO2MF0.NE.0.AND.CAS.NE.0) THEN
  DO 50,J=1,NW
    CCa0(J)=.95*(16550/DropTemp-35.62)
    IF(Slu.EQ.'A') CCa0(J)=.95*(16550/325-35.62)

  CMTSO2=(2+.6*SQRT(DropDiam(J)*(VAR(4,J)-GV)/.018E-3))*6.6E-4/
    & DropDiam(J)
  C CMTSO2=r1*CMTSO2
  Rough=1+EXP(Roughk*.2)
  BETA=6.28319*PD0*.113E-8
  GAMMA=3.14159*PD0**2*Rough*DissRate
  RATE=20.48*VAR(2,J)*6/3.14159/DropDiam(J)**3/
    & (1/GAMMA+1/BETA)
  b1=rate*dropdiam(J)/6

```

```

b2=cmtso2*Y0
b3=.8e-3*(-cmtso2)
b=(b1-b2)/b3
C0(J)=B-RATE*DropDiam(J)**2/24/.19E-8
IF(C0(J).GT.0) THEN
  R0=.03*DropDiam(J)
  C0(J)=0
ELSE
  R0=.8*SQRT((DropDiam(J)**2/4-B*6*.19E-8/RATE))
  C0(J)=0
  IF(R0.GT.DropDiam(J)) R0=.9*DropDiam(J)
ENDIF
dRSO2(J)=DropDiam(J)/2-R0
50  Rold1(J)=0
ELSE
  NStart(1)=1
ENDIF
SMFO=(SMFO+RECYCLE)/DuctArea

C Print input data.

IF(III.GT.1) PRINT 21
21  FORMAT(1H1)
PRINT *
PRINT *, ' Input file=' ,FILEIN

C Print input sulfur capture parameters.

IF(CaS.NE.0.AND.PPM.NE.0) THEN
  PRINT *
  PRINT 55,'Sorbent Diameter =',PD0*1e6,' microns'
  PRINT 55,'Sorbent Surf Area=',SurfArea,' m2/g '
  PRINT 55,'Ca/S      =',CaS
  IF(PRECYCLE.NE.0.OR.add.NE.0) THEN
    PRINT 55,'Effective Ca/S  =',EFFCAS,' (Due to recyc/addi.,'
    &,' calculated)'
    PRINT 55,'Initial Ave.Util.=',UT0*100,' % (Due to recycle,'
    &,' calculated)'
  ENDIF
  IF(Slu.NE.'S') THEN
    PRINT 55,'Sorbent Mass Rate=',SMFO*DuctArea,' g/sec
(calculated)'
  ELSE
    PRINT 55,'Slurry Conc.      =',SluConc*100,' % Wt. (sorbent'
    &,' only, calculated)'
  ENDIF

  IF(PPM.NE.0) THEN
    PRINT 55,'SO2 Concentration=',PPM,' ppm      '
    PRINT 56,'Additive          =',add,'% initial mass of water
    PRINT 59,'Additive flow      =',SOR,'g/s'
    IF(type.eq.1) THEN
      PRINT 57,'Type of additive = CaCl2 '

```

```
Endif
IF(type.eq.2)THEN
PRINT 57,'Type of additive = NaCl '
Endif
IF(type.eq.3) THEN
PRINT 57,'Type of additive = Na2CO3 '
endif
IF(type.eq.4) THEN
PRINT 57,'Type of additive = NaOH '
Endif
ENDIF
ENDIF
```

C Print recycle variables.

```

        IF(RECYCLE.GT.0) THEN
          PRINT 55,'Recycle      =' ,PRECYCLE*100,' % Wt. of Duct
Output'
          PRINT 55,'Util. of Recycle =',ReUt*100,' %'
          IF(Slu.NE.'D') THEN
            PRINT 55,'Ash in Recycle      =' ,ReAsh*100,' % Wt.
(calculated)'
            ENDIF
            IF(Slu.EQ.'S') THEN
              PRINT 55,'Total Solids Conc=',SolidFrac*100,' % Wt.
(calculated)'
              ENDIF
              ENDIF

```

C Print ash properties.

```

IF(ASHFLUX0.NE.0.AND.S1u.NE.'D') THEN
  PRINT 55,'Ave. Ash Diameter=',DASH*1E6,' microns'
  PRINT 55,'Ash Mass Rate      =',ASHLOAD,' g/sec'
ENDIF

```

C Print input humidification parameters.

```

IF(GasMassRate.GT.1) THEN
  PRINT 55,'Gas Mass Rate      =',GasMassRate,' Kg/sec '
ELSEIF(GasMassRate.GT..001) THEN
  PRINT 55,'Gas Mass Rate      =',GasMassRate*1000,' g/sec '
ELSE
  PRINT 55,'Gas Mass Rate      =',GasMassRate*1E6,' mg/sec '
ENDIF
PRINT 55,'Gas Temperature    =',T0,' K
PRINT 55,'Gas Humidity       =',DHum*100,' %
PRINT 55,'Gas CO2 Conc.      =',CO20*100,' %
IF(DuctArea.GT..1) THEN
  PRINT 55,'Duct Area          =',DuctArea,' m2
ELSE
  PRINT 55,'Duct Area          =',DuctArea*1E4,' cm2
ENDIF
PRINT 55,'Duct Length         =',DuctLength,' m

```

```

IF(Slu.EQ.'D') PRINT 55,'App. To Sat.      =' ,ASat,' K (calc.)'
IF(Slu.NE.'D') THEN
IF(WMR0.GT.1) THEN
    PRINT 55,'Water Mass Rate  =' ,WMR0,' g/sec '
ELSE
    PRINT 55,'Water Mass Rate  =' ,WMR0*1000,' mg/sec '
ENDIF
PRINT 55,'Water Velocity   =' ,WaterVel,' m/sec '
ENDIF
55  FORMAT(15X,A18,F8.2,A,A)
56  FORMAT(15X,A18,F5.2,A,A)
57  FORMAT(15x,A26)
59  FORMAT(15x,A18,F6.2,A,A)

IF(DIR.EQ.'U') THEN
    PRINT *,'                                Gas flow direction is up'
ELSEIF(DIR.EQ.'D') THEN
    PRINT *,'                                Gas flow direction is down'
ELSE
    PRINT *,'                                Gas flow direction is horizontal'
ENDIF

IF(DAVE.EQ.'Y') THEN
PRINT *,'                                in Daves Reactor'
ENDIF

IF(Slu.NE.'D') THEN
PRINT *
PRINT *,'                                Drop Size Distribution:'
PRINT *
IF(DAVE.EQ.'N') THEN
PRINT *,'                                Drop Diameter          Weight'
PRINT *,'                                (Microns)          Fraction'
DO 500,I=1,NW
    PRINT 90,DropDiam(I)*1E6,WF(I)
ELSE
PRINT *,'                                Drop Diameter          Weight
& Drop'
PRINT *,'                                (Microns)          Fraction
&Velocity'
DO 501,I=1,NW
    PRINT 91,DropDiam(I)*1E6,WF(I),VAR(4,I)
ENDIF
ENDIF

90  FORMAT(18X,F6.1,15X,F6.3)
91  FORMAT(16X,F6.1,13X,F6.3,10X,F6.1)
PRINT *

```

C Print results heading.

CALL HEADING()

RETURN

END

Table A-14. Subroutine PDIF.

SUBROUTINE PDIF(HMIN, VAR, PD)

C Calculate the change in the number of particles from shell to shell
C due to diffusion of the particles.

```
REAL VAR(7,15), PD(15,50), dR(15,50), NPart(15,50), DropDiam(15)
REAL *8 HMIN
INTEGER Mevap(15), NShell(15)
```

```
COMMON/DR/dR
COMMON/NPDR/NPart
COMMON/RKPR/NW, NE
COMMON/MEVAP/Mevap
COMMON/DROP/DropDiam
COMMON/NS/NShell
COMMON/T0/T0
common/dis/dis
```

```
N=HMIN/.001
IF(N.LT.1) N=1
H=HMIN/N
DO 10, J=1, NW
IF(Mevap(J).EQ.0.OR.VAR(2,J).EQ.0) GO TO 10
DIFFPART0=6.782E-35*(T0*VAR(6,J))**6.416
```

```
DO 100, I=1, N
R=DropDiam(J)/2
```

```
IF(Mevap(J).EQ.NShell(J)) THEN
  ME=NShell(J)
ELSE
  ME=Mevap(J)+1
ENDIF
```

```
DO 20, M=ME, 2, -1
```

```
IF(PD(J,M).LT.1E-10) GO TO 20
DIFFPART=DIFFPART0/PD(J,M)
R=R-dR(J,M)
C1=NPart(J,M)/((R+dR(J,M))**3-R**3)
C0=NPart(J,M-1)/(R**3-(R-dR(J,M-1))**3)
DRBAR=(dR(J,M)+dR(J,M-1))/2
dN=3*R**2*DIFFPART*(C1-C0)/DRBAR*H/VAR(4,J)
IF(dN.GT.NPart(J,M)) dN=.9*NPart(J,M)
NPart(J,M)=NPart(J,M)-dN
IF(dN.GT.0) THEN
  PD(J,M-1)=((PD(J,M)**3*(dN)+PD(J,M-1)**3*NPart(J,M-1))
  &           /(dN+NPart(J,M-1)))**.33333333
ELSE
  PD(J,M)=((PD(J,M-1)**3*(-dN)+PD(J,M)**3*NPart(J,M))
```

```
&           / ( -dN+NPART (J,M) ) )**.3333333
ENDIF
NPart (J,M-1) =NPart (J,M-1) +dN
20  CONTINUE

100 CONTINUE
10  CONTINUE

RETURN
END
```

Table A-15. Subroutine PHY.

```
SUBROUTINE PHY (IT,I,J,Q,ER,ERate,CpW,WVMFlux,HtCapG,SMF,
& DropDens,Re,DenG,HTVAP,HtCapW)

REAL CD0(15),DropNFlux(15),DropDiam(15),Nu,NPart(15,50)
REAL W(7,15),WPD(15,50),NPartOld(15),DsSolids(15),dR(15,50)
REAL KDISSOC,RWCore(15),Rdry0(15,50),Dmin(15),VolPart(15,50)
REAL MWF,MWG,MUAIR,MUW,MolWt,MWG0,SolFrac(15,50),NASH(15,50)
REAL NASHOLD(15)
REAL rl
INTEGER ISTOP(15),IVSTOP(15),NSHELL(15),Mevap(15),NSTART(15)
INTEGER IFlux(15)
INTEGER type
CHARACTER *1 Slu

common/AG/DissRate,RateK,Dprod
COMMON/DUM/W,WPD
COMMON/FN/DropNFlux,DuctArea,AirMassFlux,WVMFlux0
COMMON/DROP/DropDiam
COMMON/PP/P
COMMON/I/ISTOP
COMMON/C/IVSTOP
COMMON/E/SD,PDO,SP,PDD
COMMON/P/CD0,SMF0
COMMON/RKPR/NW,NE
COMMON/PRNT/GV
COMMON/VOL/VolMol,CaUt
COMMON/MOL/MolWt
COMMON/Y/SO2MF0
COMMON/IMIN/IMIN
COMMON/CO2/CO2,MWG0
COMMON/SLU/Slu
COMMON/T0/T0
COMMON/IDRY/IDRY
COMMON/ET/ReG,VisG
COMMON/DS/DsSolids
COMMON/NS/NSHELL
COMMON/DR/dR
COMMON/NPDR/NPart
COMMON/MEVAP/Mevap
COMMON/RW/RWCore
COMMON/SO2/DSO2,CMTSO2,HE,KDISSOC,DH2SO3,DHSO3,YS8
COMMON/LIME/Dlime,ClimeEq
COMMON/RD/Rdry0
COMMON/CG/Cg
COMMON/A/ALPHA
COMMON/SA/RoughK
COMMON/NT/NSTART
COMMON/VL/VolPart
COMMON/SOL/SolFrac
COMMON/CAS/CAS
COMMON/NP/NPartOld
```

```

COMMON/IF/IFlux
COMMON/ICE/ICEASE
COMMON/DV/DelV0
COMMON/NASH/NASH
COMMON/ASH/ASHFLUX0,DASH,ASHFLUX
COMMON/NAOLD/NASHOLD
COMMON/UT0/UT0,EFFCAS,PDR0
common/dis/dis
common/typ/type
common/add/add
common/r1/r1
common/phin/phin
common/s1/s1

```

C Calculate gas, film, and drop temperatures.

```

Td=W(6,J)*T0
Tg=W(1,1)*T0
Tf=(Tg+Td)/2
Cf=P/8.206E-5/Tf
Cg=P/8.206E-5/Tg

```

C If the drop has stopped evaporating, calculate its final water content.

```

IF(SMF0.EQ.0.AND.W(5,J).LT.0.001.AND.ISTOP(J).EQ.0.AND.Slu.NE.
& 'D') THEN
  W(5,J)=1E-30
  ISTOP(J)=1
  IF(SO2MF0.EQ.0) IMIN=IMIN+1
ENDIF

```

C Calculate Sorbent Mass Rate, Water Vapor Mass Flux and Gas Velocity.

```

IF(J.EQ.IMIN) THEN

  SMF=SMF0
  ASHFLUX=ASHFLUX0
  WVMFlux=WVMFlux0
  DO 100,L=1,NW
    IF(Slu.NE.'S') SMF=SMF-DropNFLux(L)*W(2,L)*3.14159/6*
    & SD*(1-SP)*PDD**3
    IF (Slu.NE.'D'.AND.ASHFLUX0.GT.0)
ASHFLUX=ASHFLUX-DropNFLux(L)
    & *W(3,L)*3.14159/6*SD*DASH**3
100   WVMFlux=WVMFlux+DropNFLux(L)*CD0(L)*(1-W(5,L))
    IF(Slu.EQ.'D') THEN
      WVMFlux=WVMFlux0
      DO 103,L=1,NW
        WVMFlux=WVMFlux-CD0(L)*W(5,L)*DropNFLux(L)
    ENDIF
    DenG=P/8.206E-5/Tg
    GV=(AirMassFlux/MWG0+WVMFlux/18)/DenG
    GasMassFlux=WVMFlux+AirMassFlux

```

```

YG=WVMFlux/GasMassFlux
XG=WVMFlux/18/(AirMassFlux/MWG0+WVMFlux/18)
ENDIF

C Calculate the number of sorbent particles (for the scavenging
case)
C and the volume of sorbent in each radial shell.

IF(Slu.NE.'D') THEN
  R=0
  XRSUM=0
  ASHSUM=0
  VolSum=0
  DO 107,M=1,NShell(J)
    IF(IVSTOP(J).EQ.0) then
      IF(M.LT.NShell(J)) THEN
        NPart(J,M)=NPart(J,M)+(W(2,J)-NPartOld(J))*4*
        & ((R+dR(J,M))**3-R**3)/DropDiam(J)**3
        XRSUM=XRSUM+NPart(J,M)
        NASH(J,M)=NASH(J,M)+(W(3,J)-NASHOLD(J))*4*
        & ((R+dR(J,M))**3-R**3)/DropDiam(J)**3
        ASHSUM=ASHSUM+NASH(J,M)
      ELSE
        NPart(J,M)=W(2,J)-XRSUM
        NASH(J,M)=W(3,J)-ASHSUM
      ENDIF
      R=R+dR(J,M)
    ENDIF
    IF(W(2,J).EQ.0) THEN
      VolPart(J,M)=0
    ELSE

      VolPart(J,M)=.5236*(NPart(J,M)*(1-SP)*(WPD(J,M)**3+(PD0**3-
      & WPD(J,M)**3)*ALPHA)
      & +NASH(J,M)*DASH**3)
    ENDIF
  107  VolSum=VolSum+VolPart(J,M)
  ELSE
    VolSum=.5236*(WPD(J,1)**3+(PD0**3-WPD(J,1)**3)*ALPHA)
  ENDIF

C Calculate the solid mass in the drop (SMass).

IF(ISTOP(J).EQ.0) THEN
  DUM=0
  IF(IVSTOP(J).EQ.0.AND.Slu.NE.'S') THEN
    DUM=((PD0**3-WPD(J,1)**3)*129/74+WPD(J,1)**3)*W(2,J)
  ELSE
    DO 5,M=1,NSHELL(J)
      IF(WPD(J,M).LT.0) WPD(J,M)=0
  5  DUM=DUM+((PD0**3-WPD(J,M)**3)*129/74+WPD(J,M)**3)*NPart(J,M)
  ENDIF
  SMass=3.14159/6*SD*(1-SP)*DUM+DsSolids(J)+W(3,J)*3.14159*

```

```

&           DASH**3/6*SD
ENDIF

C Calculate an average sorbent particle diameter for the scavenging
case
C   except when W has just been set equal to VAR.

IF (IT.NE.1.AND.W(2,J).GT.NPartOld(J)) THEN

WPD(J,1)=((NPartOld(J)*WPD(J,1)**3+(W(2,J)-NPartOld(J))*PDD**3)
&           /W(2,J))**.333333333
      DO 105,M=2,NSHELL(J)
105      WPD(J,M)=WPD(J,1)
      ENDIF

C Calculate drop diameter, drop density.

IF (DropDiam(J).NE.Dmin(J)) THEN
  DropDiam(J)=(1.9099*(W(5,J)*CD0(J)/1E6+VolSum))**.333333333
  IF (VolSum.EQ.0) THEN
    Dmin(J)=0
  ELSE
    Dmin(J)=(2.546479*VolSum)**.333333333
  ENDIF
  IF (DropDiam(J).LT.Dmin(J).AND.Slu.NE.'D') THEN
    DropDiam(J)=Dmin(J)
    Mevap(J)=0
    ISTOP(J)=1
    R=0
    DO 201,M=1,NShell(J)
      dR(J,M)=(R**3+VolPart(J,M)/3.14159)**.333333333-R
201      R=R+dR(J,M)
      DropDiam(J)=2*R
      Dmin(J)=DropDiam(J)
    ENDIF
  ENDIF

  D2=DropDiam(J)**2
  D3=DropDiam(J)*D2
  IF (ISTOP(J).EQ.0) DropDens=1.90986/D3*(W(5,J)*CD0(J)+SMass)

C Calculate size of differential radial shells.

IF (Slu.NE.'D'.AND.SO2MF0.NE.0.AND.CaS.NE.0
&           .AND.IT.EQ.1.AND.DropDiam(J).NE.Dmin(J)) CALL DELR(J)

C Calculate the volume of sorbent and product in each radial shell.

IF (Slu.NE.'D') THEN
  R=0
  DO 108,M=1,NShell(J)
    SolFrac(J,M)=VolPart(J,M)/4.1888888/((R+dR(J,M))**3-R**3)
108      R=R+dR(J,M)

```

```
ENDIF
```

```
C Determine whether the flux of water due to evaporation should be  
C included in SO2 and Ca flux calculations.
```

```
IF(Slu.NE.'D') THEN  
  PNSum=0  
  R=DropDiam(J)/2  
  IF(W(2,J).GT.0.OR.W(3,J).GT.0) THEN  
    Dave=(W(2,J)*PDD+W(3,J)*DASH)/(W(2,J)+W(3,J))  
  ELSE  
    Dave=PDD  
  ENDIF  
  DO 133,M=NShell(J),1,-1  
  IF(SolFrac(J,M).LT..7) GO TO 134  
  PNSum=PNSum+NPart(J,M)+NASH(J,M)  
133  R=R-dR(J,M)  
134  FluxN=6*((DropDiam(J)/2)**3-R**3)/Dave  
  IFlux(J)=0  
  IF(PNsum.GT.FluxN) Then  
    IFlux(J)=1  
  Endif  
ENDIF
```

```
C Calculate radius of water core.
```

```
c  IF(DropDiam(J).EQ.Dmin(J).AND.ISTOP(J).EQ.0) THEN  
    IF(DropDiam(J).EQ.Dmin(J)) THEN  
      R=0  
      WMass=0  
      WMold=0  
      DO 120,M=1,NSHELL(J)  
      WMass=WMass+4.1888*((R+dR(J,M))**3-R**3)*(1-SolFrac(J,M))  
      &           *1E6  
      IF(WMass.LT.W(5,J)*CD0(J)) THEN  
        R=R+dR(J,M)  
        WMold=WMass  
      ELSE  
        RWCore(J)=(R**3+((R+dR(J,M))**3-R**3)*((W(5,J)*CD0(J)-WMold)  
        &           /(WMass-WMold)))**.333333333  
        GO TO 125  
      ENDIF  
120  CONTINUE  
    ENDIF  
    IF(ISTOP(J).EQ.0) THEN  
      RWCore(J)=DropDiam(J)/2  
    ELSE  
      RWCore(J)=0  
    ENDIF
```

```
C If water core has receded past a radial shell, store sorbent  
C particle  
C radius.
```

```

125  IF(ISTOP(J).EQ.0) THEN
      R=DropDiam(J)
      DO 130,M=NSHELL(J),1,-1
      IF(Rdry0(J,M).EQ.0.AND.R.GT.RWCore(J)) Rdry0(J,M)=WPD(J,M)/2
130  R=R+dR(J,M)
      ENDIF

C Calculate the film temperature (Tf), water mole fraction at the
drop
C surface (XO), mass fraction in the film (YF) and in the bulk gas
C phase (YG), the Gas Mass Rate and Molecular Weights.

      IF(ISTOP(J).EQ.1) THEN
          XO=XG
          YF=YG
      ELSEIF(IDRY.EQ.0) THEN

          IF(type.eq.1)THEN
              DsMol=DsSolids(J)/W(5,J)/CD0(J)/.111
              ActW=.9899-8.678E-3*DsMol-3.676E-2*DsMol**2+4.624E-3*DsMol**3
              & -1.667E-4*DsMol**4
C          ActW = 0.9899
          ENDIF

          IF(type.eq.2)THEN
              DsMol=DsSolids(J)/W(5,J)/CD0(J)/0.058
              ActW=.9899-3.7055E-2*DsMol+1.416E-3*DsMol**2-1.055E-3*DsMol**3
              & +2.5E-5*DsMol**4
C          ActW=0.9899
          ENDIF

          IF(type.eq.3)THEN
              DsMol=DsSolids(J)/W(5,J)/CD0(J)/0.106
              ActW=.9899-0.036543*DsMol-5.743E-3*DsMol**2+3.088E-3*DsMol**3
              & -0.001046*DsMol**4
          ENDIF

          IF(type.eq.4)THEN
              DsMol=DsSolids(J)/W(5,J)/CD0(J)/0.04
              ActW=.9899-0.023276*DsMol-3.106E-3*DsMol**2+1.66E-4*DsMol**3
              & -0.000002*DsMol**4
C          ActW=0.9899
          ENDIF

          IF(Slu.EQ.'D') ActW=1

          IF(type.eq.1) THEN
              XO=ActW*EXP(18.3036-3816.44/(Td-46.13))/P/760
          ENDIF

          IF(type.eq.2) THEN
              XO=ActW*EXP(18.520757-3935.37889/(Td-41.365668))/P/760

```

```
ENDIF
```

```
IF(type.eq.3)THEN
  XO=ActW*EXP(17.991841-3623.981161/(Td-53.375442))/P/760
ENDIF
```

```
IF(type.eq.4)THEN
  XO=ActW*EXP(18.30277-3722.230398/(Td-53.436414))/P/760
ENDIF
```

```
  YF=XO*18/((1-XO)*MWG0+XO*18)
ELSE
  XO=1
  YF=1
  IDRY=1
ENDIF
IF(XO.GE.1.OR.YF.GE.1) THEN
  XO=1
  YF=1
  IDRY=1
ELSEIF(XO.LE.0.OR.YF.LE.0) THEN
  XO=0
  YF=0
ENDIF
YF=(YF+YG)/2
XF=(XG+XO)/2
MWF=18*XF+MWG0*(1-XF)
MWG=18*XG+MWG0*(1-XG)
DenF=Cf*MWF

IF(XG.LT.0.OR.XG.GT.1.OR.XO.LT.0.OR.XO.GT.1) THEN
  print *, 'xo=',xo,' xg= ',xg,' w(6,j)= ',w(6,j)
  RETURN
ENDIF
```

C Calculate drop independent variables.

```
IF(J.EQ.IMIN) THEN
```

C Calculate the SO2 Mass Flux and the SO2 mole fraction in the bulk
C gas phase (YS8).

```
IF(SO2MF0.NE.0) THEN
  SO2MFlux=SO2MF0
  DO 200,L=1,NW
  DUM=0
  IF(IVSTOP(L).EQ.0.AND.Slu.NE.'S') THEN
    DUM=W(2,L)*(PDD**3-WPD(L,1)**3)
  ELSE
    DO 205,M=1,NSHELL(L)
    IF(Slu.NE.'D') THEN
      DUM=DUM+NPart(L,M)*(PDD**3-WPD(L,M)**3)
```

```

        ELSE
          IF(L.EQ.1) THEN
            DUM=DUM+(PD0**3-WPD(L,M)**3)
          ELSE
            DUM=DUM+(PDR0**3-WPD(L,M)**3)
          ENDIF
        ENDIF
205      CONTINUE
      ENDIF
200      SO2MFlux=SO2MFlux-DropNFlux(L)/(1.90986/(1-SP))/VolMol
      &      *(1-CaUt)*DUM
      YS8=SO2MFlux/(AirMassFlux/MWG0+WVMFlux/18+SO2MFlux)
      IF(YS8.LE.0) THEN
        ICease=1
        RETURN
      ENDIF
      ENDIF

```

C Calculate viscosities (Mu or Vis), heat capacities (Cp or HtCap),
 C molecular weights (MW), thermal conductivities (Cond), heat of
 C vaporization (HTVAP), and densities (Den) for air (A), gas (G),
 C water (W), and film (F).
 C Calculate bulk diffusivity of SO2 and coefficient of external
 mass
 C transfer.
 C Calculate calcium hydroxide diffusivity in water (Dlime),
 equilibrium
 C concentration of lime in water (CLimeEq), and Henry's Constant.
 C Calculate Henry's Constant.

```

      IF(ISTOP(NW).EQ.0.AND.ABS(Tg-TGold).GT.0.5) THEN
        MuAir=2.484E-4*Tg**.7319
        MuW=2.109E-5*Tg**1.0776
        VisG=(1-YG)*MuAir+YG*MuW
        CpA=(28.09+.1965E-2*Tg+.4799E-5*Tg**2-1.965E-9*Tg**3)
        CpW=(33.46+.688E-2*Tg+.7604E-5*Tg**2-3.593E-9*Tg**3)
        TC=Tg-273
        CpCO2=(36.11+4.233E-2*TC-2.887E-5*TC**2+7.464E-9*TC**3)
        HtCapG=((1-XG)*(1-CO2)*CpA+XG*CpW+CO2*(1-XG)*CpCO2)/MWG
        TGold=Tg
      ENDIF
      DenG=DenG*MWG
    ENDIF

    IF(ISTOP(J).EQ.0) THEN
      MuAir=2.484E-4*Tf**.7319
      MuW=2.109E-5*Tf**1.0776
      VisF=(1-YF)*MuAir+YF*MuW
      CondA=2.032E-4*Tf**.8522
      CondW=2.593E-5*Tf**1.154
      CondF=(1-YF)*CondA+YF*CondW
      DSO2=3.851E-10*Tf**1.824
      Sc=VisF/DenF/DSO2
      IF(IVSTOP(J).EQ.0) THEN

```

```

        DeltaV=W(4,J)-GV
        Re=DropDiam(J)*DeltaV/(VisF/DenF)
        Sh=2+.6*SQRT(Re)*Sc**.33333333
        ELSE
        Sh=2
        ENDIF
        CMTSO2=Sh*DSO2/DropDiam(J)*Cf

        IF (ABS(Td-TDold).GT.0.5.OR.Slu.EQ.'A'.AND.DeltaV.GT..4*DelV0.
        &      AND.DeltaV.LT..45*DelV0) THEN
        HTVAP=(2.897E5*Td**(-.3309)+5.703E4-43.68*Td)/2
        HtCapW=3.251*Td**.044
        CpA=(28.09+.1965E-2*Td+.4799E-5*Td**2-1.965E-9*Td**3)
        CpW=(33.46+.688E-2*Td+.7604E-5*Td**2-3.593E-9*Td**3)
        Dlime=3.954E-9*Td*EXP(-2046/Td)

        IF (type.eq.1) then
        CLimeEq=16550/Td-35.62 + 0.394551*add
        C L i m e E q = 1 6 5 5 0 / T d - 3 5 . 6 2 +
        1.1355578*DsSolids(J)/W(5,J)/CD0(J)
        ENDIF
        IF (type.eq.2) then
        CLimeEq=16550/Td-35.62 +0.9814357*DsSolids(J)/W(5,J)/CD0(J)
        CLimeEq=16550/Td-35.62 +0.4510510442*add
        ENDIF

        IF (type.eq.3) then
        CLimeEq=16550/Td-35.62
        ClimeEq= ClimeEq*s1
        ENDIF

        IF (type.eq.4) then
        CLimeEq=16550/Td-35.62 -17.21182*DsSolids(J)/W(5,J)/CD0(J)
        ENDIF

        HE=EXP(2.4717-2851.1/Td)
        KDISSOC=EXP(22.426-1775/Td-.046*Td)
        DH2SO3=phin*Td*EXP(-19.895-1800/Td)
        DHSO3=phin*1.7856e-13*tD/(1/(4.86*tD-1100)+1/(1.46*Td-390))
        TDold=Td

        ENDIF

        TC=Td-273
        CpCO2=(36.11+4.233E-2*TC-2.887E-5*TC**2+7.464E-9*TC**3)
        HtCapF=((1-XF)*(1-CO2)*CpA+XF*CpW+CO2*(1-XF)*CpCO2)/MWF

C Calculate the difference between drop and gas velocities
(DeltaV),
C Reynolds (Re), Schmidt (Sc), Prandtl (Pr), Sherwood (Sh), and
C Nusselt (Nu) numbers and the water diffusivity in the film (Dv).

```

```

Dv=4.3E-11*Tf**2.334/P
IF(IVSTOP(J).EQ.1.OR.W(4,J)-GV.LE..01) THEN
  W(4,J)=GV
  Re=0
  ReG=0
  Sh=2
  Nu=2
  IVSTOP(J)=1
ELSE
  DeltaV=W(4,J)-GV
  ReG=DropDiam(J)*DeltaV*DenG/VisG
  Sc=VisF/DenF/Dv
  Re=DropDiam(J)*DeltaV/(VisF/DenF)
  Pr=HtCapF*VisF/CondF
  Sh=2+.6*SQRT(Re)*Sc**.33333333
  Nu=2+.6*SQRT(Re)*Pr**.33333333
ENDIF

C Calculate water Heat Transfer Coefficient in the film and heat
flow to
C   the drop (Q) .

HTC=Nu*CondF/DropDiam(J)
Q=3.14159*D2*(Tg-Td)*HTC

C Calculate the drop evaporation rate (ERate) and the heat flow
C to the drop (Q) .

IF(ISTOP(J).EQ.0.AND.IDRY.EQ.0) THEN
  CMTW=Sh*Dv/DropDiam(J)
  IF(Mevap(J).NE.0) THEN
    ER=-Cf*CMTW* ALOG((1-XO)/(1-XG))
  ELSE
    Cd=P/8.206E-5/Td
    Deff=.25*Dv
  ENDIF
  A=Deff*Cd/DropDiam(J)*2*RWCore(J)/(RWcore(J)-DropDiam(J)/2)
  ER=-Cf*(XG-XO)/(1/CMTW-1/A)
  print *, 'a=',a,' cmtw=',cmtw,' er=',er
  print *, 'Td=',w(6,1)*t0,w(5,1),'MEVAP=',MEVAP(j)
  print *, 'dmin=',dmin,'D=',dropdiam(J)
  If(XG.ge.0.14.and.(XO-XG).le.1e-3) then
    ERate=0
    ER=0
  ISTOP(J) = 1
  endif
  ELSE
    ERate=0
    ER=0
  ENDIF

```

```

IF(ERate.NE.0.AND.IDRY.EQ.0) THEN
  EP=9./3.14159*ERate*18*HtCapF/CondF/DropDiam(J)
  IF(EP.LT.88) THEN
    Q=Q*EP/(EXP(EP)-1)
  ELSE
    Q=0
  ENDIF
ENDIF

ENDIF

C      Sulfur Capture constants in wet agglomerate

RateK= 0.01
Dprod=1e-6

C      Dissolution rate constant of lime (basecase) and with NaOH

DissRate =rl*3e-4

If (type.eq.4) then
  D      i      s      s      R      a      t      e      =
DissRate*(DsSolids(J)/W(5,J)/CD0(J))**-.876132/733.88
ENDIF

RETURN
END

```

Table A-16. Subroutine PRINT.

SUBROUTINE PRINT(Dist, VAR, PD, ID, IA)

C Print results.

```
REAL CD0(15),DropNFlux(15),DropDiam(15),PD(15,50),NPart(15,50)
REAL VAR(7,15),WF(15),MWG0,DTime(15),MolWt,DsSolids(15)
REAL dR(15,50)
real CP(15,0:51),r0(15)
REAL *8 Dist
INTEGER ISTOP(15),NSHELL(15),nstart(15),l1(15)
    integer type
CHARACTER *1 Slu

COMMON/RKPR/NW,NE
COMMON/P/CD0,SMF0
COMMON/I/ISTOP
COMMON/E/SD,PD0,SP,PDD
COMMON/T/Time
COMMON/RW/RWCore
COMMON/Y/SO2MF0
COMMON/PP/P
COMMON/FN/DropNFlux,DuctArea,AirMassFlux,WVMFlux0
COMMON/DROP/DropDiam
COMMON/WF/WF
COMMON/VOL/VolMol,CaUt
COMMON/CO2/CO2,MWG0
COMMON/SLU/Slu
COMMON/CAS/Cas
COMMON/DTIME/DTime
COMMON/T0/T0
COMMON/DS/DsSolids
COMMON/NS/NSHELL
COMMON/NPDR/NPart
COMMON/DR/dR
COMMON/MOL/MolWt
COMMON/ASH/ASHFLUX0,DASH,ASHFLUX
COMMON/UT0/UT0,EFFCAS,PDRO
COMMON/IDRY/IDRY
COMMON/PRE/PRECYCLE
COMMON/IHED/IHED
common/CP/cp
common/nt/nstart
    common/typ/type
```

C Calculate captured Sorbent Mass Flux, Water Vapor Mass Flux,
fraction
C water unevaporated (XW), SO2 Mass Flux captured, water mole
fraction
C in the bulk gas phase (YG), and SO2 capture (Cap).

XW=0

```

SMF=0
WVMFlux=WVMFlux0
Util=0
SO2MF=0
NUM=NW
DO 59, I=1, NW
    I F ( S l u . N E . ' S ' . O R . S l u . N E . ' D ' )
SMF=SMF+DropNFlux(I)*VAR(2,I)/6
&           *3.14159*(1-SP)*SD*PDD**3
    WVMFlux=WVMFlux+DropNFlux(I)*CD0(I)*(1-VAR(5,I))
    XW=XW+WF(I)*VAR(5,I)
    IF(ISTOP(I).EQ.1) NUM=NUM-1
DUM=0
DUM2=0
DO 205, M=1, NSHELL(I)
IF(Slu.NE.'D') THEN
    DUM=DUM+NPart(I,M)*(PDD**3-PD(I,M)**3)
    DUM2=DUM2+NPart(I,M)*(PD0**3-PD(I,M)**3)
ELSE
    IF(I.EQ.1) THEN
        DUM=DUM+(PD0**3-PD(I,M)**3)
    ELSE
        DUM=DUM+(PDR0**3-PD(I,M)**3)
    ENDIF
    DUM2=DUM2+(PD0**3-PD(I,M)**3)
ENDIF
205  CONTINUE
Util=Util+DUM2/VAR(2,I)*WF(I)
59  SO2MF=SO2MF+DropNFlux(I)/(1.90986/(1-SP))/VolMol*(1-CaUt)
&           *DUM

    IF(Slu.EQ.'D') THEN
        WVMFlux=WVMFlux0-CD0(1)*VAR(5,1)*DropNFlux(1)
        XW=VAR(5,1)*CD0(1)/(3.14159*PD0**3/6*(1-SP))*VolMol/18
    ENDIF
    Cap=SO2MF/SO2MF0
    Util=Util/PD0**3

```

C Calculate the water mole fraction in the gas phase (X0), the
C saturation temperature (TSat), and the approach to saturation
(ASat).

```

XO=WVMFlux/18/(WVMFlux/18+AirMassFlux/MWGO)

    IF(type.eq.1)THEN
    TSat=46.13+3816.44/(18.3036-ALOG(XO*P*760))
    ASat=(VAR(1,1)*T0)-TSat
    ENDIF

    IF(type.eq.2)THEN
    TSat=41.381798+3934.936165/(18.520014-ALOG(XO*P*760))
    ASat=(VAR(1,1)*T0)-TSat
    ENDIF

```

```

        IF(type.eq.3)THEN
TSat=45.2469564+3824.134017/(18.321794-ALOG(XO*P*760))
ASat=(VAR(1,1)*T0)-TSat
        ENDIF

        IF(type.eq.4)THEN
TSat=46.13+3816.44/(18.3036-ALOG(XO*P*760))
ASat=(VAR(1,1)*T0)-TSat
        ENDIF

C Print the results.

IF(SO2MF0.EQ.0.OR.SMF0.EQ.0) THEN
  PRINT 15,Dist,Time,XW,(VAR(1,1)*T0),ASat,NUM,XO
ELSEIF(Slu.EQ.'D') THEN
  IF(ID.EQ.0) THEN
    IF(CAP.LT..02) THEN
      PRINT 11,Dist,Time,XW,Util*100,Cap*100
    ELSE
      PRINT 10,Dist,Time,XW,Util*100,Cap*100
    ENDIF
  ENDIF
  IF(IDRY.EQ.1.AND.ID.EQ.0) THEN
    ID=1
  ELSEIF(IDRY.EQ.1) THEN
    IF(CAP.LT..02) THEN
      PRINT 21,Dist,Time,Util*100,Cap*100
    ELSE
      PRINT 20,Dist,Time,Util*100,Cap*100
    ENDIF
  ENDIF
  ELSEIF(Slu.EQ.'S') THEN
    IF(CAP.LT..02) THEN
      PRINT11,Dist,Time,XW,Util*100,Cap*100,(VAR(1,1)*T0),ASat
      & ,NUM,XO
    ELSE
      PRINT10,Dist,Time,XW,Util*100,Cap*100,(VAR(1,1)*T0),ASat
      & ,NUM,XO
    ENDIF
  ELSE
    IF(IHED.EQ.0) THEN
      P          R          I          N          T
11,Dist,Time,XW,SMF/SMF0*100,Cap*100,(VAR(1,1)*T0),ASat
      & ,NUM,XO
    ELSE
      PRINT10,Dist,Time,XW,Util*100,Cap*100,(VAR(1,1)*T0),ASat
      & ,NUM,XO
    ENDIF
  ENDIF
11  FORMAT(F7.2,1X,F6.3,4X,F5.3,4X,F6.2,4X,F6.3,4X
      & ,F5.1,3X,F5.1,2X,I5,4X,F5.4,4X,F6.2)
10  FORMAT(F7.2,1X,F6.3,4X,F5.3,4X,F6.1,4X,F6.2,4X
      & ,F5.1,3X,F5.1,2X,I5,4X,F5.4,4X,F6.2)

```

```

15  FORMAT(F7.2,4X,F6.3,7X,F5.3,10X,F5.1,6X,F5.1,5X,I5,7X,F5.4)
21  FORMAT(F7.2,1X,F6.3,5X,'  ',5X,F6.2,4X,F6.3,4X
&           ,F5.1,3X,F5.1,2X,I5,4X,F5.4,4X,F6.2)
20  FORMAT(F7.2,1X,F6.3,5X,'  ',5X,F6.1,4X,F6.2,4X
&           ,F5.1,3X,F5.1,2X,I5,4X,F5.4,4X,F6.2)

```

C Optional printout of drop size distribution either when called
for
C or at the end of the duct.

```

IF(IA.EQ.0) THEN
PRINT *
PRINT 77,'At ',Dist,' meters the individual drop parameters
are:
&
PRINT *
77 FORMAT(A13,F7.3,A)
IF(Slu.NE.'D') THEN
PRINT *, 'Drop Diam  Frac Water  %Water',
&      'Drop Temp  Drop Time  Drop Vel  % Util  %Ash'

```

C Calculate the mass of solids in each drop, SMass, the cumulative
C capture of the large drops, and weighted cumulative capture
C of the large drops.

```

CUM=0
WFSUM=0
DO 111,I=NW,1,-1
DUM=0
DUM2=0
DO 5,M=1,NSHELL(I)
DUM2=DUM2+(1-(PD(I,M)/PD0)**3)*NPart(I,M)
5  DUM=DUM+((PD0**3-PD(I,M)**3)*129/MolWt+PD(I,M)**3)*NPart(I,M)
ASHMASS=3.14159/6*SD*DASH**3*VAR(3,I)
SMass=3.14159/6*SD*(1-SP)*DUM+DsSolids(I)+ASHMASS
DUM2=DUM2/VAR(2,I)*100

111  PRINT 12,DropDiam(I)*1E6,VAR(5,I)*WF(I)
      &
      ,VAR(5,I)*CD0(I)/(VAR(5,I)*CD0(I)+SMass)*100,(VAR(6,I)*T0),
      &
      DTime(I),VAR(4,I),DUM2,ASHMASS/(SMass+VAR(5,I)*CD0(I))
      &          *100

12
FORMAT(2X,F6.2,6X,F5.3,5X,F6.2,5X,F5.1,5X,F6.3,4X,F6.2,4X,F6.2,
&           2X,F4.1,3X,F5.1)
PRINT *

ELSE
PRINT*, 'Particle Diameter      Core Diameter'

```

```
      PRINT*, '      (microns)          (microns)      %  
Utilization'  
      DO 118, I=1, NW  
      DUM2=(1-(PD(I,1)/PD0)**3)*100  
118  PRINT 119,DropDiam(I)*1E6,PD(I,1)*1E6,DUM2  
      PRINT *  
      ENDIF  
119  FORMAT(5X,F6.2,16X,F6.2,13X,F6.2)  
  
      ENDIF  
  
      RETURN  
      END
```

Table A-17. Subroutine RUNGKUTT.

```
SUBROUTINE RUNGKUTT(VAR, PD, Dist, HMIN, IWARN)

C Perform 4th order Runge Kutta on the differential equations.
Each
C drop size has an individual step size and calculations are
performed
C only when appropriate.

REAL(K4,7,15),VAR(7,15),W(7,15),CD0(15),MWG0,MWG,NASH(15,50)
      R           E           A           L
NPartOld(15),DropNFlux(15),DropDiam(15),DTime(15),PD(15,50)
      REAL KPD(4,15,50),WPD(15,50),dR(15,50),NPart(15,50),Tave(15)
      REAL NPold(15,50),NASHOLD(15),XW(15)
      REAL *8 Dist,Hmin
      INTEGER ISTOP(15),Iold(15),IVSTOP(15)
      INTEGER NSHELL(15),NStart(15),Mevap(15)
      CHARACTER *1 Slu

COMMON/FN/DropNFlux,DuctArea,AirMassFlux,WVMFlux0
COMMON/PP/P
COMMON/DROP/DropDiam
COMMON/DUM/W,WPD
COMMON/IMIN/IMIN
COMMON/RKPR/NW,NE
COMMON/I/ISTOP
COMMON/PRNT/GV
COMMON/Iold/Iold
COMMON/P/CD0,SMF0
COMMON/Y/SO2MF0
COMMON/CAS/CaS
COMMON/E/SD,PD0,SP,PDD
COMMON/T/Time
COMMON/CO2/CO2,MWG0
COMMON/SLU/Slu
COMMON/DTIME/DTime
COMMON/T0/T0
COMMON/IDRY/IDRY
COMMON/IC/ICOUNT
COMMON/C/IVSTOP
COMMON/NP/NPartOld
COMMON/NS/NSHELL
COMMON/NT/NStart
COMMON/DR/dR
COMMON/NPDR/NPart
COMMON/MEVAP/Mevap
COMMON/TAVE/Tave,NSTEPS
COMMON/DV/DelV0
COMMON/ICE/ICEASE
COMMON/NASH/NASH
COMMON/NAOLD/NASHOLD
```

```
C Determine on which drop sizes calculations are to be performed  
and  
C calculate Water Vapor Mass Flux, and Gas Velocity.
```

```
ICOUNT=ICOUNT+1  
WVMFlux=WVMFlux0
```

```
DO 899,J=1,NW
```

```
IF(ISTOP(J).EQ.1.AND.SO2MF0.EQ.0) THEN  
IMIN=J+1  
ELSEIF(ISTOP(J).EQ.1) THEN  
VAR(6,J)=VAR(1,1)  
ENDIF
```

```
C If condensation has stopped reset step size.
```

```
IF(XW(J).GE.1.AND.VAR(5,J).LT.1) CALL CHK(HMIN,Dist,VAR)  
XW(J)=VAR(5,J)
```

```
899 WVMFlux=WVMFlux+DropNFlux(J)*CD0(J)*(1-VAR(5,J))
```

```
IF(Slu.EQ.'D') WVMFlux=WVMFlux0-CD0(1)*VAR(5,1)*DropNFlux(1)  
GV=(AirMassFlux/MWG0+WVMFlux/18)/(P/8.206E-5/VAR(1,1)/T0)  
GVOld=GV
```

```
C Initialize the dummy variable.
```

```
9 DO 10,I=1,NE  
DO 20,J=1,NW  
IF(I.EQ.7) THEN  
DO 15,M=1,NSHELL(J)  
15 WPD(J,M)=PD(J,M)  
ELSE  
W(I,J)=VAR(I,J)  
ENDIF  
IF(I.EQ.1) GO TO 10  
20 CONTINUE  
10 CONTINUE
```

```
C Perform Runge Kutta calculations.
```

```
C Evaporation from all drops contributes to the change in the duct  
gas
```

```
C temperature, VAR(1,1).
```

```
C For the dry sorbent injection case don't calculate the  
differential
```

```
C equations for sorbent capture and particle deceleration.
```

```
C For the slurry spray case don't calculate the differential  
equation
```

```
C for sorbent capture.
```

```
C If the drop temperature of the smallest evaporating drop becomes  
C unstable (changes by more than one degree Kelvin in one step)  
C reduce step size.
```

```
DO 55, L=1, 4
```

```
C Calculate K's.
```

```
DO 40, J=IMIN, NW
DO 50, I=1, NE
IF (I.EQ.7.AND.SO2MF0.NE.0.AND.CaS.NE.0) THEN
  DO 45, M=NShell(J), 1, -1
    IF (W(4,J)-GV.GT..4*DelV0.AND.M.NE.NShell(J)) THEN
      KPD(L,J,M)=KPD(L,J,NShell(J))
    ELSE
      KPD(L,J,M)=HMIN*FNC(L,I,J,M)
    ENDIF
 45  CONTINUE
ELSE
  K(L,I,J)=HMIN*FNC(L,I,J,0)
  IF (ICEASE.EQ.1) RETURN
ENDIF
IF (ISTOP(J).EQ.1.AND.SO2MF0.EQ.0) GO TO 40
50  CONTINUE
40  CONTINUE
```

```
C Calculate new dummy variable value.
```

```
IF (L.EQ.4) GO TO 100
DO 60, I=1, NE

IF (Slu.EQ.'D') THEN
  IF (I.EQ.2.OR.I.EQ.3.OR.I.EQ.4) GO TO 60
  IF (W(1,1).EQ.W(6,J).AND.I.EQ.6) GO TO 60
ENDIF
IF (Slu.EQ.'S'.AND.I.EQ.2) GO TO 60

DO 70, J=IMIN, NW

IF (I.EQ.1) THEN
  JJ=1
ELSE
  JJ=J
ENDIF

IF (I.EQ.7.AND.SO2MF0.NE.0.AND.CaS.NE.0) THEN
  DO 65, M=1, NSHELL(J)
    IF (L.NE.3) THEN
      DUM=PD(J,M)+KPD(L,J,M)/2
    ELSE
      DUM=PD(J,M)+KPD(L,J,M)
    ENDIF
    WPD(J,M)=DUM
    IF (WPD(J,M).LT.1E-3*PD0) WPD(J,M)=0
  65  CONTINUE
ELSE
  IF (L.NE.3) THEN
```

```

        DUM=VAR(I,JJ)+K(L,I,J)/2
    ELSE
        DUM=VAR(I,JJ)+K(L,I,J)
    ENDIF
    IF(I.EQ.6.AND.ICOUNT.GT.5.AND.
&           ABS(DUM-VAR(6,JJ)).GT..5/T0.AND.Slu.NE.'D') GO TO
131
        IF(I.EQ.4.AND.DUM.LT.0) GO TO 131
        W(I,JJ)=DUM
    ENDIF

70  CONTINUE
60  CONTINUE
55  CONTINUE

C Calculate new variable value.

100 DO 150,I=1,NE

        IF(Slu.EQ.'D') THEN
            IF(I.EQ.2.OR.I.EQ.3.OR.I.EQ.4) GO TO 150
            IF(I.EQ.6.AND.(VAR(1,1)-VAR(6,1)).LT..1/T0) THEN
                VAR(6,1)=VAR(1,1)
                GO TO 150
            ENDIF
        ENDIF
        IF(Slu.EQ.'S'.AND.I.EQ.2) GO TO 150

        DO 160,J=IMIN,NW

            IF(I.EQ.1) THEN
                JJ=1
            ELSE
                JJ=J
            ENDIF

            IF(I.EQ.7.AND.SO2MF0.NE.0) THEN
                DO 155,M=1,NSHELL(J)
                PD(J,M)=PD(J,M)+(KPD(1,J,M)+2*KPD(2,J,M) +
&                           2*KPD(3,J,M)+KPD(4,J,M))/6
                IF(PD(J,M).LT.1E-3*PDO) PD(J,M)=0
155  CONTINUE
            ELSE
                DUM=VAR(I,JJ)+(K(1,I,J)+2*K(2,I,J)+2*K(3,I,J)+K(4,I,J))/6
                IF(Slu.EQ.'D'.AND.IDRY.EQ.0.AND.VAR(5,1).GE.DUM.AND.I.EQ.5)
THEN
                    IDRY=1
                    GO TO 160
                ENDIF
                IF(I.EQ.4.AND.DUM.LT.0) GO TO 131
                VAR(I,JJ)=DUM
            ENDIF
        ENDIF
    ENDIF

```

```
ENDIF
```

```
C If variable is outside normal ranges default program.
```

```
IF(VAR(I,JJ).LT.0.OR.VAR(I,JJ).GT.1000.AND.I.NE.2) THEN
  IF(Slu.NE.'D') THEN
    IWARN=3
  ELSE
    IWARN=6
  ENDIF
  RETURN
ENDIF
```

```
160  CONTINUE
```

```
150  CONTINUE
```

```
C Calculate the change in the number of sorbent particles in each
shell
```

```
C due to diffusion of the particles.
```

```
IF(Slu.NE.'D'.AND.SO2MFO.NE.0.AND.CAS.NE.0) THEN
  CALL PDIF(HMIN,VAR,PD)
```

```
C If an outer radial shell is too small, combine it with the next
one in.
```

```
DO 285,J=1,NW
  IF(MEVAP(J).GT.0) THEN
    DO 286,M=NShell(J),Mevap(J),-1
      IF(dR(J,M).LE..001E-6) THEN
        IF(M.NE.NShell(J)) THEN
          PD(J,M)=(PD(J,M)*NPart(J,M)+PD(J,M+1)*NPart(J,M+1))
          &           /(NPart(J,M)+NPart(J,M+1))
          NPart(J,M)=NPart(J,M)+NPart(J,M+1)
          NASH(J,M)=NASH(J,M)+NASH(J,M+1)
          DO 287,MM=M+1,NShell(J)-1
            NPart(J,MM)=NPart(J,MM+1)
            NASH(J,MM)=NASH(J,MM)+1
            PD(J,MM)=PD(J,MM+1)
          287  ELSE
            PD(J,M-1)=(PD(J,M)*NPart(J,M)+PD(J,M-1)*NPart(J,M-1))
            &           /(NPart(J,M)+NPart(J,M-1))
            NPart(J,M-1)=NPart(J,M)+NPart(J,M-1)
            NASH(J,M-1)=NASH(J,M)+NASH(J,M-1)
            Mevap(J)=Mevap(J)-1
          ENDIF
          NShell(J)=NShell(J)-1
        ENDIF
      CONTINUE
    ENDIF
  285  CONTINUE
ENDIF
```

```
Time=Time+Hmin/(GV+GVOld)*2
```

```

DO 290,J=1,NW

C If IVSTOP(J) equals 1 set the drop velocity equal to the gas
velocity.

IF(IVSTOP(J).EQ.1.AND.SO2MF0.NE.0) VAR(4,J)=GV

C Calculate an average particle diameter in each drop size for the
C scavenging case.

IF(Slu.NE.'S'.AND.SO2MF0.NE.0.AND.J.GE.IMIN.AND.VAR(4,J)-GV.GT.
& .9*DelV0.AND.Slu.NE.'D') THEN
  M=1
  PD(J,M)=((NPold(J,M)*PD(J,M)**3+(NPart(J,M)-NPold(J,M))*PDD**3)/NPart(J,M))**.3333333
  &
  DO 295,M=1,NSHELL(J)
  PD(J,M)=PD(J,1)
295  NPold(J,M)=NPart(J,M)
  ENDIF
  NPartOld(J)=VAR(2,J)
  NASHOLD(J)=VAR(3,J)

C Calculate the drop time in the duct.

IF(Iold(J).EQ.0.OR.SO2MF0.NE.0.and.istop(J).eq.0) DTime(J)=
& DTime(J)+HMIN/VAR(4,J)

C If evaporation has ceased set the final mass of water in
VAR(5,J),
C call CHK to find the new step size, and set the K's to zero.

IF(Iold(J).NE.ISTOP(J).AND.Slu.NE.'D') THEN

  CALL CHK(HMIN,Dist,VAR)
  ICOUNT=5

  DO 200,I=1,NE
  DO 210,L=1,4
  IF(I.EQ.7.AND.SO2MF0.NE.0) THEN
    DO 205,M=1,NSHELL(J)
    KPD(L,J,M)=0
205  ELSE
    K(L,I,J)=0
    ENDIF
210  CONTINUE
200  CONTINUE

  ENDIF

290  Iold(J)=ISTOP(J)

C If evaporation has ceased, stop evaporation calculations.

```

```

NSTEPS=NSTEPS+1
DO 300,J=IMIN,NW
  Tave(J)=(Tave(J)*NSTEPS+VAR(6,1))/NSTEPS+1
300
IF(VAR(6,1).GT..3*(VAR(1,1)-Tave(J))+Tave(J).AND.VAR(5,1).LT..1
  &.AND.Slu.NE.'D'.AND.VAR(1,1)-VAR(6,NW).GT..1/T0) ISTOP(J)=1

C Send message to main program when evaporation of all drops has
ceased.

  IF(ISTOP(NW).EQ.1.AND.SO2MF0.EQ.0) IWARN=4

  RETURN

C If variable is diverging, reduce the step size.

131  HMIN=HMIN/SQRT(10.)
  IF(HMIN.LT.1D-8) THEN
    IWARN=2
    print *, 'w(1,1)= ', w(1,1), ' imin= ', imin
    print *, 'var(6,imin)= ', var(6,imin), ' w(6,imin)= ', w(6,imin)
    print *, 'var(1,1)= ', var(1,1), ' iminwarn= ', iminwarn
    print *, 'pd( ,j,m, )= ', pd(j,m), ' dum= ', dum
    print *, 'wpd( ,j,m, )= ', wpd(j,m), ' dum= ', dum
    RETURN
  ENDIF
  ICOUNT=0
  GO TO 9

  END

```

Table A-18. Subroutine SULF.

SUBROUTINE SULF(J,M,FNC,ER)

```
REAL W(7,15),WPD(15,50),DropDiam(15),NPART(15,50),RWCore(15)
REAL MolWt,KDISSOC,Rdry0(15,50),CD0(15)
REAL ShellFlux(15,50)
INTEGER ISTOP(15)
CHARACTER *1 Slu

COMMON/DUM/W,WPD
COMMON/SLU/Slu
COMMON/E/SD,PDO,SP,PDD
COMMON/P/CD0,SMFO
COMMON/SA/RoughK
COMMON/AG/DissRate,RateK,Dprod
COMMON/DROP/DropDiam
COMMON/VOL/VolMol,CaUt
COMMON/SO2/DSO2,CMTSO2,HE,KDISSOC,DH2SO3,DHSO3,YS8
COMMON/LIME/Dlime,ClimeEq
COMMON/NPDR/NPart
COMMON/MOL/MolWt
COMMON/RW/RWCore
COMMON/RD/Rdry0
COMMON/A/ALPHA
COMMON/CG/Cg
COMMON/SHEL/ShellFlux
COMMON/I/ISTOP
COMMON/PRNT/GV
COMMON/DV/DelV0
COMMON/IDRY/IDRY
COMMON/XW/XW
common/dis/dis
```

C Calculate the rate of sorbent consumption (dDp/dt) for the case
when

C sorbent particle is within the droplet surface (both
C moving and stopped relative to the gas velocity).

```
IF(ISTOP(J).EQ.0.AND.Slu.NE.'D') THEN
  IF(Slu.EQ.'S'.OR.W(4,J)-GV.LT..4*DelV0) THEN
    IF(WPD(J,M).EQ.0) THEN
      FNC=0
      RETURN
    ENDIF
    IF(M.NE.1) THEN
      FNC=-2*VolMol*(ShellFlux(J,M)-ShellFlux(J,M-1))/(1-SP) /
      & WPD(J,M)**2/NPart(J,M)
    ELSE
      FNC=-2*VolMol*ShellFlux(J,M)/(1-SP) /
```

```

&           WPD(J,M)**2/NPart(J,M)
ENDIF

C Else calculate the rate of sorbent consumption during
deceleration.

ELSE

Rough=1+EXP(RoughK*((WPD(J,M)/PD0)**3-.8))
U=4*Dlime*ClimeEq/WPD(J,M)**2
V=Dlime/Rough/DissRate
EP=W(2,J)**6/DropDiam(J)**3
DUM=WPD(J,M)**2*ClimeEq
DUM2=1/Rough/DissRate
A1=W(2,J)*ClimeEq*(WPD(J,M)/DropDiam(J))**2
A2=CMTSO2*YS8
A3=ER-CMTSO2
B1=KDISSOC**2
B2=4*KDISSOC/HE

C Iteratively calculate film thickness and therefore XS.

XS=0
C=0
DO 20, I=1,10
A=A1/(Del(C,WPD(J,M),U,V,J,M)/DLime+DUM2)
XS=(A-A2)/A3
C=(-KDISSOC+SQRT(B1+B2*XS))/2
IF(ABS(XS-XSOLD).LT..00001*XS) GO TO 21
20   XSOLD=XS

21   FNC=-2*VolMol*DropDiam(J)**2/(1-SP)/W(2,J)/WPD(J,M)**2*
&           (CMTSO2*(YS8-XS)+XS*ER)
ENDIF

C Else calculate the rate of sorbent consumption (dDp/dt) for the
case
C when the water core has receded past a sorbent particle.

ELSEIF(Slu.NE.'D') THEN

  IF(WPD(J,M).GT.0) THEN
    C=Cg*YS8
    Rough=1+EXP(RoughK*((WPD(J,M)/PD0)**3-.8))

Rratio=1/(ALPHA*(2*Rdry0(J,M)/WPD(J,M))**3+1-ALPHA)**.33333333
      FNC=-VolMol*RateK*Rough*C/(1+RateK*Rough/Dprod*WPD(J,M) /
&           2*(1-Rratio))
      FNC33 = FNC
  ENDIF

  if(fnc.gt.0) then
  print *

```

```

      print2,'in dry sulf, fnc=',fnc,' rratio=',rratio,' c=',c,
      & ' m=',m
      print *, 'ratek=',ratek,' rough=',rough,' dprod=',dprod,
      & ' wpd=',wpd(j,m)
2  format(1x,3(a,e12.5),a,i2)
      endif

C Else calculate the rate of sorbent consumption (dDp/dt) for the
dry
C   sorbent injection case.

      ELSE

      XW=W(5,J)*CD0(J)/(3.14159*PD0**3/6*(1-SP))*VolMol/18
      IF(XW.GT..25) THEN
          XW=.25
          IDRY=1
      ENDIF
      Rough=1+EXP(RoughK*((WPD(J,M)/PD0)**3-.8))
      RK=RateK*Rough*(XW/.25)
      Rs3=(ALPHA*PD0**3+WPD(J,M)**3*(1-ALPHA))/8
      Rratio=1/(ALPHA*PD0**3/Rs3+1-ALPHA)**.33333333
      FNC=-2*MolWt*YS8*Cg/SD/(1/RK+Rratio**2*Cg
      & /CMTSO2+1/Dprod/(XW/.25)*WPD(J,M)*(1-Rratio))

      ENDIF

      FNC=FNC/W(4,J)
      RETURN
      END

```

100-
200-
300-
400-
500-

46196

FILED

DATE